

**STUDY ON DEFLECTIONS OF REINFORCED CONCRETE
FLAT PLATES UNDER SERVICE LOAD**

by

SALAH UDDIN AHMED

MASTER OF SCIENCE IN CIVIL ENGINEERING (STRUCTURAL)



**Department of Civil Engineering
BANGLADESH UNIVERSITY OF ENGINEERING AND TECHNOLOGY,
DHAKA**

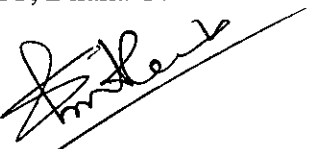


#104304#

2007

The thesis titled “**STUDY ON DEFLECTIONS OF REINFORCED CONCRETE FLAT PLATES UNDER SERVICE LOAD**”, Submitted by Salah Uddin Ahmed, Roll No: 100004304P, Session: October-2000, has been accepted as satisfactory in partial fulfilment of the requirement for the degree of **Master of Science in Civil Engineering (Structural)** on 20th March 2007.

BOARD OF EXAMINERS

1. 
Dr. Tahsin Reza Hossain
Associate Professor
Department of Civil Engineering
BUET, Dhaka-1000
2. 
Dr. Md. Mazharul Hoque
Professor and Head
Department of Civil Engineering
BUET, Dhaka-1000
3. 
Dr. Raquib Ahsan
Associate Professor
Department of Civil Engineering
BUET, Dhaka-1000
4. 
Dr. Md. Saiful Alam Siddiquee
Professor
Department of Civil Engineering
BUET, Dhaka-1000
5. 
Dr. Md. Afsar Ali
Associate Professor
Department of Mechanical Engineering
BUET, Dhaka-1000
- Chairman**
(Supervisor)
- Member**
(Ex-officio)
- Member**
- Member**
- Member**
- Member**
(External)

CANDIDATE'S DECLARATION

It is hereby declared that this thesis or any part of it has not been submitted elsewhere for the award of any degree or diploma.

Salahuddin Ahmed

(Salah Uddin Ahmed)

ACKNOWLEDGEMENTS

First of all, the author wishes to express his gratitude to Almighty Allah for giving him this opportunity and for enabling him to complete the thesis successfully.

The author wishes to express his heartiest gratitude and profound indebtedness to his supervisor Dr. Tahsin Reza Hossain, Associate Professor, Department of Civil Engineering, Bangladesh University of Engineering and Technology (BUET), Dhaka for his generous help, invaluable suggestions, continuous encouragement and unfailing enthusiasm at every stage of this study. His active interest in this topic and valuable advice was the source of author's inspiration.

The author wishes to express his sincere thanks and appreciation to Professor Dr. Md. Saiful Alam Siddiquee for providing the Artificial Neural Network program used in the current work.

The author pays his deepest homage to his parents, whom he believes to be the cardinal source of inspiration for all his achievements. Last but not the least, the author remains grateful to his friends and relatives specially to Md Ziaur Rahman, Md. Kaiser Ahamed and Sayra Monir for their contribution to complete this thesis work.

ABSTRACT

Excessive deflections of reinforced concrete slabs can cause severe serviceability problems. In recent years, realistic estimation of slab deflection under service loads has become more important due to the increasing use of high strength materials and due to the ultimate limit state design that generally leads to thinner members. Short-term deflection of concrete slab is affected by level of cracking and cannot be calculated by elastic analysis. Long-term deflection is further increased due to the effect of creep and shrinkage of concrete. Deflection calculations of slabs using nonlinear Finite Element (FE) analysis are complicated and time consuming. The main objective of this work is to develop an easy method of deflection estimation that will be useful in selecting thickness of flat plate slabs.

The effect of cracking in flat plate slab can be simulated using a number of nonlinear FE models of which ACI/Branson equation is the simplest. A global plate stiffness approach incorporating this equation has been used in this current work. The performance of ACI/Branson crack model in predicting short- and long-term experimental deflections is reasonably good. However, use of this rigorous nonlinear FE analysis is not particularly suitable for everyday use of the designer. With an aim to develop a simplified method of deflection calculation, a general purpose Artificial Neural Network (ANN) prediction software has been selected. A large number of FE analysis has been carried out on slabs with varying spans, column sizes, loads, material properties etc. and a database have been created for training the ANN prediction tool. The ANN program has been trained using this database until the amount of error in predicting deflection become very small. Once trained, the prediction tool has been validated against experimental and numerical results from previous FE analysis. Use of the trained ANN software to estimate short-and long-term deflections have been demonstrated with example. Now, a designer will be able to estimate deflection of flat plate slab easily for different span, column size, loading, material properties etc. by using the developed ANN prediction tool and will be able to select the appropriate thickness for the flat plate slab.

CONTENTS

	<u>Page No.</u>
DECLARATION	iii
ACKNOWLEDGEMENT	iv
ABSTRACT	v
CONTENTS	vi
LIST OF FIGURES	x
LIST OF TABLES	xiii
LIST OF SYMBOLS	xv
CHAPTER-1: INTRODUCTION	1
1.1 Background	1
1.2 Objective with specific aims, scope and possible outcome	2
1.3 Outline of the thesis	3
CHAPTER-2: LITERATURE REVIEW	5
2.1 Introduction	5
2.2 Behavior of column supported slab	6
2.3 Design methods of two way slabs	7
2.4 Equivalent frame method	9
2.4.1 Basis of analysis	9
2.4.2 Moments of inertia of slab beam	9
2.4.3 The equivalent column	10
2.4.4 Moment analysis	12
2.4.5 Flexural reinforcement	13
2.5 Strength and serviceability	15
2.6 Creep and shrinkage	16
2.6.1 Creep effect on deflections under sustained loads	16
2.6.2 Shrinkage effect on deflections under sustained loads	19
2.7 Deflection calculation by uncracked model	20
2.7.1 Deflection of two-way slab by Lagrange equation	20
2.7.2 Finite element method	21

2.8	Deflection calculation by cracked model	22
2.8.1	Immediate deflection (ACI method) using Branson's crack model	22
2.8.2	Nilson's approach	24
2.8.3	Hossain's model	27
2.9	Long-term deflection	28
2.9.1	Long-term deflection multiplier	28
2.10	Restraint cracking	30
2.11	Control of deflection	31
2.11.1	ACI Code provisions for deflection control	32
2.12	Permissible deflection	34
2.13	Artificial Neural Network	35
2.13.1	Introduction to Artificial Neural Network	35
2.13.2	Artificial Neural Network	35
2.13.3	Structures of Neural Network	37
2.13.4	The iterative learning process of ANN	38
2.13.5	Feed forward, Back-Propagation	40
2.13.6	Use of Neural Network	41
2.14	Conclusion	42
CHAPTER-3: NONLINEAR FINITE ELEMENT ANALYSIS		43
3.1	Introduction	43
3.2	Incorporation of Branson's equation	43
3.3	Incorporation of ACI method	44
3.4	Formation of [E] matrices	45
3.5	Sequence of analysis	46
3.6	Comparison of experimental results with FE analysis	48
3.6.1	McNeice corner supported slab	48
3.6.2	McNeice one way slab	50
3.6.3	Shukla and Mittal slabs	51
3.7	Conclusion	54



CHAPTER-4: LONG TERM DEFLECTION CALCULATION:	
CARDINGTON ECBP BUILDING	55
4.1 Introduction	55
4.2 Description of the Cardington ECBP building	56
4.2.1 Material properties	58
4.2.2 Loading	58
4.3 Finite element analysis and deflection calculation	59
4.4 Deflection calculation of Cardington Slab 3	62
4.4.1 Short-term deflection calculation	62
4.4.2 Long-term Deflection Calculation	63
4.5 Deflection calculation of Cardington Slab 4	70
4.5.1 Short-term deflection calculation	70
4.5.2 Long-term Deflection Calculation	70
4.6 Deflection calculation of Cardington Slab 6	75
4.6.1 Short-term deflection calculation	75
4.6.2 Long-term Deflection Calculation	76
4.7 Conclusion	80
CHAPTER-5: DEFLECTION ESTIMATION OF FLAT PLATE SLAB BY ARTIFICIAL NEURAL NETWORK	82
5.1 Introduction	82
5.2 Database development for training the ANN	82
5.2.1 The automated data file	83
5.2.2 The automated mesh file	85
5.2.3 The property file	85
5.3 Sensitivity analysis	86
5.3.1 Sensitivity of plate elements	86
5.3.2 Sensitivity of brick elements	87
5.4 Input parameters for database development	88
5.4.1 Span length	88
5.4.2 Column size	88
5.4.3 Slab thickness	88

5.4.4 Loading	88
5.4.5 Reinforcement	89
5.4.6 Material properties	89
5.5 Training of the artificial neural network (ANN) simulator	90
5.6 Use of neural network simulator for predicting deflection	92
5.7 Validation of ANN results with FE analysis	93
5.8 Validation of ANN results with Cardington test result	95
5.8.1 Validation of deflection of Cardington Slab 3 with ANN	95
5.8.2 Validation of deflection of Cardington Slab 4 with ANN	101
5.8.3 Discussion of ANN prediction with Cardington experimental results	105
5.9 Deflection prediction by ANN: Case studies	105
5.9.1 Case study 1	106
5.9.2 Case study 2	108
5.9.3 Case study 3	109
5.10 Conclusion	111
CHAPTER-6: CONCLUSION AND RECOMMENDATION	112
6.1 Introduction	112
6.2 Summaries and conclusion	112
6.2.1 Nonlinear FE analysis	112
6.2.2 Deflection Prediction by Artificial Neural Network	113
6.3 Conclusion	114
6.4 Recommendations for further work	114
REFERENCES	115-117
APPENDIX A	118-125
APPENDIX B	126-140
APPENDIX C	141-148
APPENDIX D	149-156

LIST OF FIGURES

	<u>Page No</u>	
Figure 2.1	Load distribution in flat plate slab	6
Figure 2.2	Moment variation in column supported tow way slab: a) critical moment section; b) moment variation along a span; c) moment variation across the width of critical sections.	8
Figure 2.3	Torsion at transverse supporting member illustrating the basis of the equivalent column	10
Figure 2.4	Minimum length of slab reinforcement in slabs without beams	14
Figure 2.5	Change in strain of a loaded and drying specimen; t_0 is the time of application of load.	16
Figure 2.6	Typical creep and recovery relationship	18
Figure 2.7	Standard shrinkage strain variation with time after moist curing (for 4 in or less slump, 40% ambient relative humidity and minimum thickness of member 6in. or less, after 7days moist cured)	20
Figure 2.8	Typical plate bending element with 12 degrees of freedom	22
Figure 2.9	Live load deflection analysis: (a) plan of slab; (b) deflection curve for unit strip; (c) diagram for maximum positive live load moment	26
Figure 2.10	Time variations of ξ for long term deflection	29
Figure 2.11	An example of a simple feed forward network	36
Figure 2.12	Structure of weight connection	37
Figure 3.1	Flow chart showing the sequence of calculation	47
Figure 3.2	Details of corner supported slab tested by McNeice: adapted from Jorfeit & McNeice (1971)	48
Figure 3.3	Load versus deflection curve for the corner supported slab at Node 7	49
Figure 3.4	Load versus deflection curve for the corner supported slab at Node 69	49
Figure 3.5	Load versus deflection curve for the corner supported slab at Node 147	50
Figure 3.6	Load versus deflection curve for the corner supported slab at Node 157	50

Figure 3.7	Details of simply supported one-way slab tested by McNeice adapted from Jorfeit & McNeice (1971)	51
Figure 3.8	Load versus deflection curves for center point of the simply supported one-way slab tested by McNeice	51
Figure 3.9	Details of edge-supported two-way slabs tested by Shukla and Mittal (1976)	52
Figure 3.10	Load versus deflections curves for the edge supported Shukla and Mittal slab S-8	53
Figure 3.11	Load versus deflections curves for the edge supported Shukla and Mittal slab S-11	53
Figure 3.12	Load versus deflections curves for the edge supported Shukla and Mittal slab S-12	54
Figure 4.1	Cardington EPCB building	56
Figure 4.2	Plan of Cardington in situ concrete building and deflection Measurement grid. (all dimension in mm) (Adapted from Hossain and Vollum (2002))	57
Figure 4.3	Diagrammatic representation of the load history for floor 3 in Cardington building. (Adopted from Hossain and Vollum (2002))	59
Figure 4.4	Loading pattern of Cardington building. (Adopted from Hossain and Vollum, 2002)	60
Figure 4.5	Finite element mesh of one quarter of the floor used in analysis (all dimensions are in mm)	61
Figure 4.6	Experimental and predicted deflection curve of corner panel of Cardington slab 3	65
Figure 4.7	Experimental and predicted deflection curve of edge panel of Cardington slab 3	68
Figure 4.8	Experimental and predicted deflection curve of center panel of Cardington slab 3	69
Figure 4.9	Experimental and predicted deflection curve of corner panel of Cardington slab 4	72
Figure 4.10	Experimental and predicted deflection curve of edge panel Cardington slab floor 4	73

Figure 4.11	Experimental and predicted deflection curve of center panel of Cardington slab 4	75
Figure 4.12	Experimental and predicted deflection curve of corner panel of Cardington slab 6	77
Figure 4.13	Experimental and predicted deflection curve of edge panel of Cardington slab 6	78
Figure 4.14	Experimental and predicted deflection curve of center panel of Cardington slab 6	80
Figure 5.1	The finite element mesh for 3x3 panel (1/4 th slab)	84
Figure 5.2	Neural Network Simulator	91
Figure 5.3	Opening dialogue box	92
Figure 5.4	The neural network predictor to predict deflection and stress	93
Figure 5.5	Defection versus time curve for Experimental and ANN predicted deflection of corner panel of Cardington slab 3	98
Figure 5.6	Defection versus time curve for Experimental and ANN predicted deflection of edge panel of Cardington slab 3	99
Figure 5.7	Deflection versus time curve for Experimental and ANN predicted deflection of center panel of Cardington slab 3	100
Figure 5.8	Deflection versus time curve for Experimental and ANN predicted deflection of corner panel of Cardington slab 4	102
Figure 5.9	Deflection versus time curve for Experimental and ANN predicted deflection of edge panel of Cardington slab 4	103
Figure 5.10	Deflection versus time curve for Experimental and ANN predicted deflection of center panel of Cardington slab 4	105
Figure 5.11	Defection prediction by ANN	107
Figure A.1	Two-way flat plate slab	114
Figure A.2:	Design moments and shear for flat plate slab	118

LIST OF TABLES

	<u>Page No</u>	
Table 2.1	Column strip moment, percent of total moment at critical section	13
Table 2.2	Minimum thickness of slabs without interior beams (ACI 2002)	33
Table 2.3	Maximum allowable computed deflections (ACI 2002)	34
Table 4.1	Loading and concrete material properties used in the analysis. (Adapted from Hossain and Vollum, 2002)	58
Table 4.2	Experimental and predicted deflection value of corner panel of Cardington slab 3.	65
Table 4.3	Experimental and predicted deflection value of edge panel of Cardington floor 3.	67
Table 4.4	Experimental and predicted deflection value of center panel of Cardington floor 3.	69
Table 4.5	Experimental and predicted deflection value of corner panel of Cardington slab 4.	71
Table 4.6	Experimental and predicted deflection value of edge panel of Cardington floor 4.	72
Table 4.7	Experimental and predicted deflection value of center panel of Cardington floor 4.	74
Table 4.8	Experimental and predicted deflection value of corner panel of Cardington slab 6.	76
Table 4.9	Experimental and predicted deflection value of edge panel of Cardington floor 6.	78
Table 4.10	Experimental and predicted deflection value of center panel of Cardington floor 6.	79
Table 5.1	Elastic and cracked deflection of different mesh size (same no of brick element)	87
Table 5.2	Elastic and cracked deflection of different mesh size (same no of plate element)	88
Table 5.3	Comparison of FE deflection and ANN predicted deflection	95
Table 5.4	Experimental and ANN predicted deflection of corner panel	

	of Cardington slab 3	98
Table 5.5	Experimental and ANN predicted deflection of edge panel of Cardington slab 3	100
Table 5.6	Experimental and ANN predicted deflection of center panel of Cardington slab 3.	101
Table 5.7	Experimental and ANN predicted deflection of corner panel of Cardington slab 4.	102
Table 5.8	Experimental and ANN predicted deflection of edge panel of Cardington slab 4.	104
Table 5.9	Experimental and ANN predicted deflection of center panel of Cardington floor 4.	105
Table A.1	Moment distribution of load case a	117
Table A.2	Moment distribution of load case b	118
Table A.3	Moment distribution of load case c	118
Table C.1	Database used for training of ANN ($f_r = 0.62\sqrt{f'_c}$)	142
Table D.1	Database used for training of ANN ($f_r = 0.33\sqrt{f'_c}$)	150

LIST OF SYMBOLS

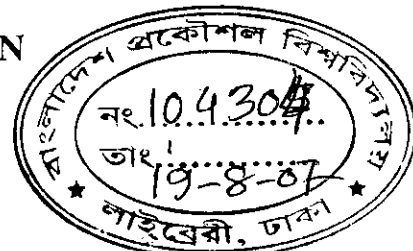
The following notations have been used in the thesis:

f'_c	Concrete cylinder strength
t, h	Thickness of section
d	Effective depth of section
E_c	Modulus of elasticity of concrete
E_s	Modulus of elasticity of steel
n	Modular ratio= E_s/E_c
f_r	Modulus of rupture of concrete
y_t	Distance from neutral axis to the tension face
I_{ut}	Moment of inertia of uncracked section
I_g	Gross moment of inertia without reinforcement
I_{eff}	Effective moment of inertia of concrete cross section
I_{cr}	Moment of inertia of cracked section
M_{cr}	Cracking moment as defined by ACI
Δ_i	Immediate deflection
A_s	Tensile reinforcement
A'_s	Compression reinforcement
l	Span length
w	Uniform transverse load
ν	Poisson's ratio
ρ	Tensile steel percentage
ρ'	Compressive steel percentage
ξ	Time-dependent coefficient for additional long-term deflection
$[E]$	Elasticity matrix in x-y directions
$[E']$	Elasticity matrix in principal directions
E_x, E_y	Reduced Young's moduli of cracked concrete in x and y-directions
ν_x, ν_y	Reduced Poisson's ratios of cracked concrete in x and y-directions
f_y	Yield strength of reinforcing steel

c_n	Depth of neutral axis
α_n, α_t	Modification factors to include the effect of cracking creep and shrinkage in the [E'] matrices
β_1	Takes in to account the bond properties of bars.
β_2	Takes in to account in the direction of tension
ε_{cs}	Shrinkage strain
σ_1, σ_2	Stress in the outer fiber of the section in principal direction
M_a	Maximum value of bending moment in the span
D	Flexural rigidity per unit width
Δ_l	Mid span live load deflection
R_c	Rigidity after cracking
λ	Multiplying factor for immediate deflection
$n'_c(t)$	Effective modular ratio
$E'_c(t)$	Effective modulus of elasticity
I_{e1}	Moment of inertia in the major principals Direction
I_{e2}	Moment of inertia in the minor principals Direction
K_t	Torsional stiffness of edge beam
K_c	Flexural stiffness of edge beam
K_{ec}	Flexural stiffness of equivalent column
C	Cross sectional constant
α_l	Relative stiffness of beam and slab
β_t	Torsional resistance of effective transverse beam
C_u	Creep coefficient
f_t, f_r	Modulus of rupture of concrete

INTRODUCTION

1.1. BACKGROUND



A structure must be safe against collapse and serviceable in use in order to serve its purpose. A structure or a part of a structure, reaches a limit state when it becomes incapable of fulfilling its function or when it no longer satisfies the conditions for which it was designed. Two categories of limit state normally have to be considered, *ultimate limit states* corresponding to failures or collapse and *serviceability limit states* at which deflection and cracking become excessive. The basic aim of structural design is to ensure that a structure should fulfill its intended function throughout its lifetime without excessive deflection and cracking or collapse and this aim must of course be met with due regard to economy and durability. Serviceability is not guaranteed simply by providing adequate strength in the member of a structure. Service load deflections under full load may be excessively large or long term deflection due to sustained loads may cause damage to partitions.

In the past, the questions of serviceability were dealt indirectly by limiting the stresses in concrete and steel at service loads to the rather conservative values that had resulted in satisfactory performance. Modern structural engineering tends to produce more economic structures with the use of higher strength materials and strength design methods through more accurate assessment of capacity. There is a tendency among designers to produce thinner sections. Particularly as for slabs, a slight decrease in thickness may save huge volume of concrete and the dead load of structure also reduces significantly. However, the reduction of slab thickness may lead to excessive deflection and cracking. Generally different codes ensure serviceability through minimum thickness provisions. The ACI Code (2002) suggests guidelines for selecting thickness of two-way column supported slabs. This guideline is for normal range of loading and geometric parameters. The designer may want to use thinner slabs, which is also allowed by the Code without

jeopardizing serviceability in situations where load is small. At the same time situations may also arise for large spans with heavy loads where ACI Code may not be adequate. In such conditions, it is important to predict short-term and long-term deflections accurately to ensure serviceability limit state design.

Calculation of deflection is a nonlinear problem even in service load range due to presence of cracks and long-term effects. Alam (2003) has developed some design charts to predict the deflection of two-way edge supported slabs based on the nonlinear FE analysis. Uddin (2005) has trained a purpose-built Artificial Neural Network (ANN) program to predict the deflection of two-way edge supported slabs based on the nonlinear FE analysis. Using these, it is possible to predict short as well as long-term slab deflections of two-way edge supported slabs without using time consuming complicated nonlinear FE analysis. In the current work, a similar attempt has been made to predict short- and long-term deflections of flat plate slab.

1.2 OBJECTIVE WITH SPECIFIC AIMS, SCOPE AND POSSIBLE OUTCOME

At present, flat plate slabs are frequently used in Bangladesh for its functional and aesthetical advantages. Often the designer wants to know whether it is possible to reduce the thickness of flat plate slab. But before reducing the slab thickness as specified by the Code, the designer must estimate the deflection correctly to ensure serviceability conditions. However, reinforced concrete is not an elastic, homogeneous, isotropic material as required by linear slab theories. Concrete possesses a comparatively low tensile strength, and most reinforced concrete slabs contain cracks in service load range. Calculation of slab deflection by the finite element analysis is complicated and time consuming. The main aim of this work is to develop an easy method of deflection estimation for flat plate slabs. To achieve this goal the objectives are set as follows:

- To study the performance of ACI/Branson crack model along with ACI long term multiplier in predicting short-term as well as long-term deflections by validating it against experimental results.

- To develop a database for training the ANN prediction tool, a large number of flat plate slabs will be analyzed by the nonlinear FE program by varying the geometric and material properties widely.
- To train a general purpose ANN program so that it can be used in estimating deflections of flat plate slabs after a proper validation against numerical and test results.

For short-term deflection calculation, a general-purpose of finite element package FE-77 (Hitchings, 1994), suitability adopted by Hossain (1999) which incorporates ACI/Branson crack model will be used in the analysis. The long-term deflection is then determined by multiplying the short-term deflection with ACI multiplier. Both the short-and long-term deflection calculation will be validated with experimental result. The database will be developed for training the ANN program by varying geometric and material properties in the usual range for a 3x3 slab system. Then the ANN program will be trained to predict deflection. It is hoped that with the successful completion of the work, it would be possible for the designer to easily estimate the short- and long-term deflections using this ANN tool.

1.3 OUTLINE OF THE THESIS

The thesis consists of six chapters, which are outlined in this section:

Chapter 1- General background of the research program and summary of aims and objectives.

Chapter 2- Behavior of column supported slabs, deflection calculation methods by uncracked and cracked models and long-term deflection by ACI method are discussed. Deflection due to creep and shrinkage are pointed out. Restrained cracking, deflection control and maximum allowable computed deflections are discussed. Artificial neural networks, neural network models, structure of neural networks, feed forward back-propagation and use of neural network are discussed.

Chapter 3- The incorporation of ACI/Branson crack model in nonlinear FE analysis is discussed. The performance of the nonlinear FE model using ACI/Branson crack model is verified against experimental short-term deflections of different slabs.

Chapter 4- Deflection calculation of Cardington test slabs with nonlinear FE analysis is discussed. The nonlinear FE program using ACI Branson's equation is used to predict both short-term and long-term deflections of flat plate slabs of Cardington European Concrete Building Projects (EBCP) full scale building.

Chapter 5 – Database development to train the ANN program is discussed. Stresses and deflections calculation of column supported slabs by Artificial Neural Network (ANN) are demonstrated. The ANN predicted deflections are verified with FE and Cardington test results. Case studies are presented to predict deflection using ANN.

Chapter 6 – Conclusions and recommendations for future work are presented.

Appendix A- Sample design calculation of flat plate slab (interior panel) are shown.

Appendix B- MS Excel sheet used in the automation of reinforcement mesh file.

Appendix C- Database used for training of ANN program for flat plate slabs is presented in tabulated form for $f_r = 0.62\sqrt{f'_c}$ N/mm². The parameters varied are span lengths in both directions, column sizes in both directions, slab thickness, loading, concrete strength and reinforcement.

Appendix D- Database used for training of ANN program for flat plate slabs is presented in tabulated form for $f_r = 0.33\sqrt{f'_c}$ N/mm². The parameters varied are span length in both directions, column sizes in both directions, slab thickness, loading, concrete strength and reinforcement.

CHAPTER 2

LITERATURE REVIEW

2.1 INTRODUCTION

In reinforced concrete construction, slabs are used to provide flat, useful surfaces. A reinforced concrete slab is a broad, flat plate, usually horizontal with top and bottom surfaces parallel or nearly so. It may be supported by reinforced concrete beams, by masonry or reinforced concrete walls, by structural steel members, directly by columns, or continuously by the ground. Its main function is to transmit load normal to their plane.

In strength design, the members are so proportioned that will have a proper safety margin against failure under a hypothetical overload state. It is also important that the member performance in normal service be satisfactory. This performance, termed serviceability, is not guaranteed simply by providing adequate strength. Excessive deflection is not acceptable in building construction. Service load deflection under full load may be excessively large, or long-term deflections due to sustained load may lead to cracking in supported walls and partition, ill-fittings of doors and windows, poor roof drainage, miss alignment of sensitive machinery and equipments, or aesthetically offensive sag. It is important therefore to control deflections, so that members designed mainly for strength as prescribed over loads will also perform well in normal service.

In the past, questions of serviceability were dealt with indirectly, by limiting the stresses in concrete and steel at service loads to the rather conservative values that had resulted in satisfactory performance. Wide availability of computers and design software and the use of higher strength concrete with steel reinforcement have permitted more material efficient reinforced concrete designs producing thinner sections. The use of high strength concrete results in smaller sections, having less stiffness that can result in larger deflections. The current approach is to investigate deflections specifically, after proportioning members based on strength requirements.

ACI Code (2002) proposes minimum slab thickness to insure serviceability and at the same time allows thinner slabs if deflection calculation permits so. ACI Code also provides a simple deflection calculation procedure.

2.2 BEHAVIOR OF COLUMN SUPPORTED SLAB

In reinforced concrete buildings slabs may be supported by beams on two opposite sides only and treated as *one-way slab*. There may be beams on all four sides of the slab and a *two-way slab* action is obtained. Concrete slab may in some cases be carried directly by columns without the use of beams or girders. Such slabs are described as *flat plates*. Flat slab construction is also beamless construction but incorporated a thickened slab region in the vicinity of the column and often employs flared column top. They are referred as drop panels and column capitals respectively.

Two-way edge slabs are supported by relatively shallow, flexible beams. 100 percent of the applied load must be carried in each direction jointly by the slab and supporting beams as far the requirement of statics. A similar situation is obtained in the flat plate slab as shown in Fig. 2.1. In this case beams are omitted. The broad strip of the slabs centered on column lines in each direction serve the same function as the beams of two-way slabs. The presence of drop panels or column capitals in the double hatched zone near the columns does not modify the requirement of statics.

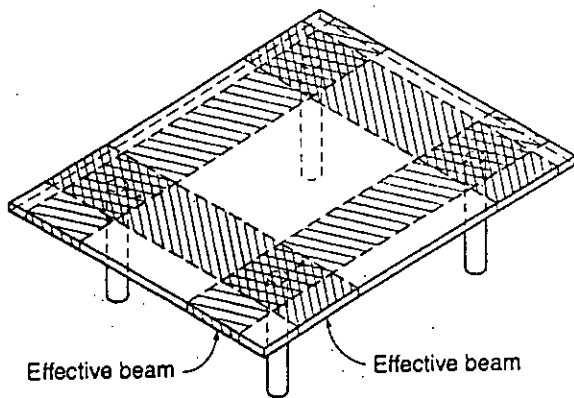


Figure 2.1 Load distribution in flat plate slab.

Figure 2.2a shows a flat plate slab supported by columns at A,B,C, and D. Figure 2.2b shows moment diagram for the direction of span l_1 . In this direction, the slab

may be considered as a broad, flat beam of width l_2 . Accordingly, the load per foot of span is wl_2 . In a span of continuous beam, the sum of the midspan positive moment and the average of negative moments at adjacent supports is equal to the midspan positive moments of a corresponding simply supported beam. In the terms of slab, this requirement of statics may be written

$$\frac{1}{2}(M_{ab} + M_{cd}) + M_{ef} = \frac{1}{8}wl_2l_1^2 \quad (2.1)$$

A similar requirement exist in the perpendicular direction, leading to the relation

$$\frac{1}{2}(M_{ac} + M_{bd}) + M_{gh} = \frac{1}{8}wl_1l_2^2 \quad (2.2)$$

These results disclose nothing about the relative magnitudes of the support moments and the span moment. The proportion of the total static moment that exists at each critical section can be found from an elastic analysis that considers the relative span lengths in adjacent panels, the loading pattern, and the relative stiffness of the supporting beams, if any and that of the columns.

The moments across the width of critical sections such as AB or EF are not constant but vary as shown qualitatively in Fig 2.2c. The exact variation depends on the presence or absence of beams on the column lines, the existence of drop panels and column capital as well as the intensity of the load. For design purpose, it is convenient to divide each panel as shown in Fig 2.2c into column strips, having the width of one fourth the panel width, on each side of the column centerlines, and middle strips in the one-half panel width between the two column strips. Moments may be considered constant within the bound of a middle strip or column strip, as shown, unless beams are present on the column lines. In the latter case, while the beam must have same curvature as the adjacent slab strip, the beam moment will be larger in proportion to its greater stiffness, producing a discontinuity in the moment variation curve at the lateral face of the beam. Since the total moment must be the same as before, according to statics, the slab moments must be correspondingly less.

2.3 DESIGN METHODS OF TWO-WAY SLABS

The ACI Code deals in a unified way with all two-way systems. Its provisions apply to slabs supported by beams and to flat slabs and flat plate as well as to two-way joist

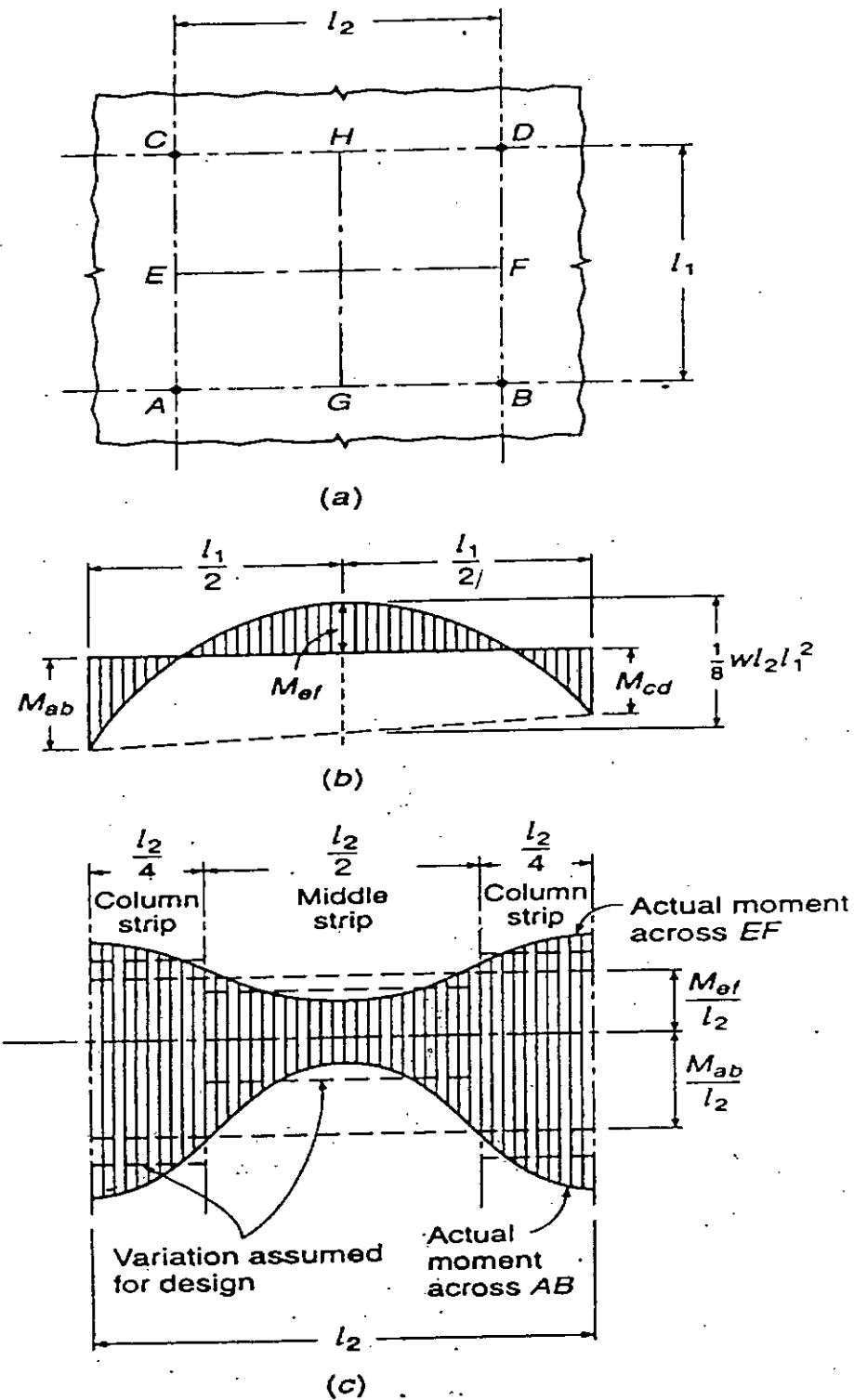


Figure 2.2 Moment variation in column supported two slabs :a) critical moment sections; b) moment variations along a span ; c) moment variation across the width of critical sections.

slabs. Two alternative approaches are suggested for design of all two-way system. First one is a semi empirical *direct design method* and the second one an approximate elastic analysis known as *the equivalent frame method*.

In either case, a typical panel is divided for purpose of design into column strip and middle strips. A column strip is defined as a strip having a width on each side of the column centerline equal to one fourth the smaller of the panel dimensions in two directions. A middle strip is a design strip bounded by two column strips. For the thesis work, the design of the flat plate is done by the equivalent frame method.

2.4 EQUIVALENT FRAME METHOD

2.4.1 Basis of analysis

By the equivalent frame method the structure is divided, for analysis, into continuous frames centered on the column lines and extending both longitudinally and transversely. Each frame is composed of a row of columns and a broad continuous beam. The beam or the slab-beam includes the portion of the slab bounded by the panel centerline on each side of the columns, together with column line beams or drop panels if used. For vertical loading each floor with its columns may be analyzed separately, the columns are assumed fixed at the floors above and below.

2.4.2 Moments of inertia of slab beam

Moment of inertia used for analysis may be based on the concrete cross section neglecting reinforcement, but variations in cross sections along the member axis should be accounted for.

According to ACI code, from the center of the column to the face of the column or capital, the moment of inertia of the slab is taken equal to that at the face of the column or capital, divided by the quantity $(1 - c_2/l_2)^2$, where c_2 and l_2 are the size of the column or capital and the panel span respectively, both measured transverse to the direction in which moments are being determined.

2.4.3 The equivalent column

In the equivalent column frame method of analysis, the columns are considered to be attached to the continuous slab beam by torsional members transverse to the direction of the span for which moments being found; the torsional member extends to the panel centerlines bounding each side of the slab beam under study. Torsional deformations of these transverse supporting members reduces the effective flexural stiffness provided by the actual column at the support.

The action of column and the transverse torsional member is easily explained with reference to Fig 2.3. From the figure, the rotational restraint provided at the end of the slab spanning in the direction l_1 is influenced not only by the flexural stiffness of the column but also by the torsional stiffness of the edge beam AC. With the distributed torque m_t applied at the slab and resisting torque M_t provided by the column, the edge beam sections at A and C will rotate to a greater degree than the section at B owing to torsional deformation of the edge beam. To allow this affect, the actual column and the edge beam are replaced by an equivalent column, so defined the total flexibility (inverse of stiffness) of the equivalent column is the sum of the flexibility of the actual column and edge beam.

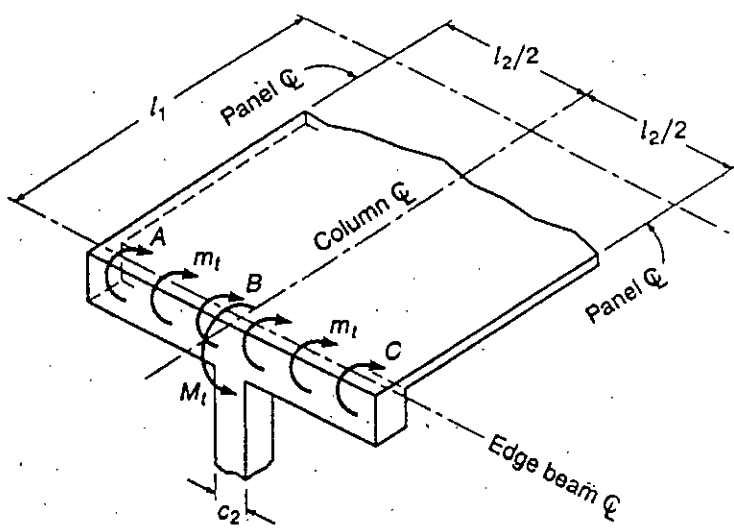


Figure 2.3 Torsion at transverse supporting member illustrating the basis of the equivalent column

Thus ,

$$\frac{1}{K_{ec}} = \frac{1}{\sum K_c} + \frac{1}{K_t} \quad (2.3)$$

where K_{ec} = flexural stiffness of equivalent column

K_c = flexural stiffness of actual column

K_t = torsional stiffness of edge beam

All expressed in terms of moment per unit rotation. In computing K_c , the moment of inertia, of the actual column is assumed to be infinite from the top of the slab to the bottom of the slab beam, and I_g is based on the gross concrete section elsewhere along the length.

The torsional stiffness K_t can be calculated by the expression

$$K_t = \sum \frac{9E_{cs}C}{l_2(1 - c_2/l_2)^3} \quad (2.4)$$

where E_{cs} = modulus of elasticity of slab concrete

c_2 = size of the rectangular column, capital or bracket in direction l_2

C = cross sectional constant

The summation applied to the typical case in which there are edge beams on both sides of the column. The constant C pertains to the torsional rigidity of the effective transverse beam which is defined as per ACI Code as the largest of

1. A portion of the slab having a equal width to that of the column or column capital in the direction in which moments are taken.
2. The portion of the slab specified in 1 plus that part of any transverse beam above and below the slab.
3. The part of the slab on each side of the beam extending a distance equal to the projection of the beam above or below the slab(whichever is greater) but not greater than 4 times the slab thickness .

The constant C is calculated by dividing the section into its component rectangles, each having smaller dimension x and larger dimension y, and summing the contributions of all the parts by means of equation

$$C = \sum \left(1 - 0.63 \frac{x}{y} \right) \frac{x^3 y}{3} \quad (2.5)$$

The subdivision can be done in such a way as to maximize C.

If a panel contains a beam parallel to the direction in which moments are being determined, the value of K_t obtained from Eq.(2.5) leads to a value of K_{ec} which are too low. Accordingly, it is recommended that in such cases the value of K_t found by Eq.(2.5) be multiplied by the ratio of the moment of inertia of the slab with such a beam to the moment of inertia of the slab without it. The concept of the equivalent column, as described with respect to an exterior column, is employed at all supporting columns for each continuous slab beam according to the equivalent frame method.

2.4.4 Moment analysis

With the effective stiffness of the slab beam strip and the supports found as described, the analysis of the equivalent frame can proceed by moment distribution or any other convenient method.

In keeping with the requirements of the statics, the equivalent beam strips in each direction must carry 100 percent of the load. If the live load does not exceed three quarter of the dead load, maximum moment may be assumed to obtain at all critical sections when the full factored live load (plus factored dead load) on the entire slab. Otherwise pattern loading must be used to maximize positive and negative moments. Maximum positive moments are calculated with the three-quarters factored live load on the panel and on alternate panes while maximum negative moment at a support is calculated with three quarters factored live load on the adjacent panels only. Use of three quarters live load rather than the full value recognizes the maximum positive and negative moments cannot occur simultaneously. Factored moments must not be taken less than those corresponding to the full factored live load on all panels.

Negative moments obtained from the analysis apply at the centerlines of supports. Since the support is not a knife-edge but rather broad band of slab spanning in the transverse direction, some reduction in the negative design moment is proper. At interior supports, the critical section for negative bending, in both column and middle strips, may be taken at the face of the supporting columns or capital, but in no case at a distance greater than the $0.175l_1$ from the center of the column.

For design purposes, the total strip width is divided into column strip and adjacent half middle strips and moments are assumed constant within the bounds of each. The distribution of moments to column and middle strips is done using the percentages given in Table 2.1.

Table 2.1 Column strip moment, percent of total moment at critical section

		l_2/l_1	0.5	1.0	2.0
Interior negative moment					
$\alpha_1 l_2/l_1 = 0$		75	75	75	
$\alpha_1 l_2/l_1 \geq 1.0$		90	75	45	
Exterior negative moment	$\beta_t = 0$	100	100	100	
$\alpha_1 l_2/l_1 = 0$	$\beta_t \geq 2.5$	75	75	75	
$\alpha_1 l_2/l_1 \geq 1.0$	$\beta_t = 0$	100	100	100	
	$\beta_t \geq 2.5$	90	75	45	
Positive moment					
$\alpha_1 l_2/l_1 = 0$		60	60	60	
$\alpha_1 l_2/l_1 \geq 1.0$		90	75	45	

$$\alpha_1 = \text{relative stiffness of the beam and slab in the direction of } l_1 = \frac{E_{cb} I_b}{E_{cs} I_s}$$

$$\beta_t = \text{torsional resistance of effective transverse beam} = \frac{E_{cb} C}{2 E_{cs} I_s}$$

2.4.5 Flexural reinforcement

Flexural reinforcement in two-way slab systems is placed in an orthogonal grid, with bars parallel to the sides of the panels. To provide for local concentrated loads, as well as to ensure the tensile cracks are narrow and well distributed, a maximum bar spacing at critical sections of 2 times the total slab thickness is specified by the ACI Code for two-way slabs. Because of the staking that results when bars are placed in perpendicular layers, the inner steel will have an effective depth 1 bar diameter less

then the outer steel. For the flat plate slab, the problem relates to middle strip positive steel and column strip positive and negative bar.

For the entire panel of a flat plate slab, including both middle strip and column strips in each direction, the moments in the long direction will be larger than those in the short direction as is easily confirmed by calculating the static moment in each direction for a rectangular panel. It is clear that the middle strip positive moments are larger in the long direction than the short direction, exactly the opposite of the situation for the slab with stiff edge beams. In the column strips, positive and negative moments are larger in the long than in the short direction. On the basis, the designer is to led place the long-direction negative and positive bars, in both middle and column strips, closer to the top or bottom surface of the slab, respectively, with the larger effective depth. The best guide in specifying steel placement order in areas where stacking occurs in the relative magnitudes of design moments obtained from analysis for a particular case, with maximum d provided for the bars resisting the largest moments. Bar cutoff point could be calculated from moment envelopes if available. Alternatively standard bar cut off points from the Fig. 2.4 should be used as recommended in the ACI Code.

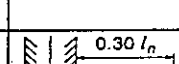
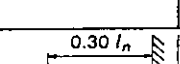
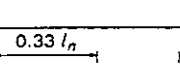
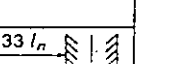
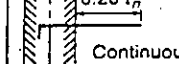
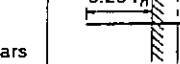
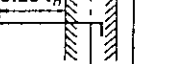
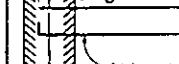
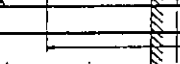
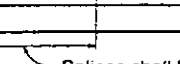
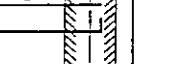
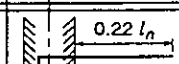
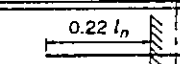
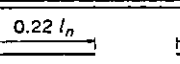
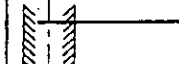
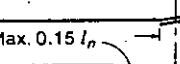
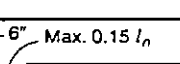
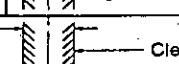
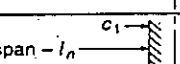
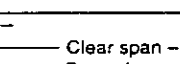
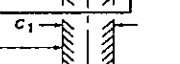
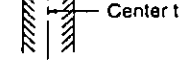
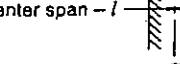
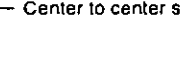
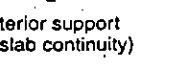
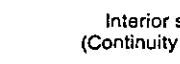
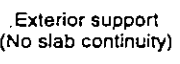
COLUMN STRIP	LOCATION	MINIMUM PERCENT A_s AT SECTION	WITHOUT DROP PANELS		WITH DROP PANELS	
			50	100	50	100
TOP	50	Continuous bars				
	Remainder					
BOTTOM	100					
		At least two bars or wires shall conform to 13.3.8.5			Splices shall be permitted in this region	
MIDDLE STRIP	TOP	100				
	BOTTOM	50 Remainder				
						
						
			Clear span - l_n	Clear span - l_n	Clear span - l_n	Clear span - l_n
			Face of support	Face of support	Face of support	Face of support
			Center to center span - l	Center to center span - l	Center to center span - l	Center to center span - l
						
			Exterior support (No slab continuity)	Interior support (Continuity provided)	Exterior support (No slab continuity)	Exterior support (No slab continuity)

Figure 2.4. Minimum length of slab reinforcement in slabs without beams

2.5 STRENGTH AND SERVICEABILITY

Members are always designed with a capacity for load that is significantly greater than that required to support anticipated service loads. This extra capacity not only provides a factor of safety against failure by accidental overload or defective construction but also limits the level of stress under service load to provide some control over deformation and cracking. Even if a member can support the design loads, it must not bend to such an extent that its function is impaired.

By providing a reserve of strength, the designer recognizes that members may be subjected to loads greater than those assumed in design. The extra strength also provides for the possibility that members may be constructed with a lower strength than specified because of under strength materials or poor workmanship. Although it is imperative that structures be designed with adequate strength to reduce the probability of failure to an acceptable level, they must also function effectively under normal service loads. Deflection must be limited to ensure that to ensure that floors will remain level within required tolerances and do not vibrate, to prevent plaster ceilings and masonry partitions from cracking, to ensure that sensitive equipment will not be thrown out of alignment, the width of cracks must be limited to preserve the architectural appearance of exposed surfaces and to protect reinforcement from attack by corrosion.

Two approaches can be applied to the problem of control of serviceability by deflection:

- a) Direct control method through the computations. The slab or plate relative to stiffness can be so proportioned that the predicted deflection falls within acceptable limit.
- b) Indirect control method through the limitation of the geometry to qualitatively accepted values of the span-to-depth-ratios.

The second approach is expectedly more conservative in many instances, while the first approach requires more effort on the part of the design engineer.

2.6 CREEP AND SHRINKAGE

Creep and shrinkage are time-dependent deformations that, along with cracking, provide the greatest concern for the designer because of the inaccuracies and unknowns that surround them. Concrete is elastic only under loads of short duration; and because of additional deformation with time, the effective behavior is that of an inelastic material. Deflection after a long period of time is therefore difficult to predict, but its control is needed to ensure serviceability during the life of the structure.

2.6.1 Creep effect on deflections under sustained loads

Creep is the property of concrete by which it continues to deform with time under sustained load at unit stresses with the accepted elastic range. This inelastic deformation increase at a decreasing rate during the time of loading, and its total magnitude may be several times as large as short-time elastic deformation. Frequently creep is associated with shrinkage, since both are occurring simultaneously and often provide the same net effect: increased deformation with time. The general relationship of deformation versus time in Fig 2.5 shows that the true elastic strain decreases since the modulus of elasticity E_c is a function of concrete strength f'_c which measures with time.

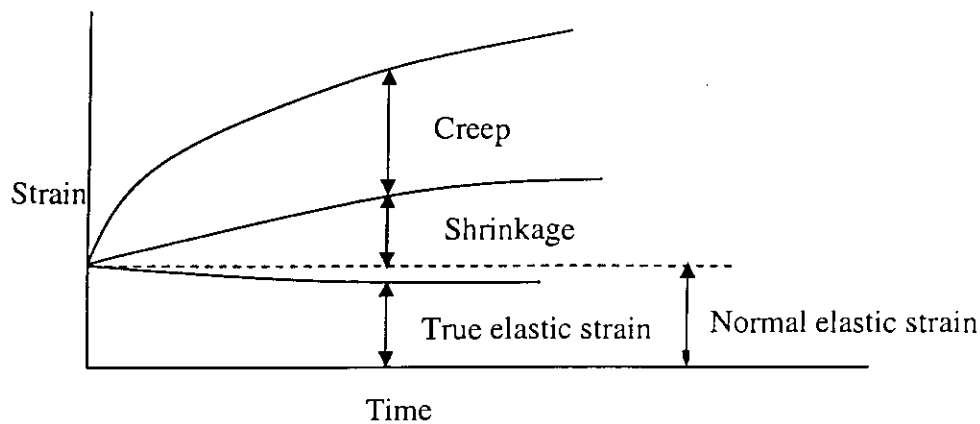


Figure 2.5 Change in strain of a loaded and drying specimen; t_0 is the time of application of load.

The internal mechanism of creep, or "plastic flow" as it is sometimes called, may be due to any one or a combination of the following:

- 1) Crystalline flow in the aggregate and hardened cement paste.
- 2) Plastic flow of the cement past surrounding the aggregate.
- 3) Closing internal voids
- 4) The flow of water out of the cement gel due to external load and drying.

Factors affecting the magnitude of creep are:

- 1) The constituents-such as the composition and fineness of the cement, the admixtures, and the size, grading, and material content of the aggregates.
- 2) Water cement ratio
- 3) Curing temperature and relative humidity
- 4) Age and duration of loading
- 5) Magnitude of stress
- 6) Surface-volume ratio of the member
- 7) Slump

Accurate prediction of creep is complicated because of the variables involved; however, a general prediction method developed by Branson gives a standard creep coefficient equation (4 inch or less slump, 40% relative humidity, moist cured, and loading age of seven days).

$$C_t = \frac{\text{creep strain}}{\text{initial elastic strain}}$$

$$= \frac{t^{0.6}}{10 + t^{0.6}} C_u \quad (2.6)$$

where, t = time in days after loading

C_u = ultimate creep coefficient

Branson (1977) suggested using an average value of $C_u = 2.35$ for standard condition but the range of C_u is from 1.3 to 4.15. The effect of unloading may be seen from Fig.2.6 where a certain time t_1 the load is removed. There is an immediate elastic recovery and a long time creep recovery but a residual deformation remains.

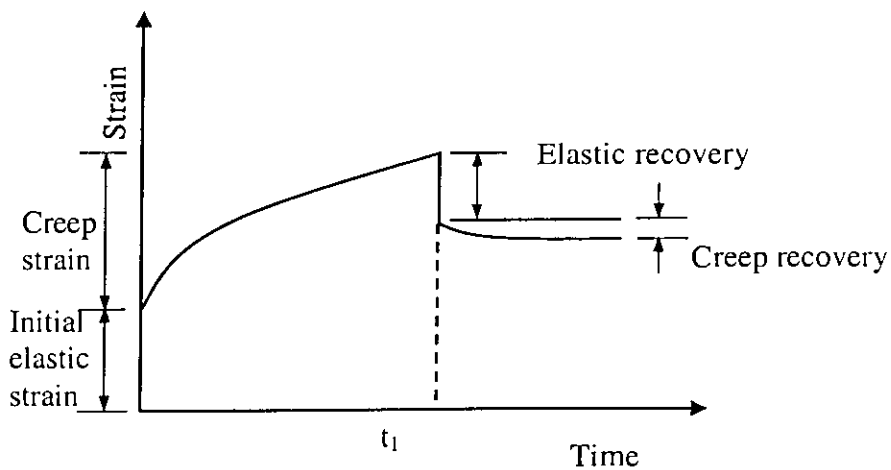


Figure 2.6 Typical creep and recovery relationship (

Deflection resulting from creep is

$$\Delta_{cp} = C_t (\Delta_i)_D \quad (2.7)$$

where, $(\Delta_i)_D$ is the instantaneous deflection due to all sustain loads.

Equation 2.7 applies to the standard condition of 40% ambient relative humidity, 4 in (100 mm) or less slump, average thickness of member 6 in (150 mm) and loading age 7 days for moist-cured concrete or 1 to 3 days for steam-cured concrete. For other condition, the standard condition value is to be multiplied by the following correction factors (CF).

1. Age of loading. For moist cured concrete,

$$(CF)_a = 1.25 t_a^{-0.118} \quad (2.8a)$$

For steam cured concrete,

$$(CF)_a = 1.13 t_a^{-0.0095} \quad (2.8b)$$

where t_a is the age of loading in days after the initial period of curing.

2. Humidity. For $H \geq 40\%$

$$(CF)_h = 1.27 - 0.0067H \quad (2.8a)$$

where H is the ambient relative humidity in percent.

3. Average thickness of member: Where the average thickness of the member in inches exceeds ~~6 in~~ (150 mm), a correction factor (reduction factor) may be applied.

However, for most design purposes such a correction may be neglected. For members whose average thickness greatly exceeds 12 in (300 mm), Meyers and

Branson (1972) provide a chart that may be used to correct for effect of average thickness.

2.6.2 Shrinkage effect on deflections under sustained load

Shrinkage, broadly defined, is volume change that is unrelated to load application. It is possible for concrete cured continuously under water to increase in volume; however the usual concern is with a decrease in volume. Shrinkage occurs more pronounced during the first few months than does creep. Typically, 90% of the shrinkage will have occurred at the end of one year, whereas not until the end of five years 90% of the creeps have occurred. Shrinkage deflection Δ_{sh} may be expressed:

$$\Delta_{sh} = \alpha_1 \phi_{sh} L^2 \quad (2.9)$$

where, ϕ_{sh} = shrinkage curvature

$$= \frac{\epsilon_{sh} - \epsilon_s}{d} \quad (2.10)$$

ϵ_s = compressive strain induced in the steel from shrinkage

α_1 = factor relating to the geometry of support system and may be taken as

$\alpha_1 = 0.5$ cantilever beams

= 0.125 simply supported beams

= 0.086 beams continuous at one end only

= 0.063 beams continuous at both ends

and L is the span length of the beam.

Branson (1977) general prediction method gives a standard shrinkage strain equation (for 4in. or less slump, 40% ambient relative humidity and minimum thickness of member 6in. or less, after 7days moist cured)

$$\epsilon_{sh} = \left(\frac{t}{35+t} \right) (\epsilon_{sh})_u \quad (2.11)$$

where, t = time in days after moist curing

$(\epsilon_{sh})_u$ = ultimate shrinkage strain (from 450 to 1000×10^{-6} in./in.)

Correction factors are given with the primary one relating to humidity H ,

$$\text{Correction factor} = 1.4 - 0.01H \text{ for } 40\% \leq H \leq 80\%$$

$$\text{Correction factor} = 3.0 - 0.03H \text{ for } 80\% \leq H \leq 100\%$$

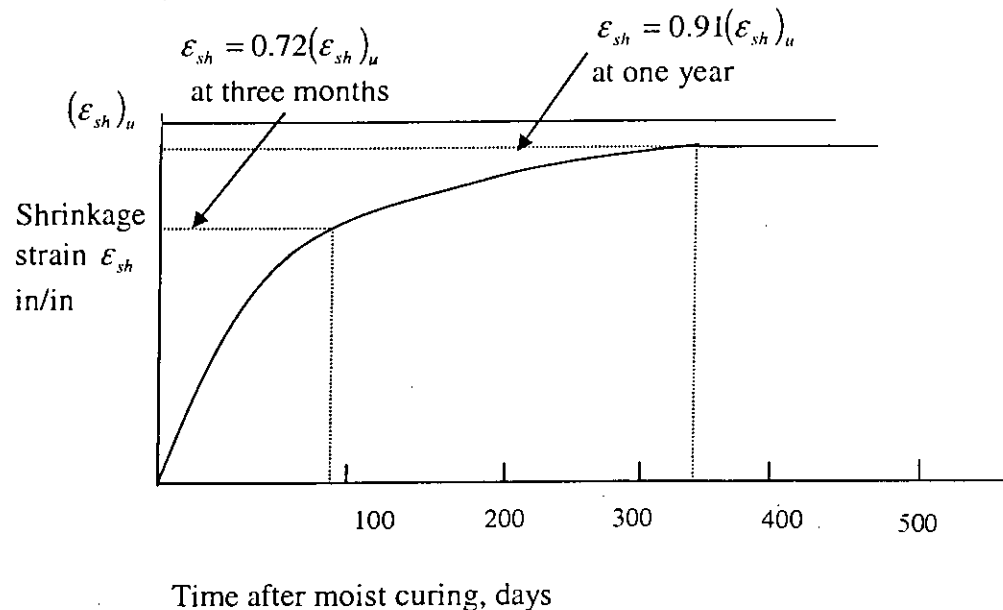


Figure 2.7 Standard shrinkage strain variation with time after moist curing (for 4 in. or less slump, 40% ambient relative humidity and minimum thickness of member 6in. or less, after 7days moist cured) (Adapted from Wang,1998)

2.7 DEFLECTION CALCULATION BY UNCRACKED MODEL

The calculation procedures of elastic deflection of edge-supported slab are discussed in this section. The analytical methods for calculation of elastic deflection are briefly discussed. From finite element analysis the elastic deflection of slab can also be calculated.

2.7.1 Deflection of two-way slab by Lagrange equation

The classical theory of elasticity-assuming thin plates of constant thickness, small deflection and low stress levels- has expressed the deflection relationship as a Lagrangian equation:

$$\frac{\partial^4 a}{\partial x^4} + 2 \frac{\partial^4 a}{\partial x^2 \partial y^2} + \frac{\partial^4 a}{\partial y^4} = \frac{w}{D} \quad (2.12)$$

where, a = deflection of the plate
 w = transverse load per unit area

$$D = \text{flexural rigidity per unit width} = \frac{Eh^3}{12(1-\nu^2)}$$

Finite difference method can be used to solve the above differential equation to get deflections of slabs.

2.7.2 Finite element method

In this method, the slab is divided into a number of sub regions of finite elements, which are generally triangular, rectangular or quadrilateral in shape. They are considered interconnected only at discrete points, called nodes, at the corners of the individual elements. The continuous displacement quantities are expressed in terms of a finite number of displacements $w(x, y)$, called degrees of freedom at the nodes. Therefore, for a rectangular plate bending element having 12 degrees of freedom (shown in Fig. 2.8), for instance,

$$[F] = [K][D] \quad (2.13)$$

where,

$[D]$ = 12x1 column vector consisting of vertical displacements and rotations about each horizontal axis of each of the four corners.

$[K]$ = 12x12 element stiffness matrix relating nodal forces and the corresponding displacements.

$[F]$ = 12x1 column vector consisting of transverse forces and bending moments at the nodes.

The main problem in the application of the finite element method to linear elastic slab systems in general is to obtain a suitable force-displacement relationship between the nodal forces and the corresponding displacements at the nodal degrees of freedom. A further complication, in applying the method to reinforced concrete, is the derivation of a suitable set of constitutive relations to model the slab behavior under various loading conditions.

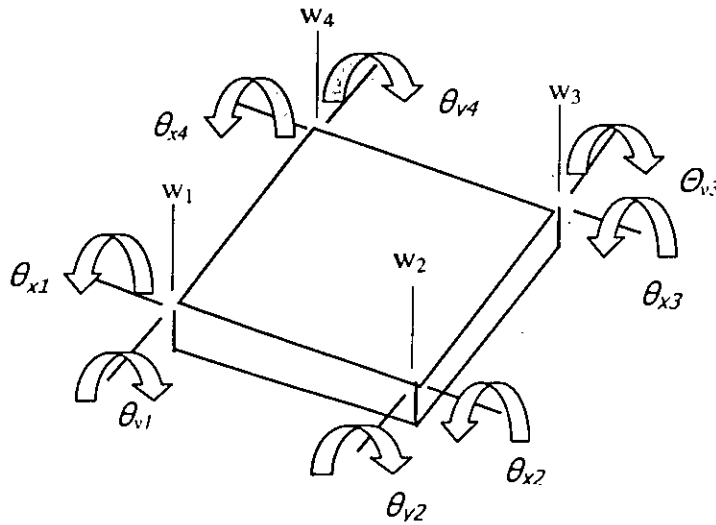


Figure 2.8 Typical plate bending element with 12 degrees of freedom

2.8 DEFLECTION CALCULATION BY CRACKED MODEL

In normal service load most of the edge-supported slabs are cracked because of the stresses greater than modulus of rupture of concrete. In this situation the instantaneous slab deflection (termed as immediate deflection) will be excess than elastic deflection. The calculation methods of immediate deflection are discussed in this section.

2.8.1 Immediate deflection (ACI method) using Branson's crack model

Elastic deflections can be expressed in the general form

$$\Delta = \frac{f(\text{loads, span, support})}{EI} \quad (2.14)$$

where, EI is the flexural rigidity and f (loads, spans, supports) is a function of the particular load, span and support arrangement. The particular problem in reinforced concrete structures is therefore the determination of the approximate flexural rigidity EI for a member consisting of two materials with properties and behavior as widely different as steel and concrete.

If the maximum moment in a flexural member is so small that the tension stress in the concrete does not exceed the modulus of rupture f_r , no flexural tension cracks

will occur. The full, uncracked section then available for resisting stress and providing rigidity. The effective moment of inertia for this low range of loads is that of the uncracked, transformed section I_{ut} , and E_c is the modulus of elasticity of concrete. For this load range, the elastic deflection is

$$\Delta_{iu} = \frac{f}{E_c I_{ut}} \quad (2.15)$$

At higher loads, flexural tension cracks are formed. In addition, if shear stresses exceed v_{cr} and web reinforcement employed to resist them, diagonal cracks can exist at service loads. In the region of flexural cracks the position of the neutral axis varies: directly at each cracks it is located at the level calculated for the cracked, transformed section; midway between cracks its dips to a location closer to that calculated for the uncracked transformed section. Correspondingly, flexural-tension cracking causes the effective moment of inertia to be that of cracked transformed section in the immediate neighborhood of flexural tension cracks, and closer to that of the uncracked transform section midway between cracks, with a gradual transition between these extremes.

It is seen that the value of local moment of inertia varies in those portions of the beam in which bending moment exceeds the cracking moment of the section

$$M_{cr} = \frac{f_r I_{ut}}{y_t} \quad (2.16)$$

where y_t is the distance from the neutral axis to the tension face and f_r is the modulus of rupture. The exact variation of I depends on the shape of the moment diagram and on the crack pattern, and is difficult to determine. This makes an exact deflection calculation impossible.

Branson (1977) proposed an equation for calculation of effective moment of inertia between uncracked and fully cracked section of a simple beam considering tension stiffening. In order to provide a smooth transition between the moment of inertia I_{cr} of the transformed cracked section and the moment of inertia I_g of the gross uncracked concrete section the ACI 318-02 (2002) proposed that, for the calculation of deflection immediately after application of load, an effective value of moment of

inertia using Branson's equation should be used. ACI Code used a power n=3 in Branson's equation:

$$I_{eff} = \left(\frac{M_{cr}}{M_a} \right)^n I_{ut} + \left[1 - \left(\frac{M_{cr}}{M_a} \right)^n \right] I_{cr} \text{ and } \leq I_{ut}. \quad (2.17)$$

where,

I_{ut} = moment of inertia of the gross uncracked concrete section

I_{cr} = moment of inertia of the cracked transformed concrete section

M_{cr} = cracking moment of the reinforced concrete beam

M_a = maximum values of bending moment in the span

Extensive documented studies (Branson, 1977) have shown that deflections of beams as well as slab are reasonably predicted by Branson's equation:

$$\Delta_{ic} = \frac{f}{E_c I_{eff}} \quad (2.18)$$

Most reinforced concrete spans are continuous, not simply supported. The effective moment of inertia for a continuous span can be found by a simple averaging procedure. A fundamental problem for continuous is that, although the deflection are based on the moment diagram, that moment diagram depends, in turn, on the flexural rigidity EI for each member of the frame. The flexural rigidity depends on the extent of cracking and the cracking depends on the moments, which are to be found.

2.8.2 Nilson's approach

Nilson (1997) has presented deflection calculation procedure of edge-supported slab. Edge-supported slabs are typically thin relative to their span, and may show large deflections even though strength requirements are met, unless certain limitations are imposed in the design to prevent this. The simplest approach to deflection control is to impose a minimum thickness-span ratio.

The calculation of deflections for slabs is complicated by many factors, such as the varying rotational restraint at the edges, the influence of alternative loading arrangements, varying ratio of side length, and the effects of cracking, as well as the time dependent influences of shrinkage and creep. The deflection of an edge-supported slab can be estimated with reasonable accuracy, based on the moment

coefficients used in the flexural analysis. The deflection components of concern are usually the long-term deflections due to sustained loads and the immediate deflection due to live load.

Maximum live load deflection will be obtained when live load acts on the given panel, but not on adjacent panels, i.e., in a checkerboard pattern. Therefore, live load deflection should be based on the maximum positive moments found corresponding to that loading arrangement, together with statically consistent negative moments at the supported edges. This will be illustrated for the slab in Fig. 2.9a, considering the middle strip of unit width in the long direction of the panel. The variation of moment for a uniformly distributed load is parabolic, and the sum of the positive and average negative moments must be

$$M = \frac{1}{8} w_b l_b^2 \quad (2.19)$$

where, w_b is the fractional part of the load transmitted in the long direction of the panel (Fig. 2.9c). The fully fixity were obtained at the supports, the negative moment would be

$$M_{neg} = \frac{1}{12} w_b l_b^2 = \frac{2}{3} M \quad (2.20)$$

and the positive moment would be

$$M_{pos} = \frac{1}{24} w_b l_b^2 = \frac{1}{3} M \quad (2.21)$$

The coefficients for maximum live load positive moments were derived assuming 50 percent, not 100 percent fixity. The zero moment baselines associated with the maximum positive moment M_b as obtained, shown in Fig. 2.9c, and the statically consistent negative moments are one-half the positive moment M_b .

Deflection calculations are thus based on the parabolic moment diagram, with maximum ordinate M_b at midspan and negative end moments one-half of that value. The midspan live load deflection, Δ_l , of the slab strip shown in Fig. 2.9b, can be found based on the moment diagram of Fig. 2.9c. For the slab with both edges continuous,

$$\Delta_l = \frac{3}{32} \frac{M_b l_b^2}{E_c I_{eff}} \quad (2.21)$$

where, M_b = Maximum live load positive moment

E_c = Elastic modulus of the concrete

I_{eff} = Effective moment of inertia of the concrete cross section of unit width

Δ_l = Mid span live load deflection

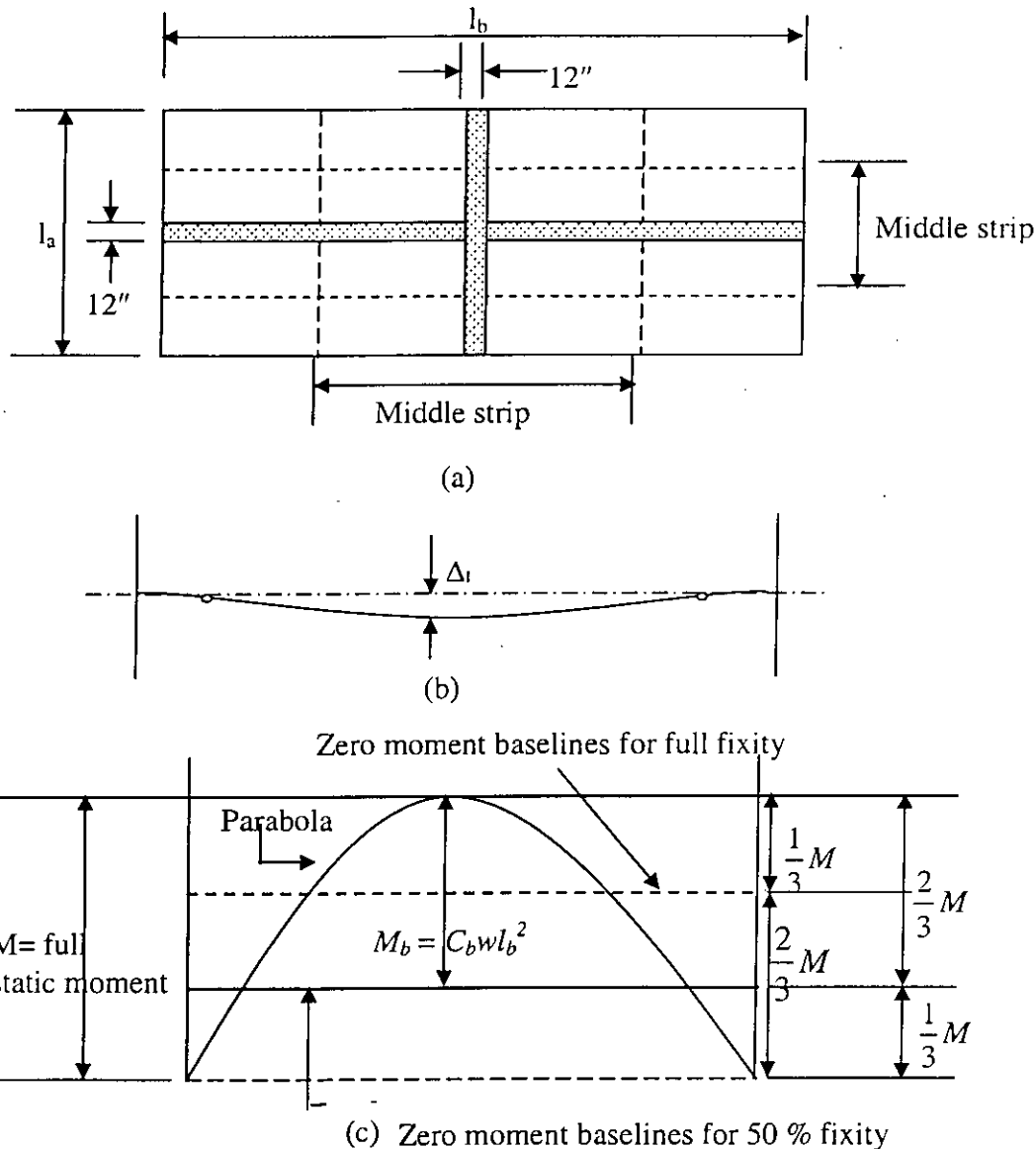


Figure 2.9 Live load deflection analysis: (a) plan of slab; (b) deflection curve for unit strip; (c) diagram for maximum positive live load moment

According to the coefficient method of moment analysis, negative moments at discontinuous slab edges are assumed equal to one third of positive moment in the same direction. The above equation (Eq.2.225) used for panel strips with one or both ends discontinuous, but monolithic with supporting beam. For the special case of slab where edges are completely free of restraint, the mid span deflection is

$$\Delta_l = \frac{5}{48} \frac{M_b l_b^2}{E_c I_{eff}} \quad (2.23)$$

The dead load deflection is based on the moment diagram found using maximum dead load positive moment assuming all panels are loaded. The mid span dead load deflection Δ_d , for both ends continuous, is

$$\Delta_d = \frac{1}{16} \frac{M_b I_b^2}{E_c I_{eff}} \quad (2.24)$$

where, M_b is the dead load positive moment. For the special case where both ends are free of restraint, the midspan dead load deflection is

$$\Delta_d = \frac{5}{48} \frac{M_b l_b^2}{E_c I_{eff}} \quad (2.25)$$

The resulting deflections at the center of the panel will be same in the short and long direction of the panel.

2.8.3 Hossain's model

Hossain (1999) has developed a nonlinear finite element (NLFE) module to calculate the deflection of reinforced concrete slabs, which is based on a global plate stiffness approach. The program is novel since it incorporates an incremental approach to calculate deflections due to a time-varying load. The global plate stiffness approach was adopted, rather than the more complex and time-consuming layered element approach, since work by others including Polak (1996) suggests that the accuracy of both methods is comparable. The global plate stiffness approach has the added benefit of being consistent with the methods given in MC90 (1990) and EC2 (1992) for calculating the curvature of cracked sections. This model with ACI/Branson equation is used in the current work and will be discussed in detail in Chapter 3.

2.9 LONG-TERM DEFLECTION

Initial deflections are increased significantly if loads are sustained over a long period of time, due to the effects of shrinkage and creep. These two effects are usually combined in deflection calculation. Creep generally dominates, but for some types of members, shrinkage deflections are large and should be considered separately. Creep deformations are directly proportional to the compressive stress up to and beyond the usual service load range. They increase asymptotically with time and, for the same stress, are larger for low-strength than for high-strength concretes.

Long-term deflection due to creep and shrinkage are influenced by many variables, including load intensity, mix components mix proportions, age of slab at first loading, curing conditions, presence of compressive reinforcement, relative humidity, and temperature. While time-dependent deflection of slabs has not been studied extensively, it is generally known that time-dependent deflections may be about two to three times initial elastic deflections (Yu and Winter, 1960), and often result in unsatisfactory service load performance. Time-depended deflection of a reinforced concrete beam in flexure at any time, t , is given by

$$\Delta(t, t_0) = \underbrace{\Delta_D(0) + \Delta_L(0)}_{\substack{\text{short-term} \\ \text{deflection} \\ \text{dead} \\ \text{load}}} + \underbrace{\Delta_D^c(t, t_0) + \Delta_L^c(t, t_0)}_{\substack{\text{time-dependent} \\ \text{deflection} \\ \text{creep deflection} \\ \text{due to} \\ \text{dead load, and} \\ \text{sustained live load}}} + \underbrace{\Delta^s(t, t_0)}_{\substack{\text{warping} \\ \text{due to} \\ \text{shrinkage}}}$$
 (2.26)

The ultimate deflection with respect to time is obtained by substituting ultimate values of creep and shrinkage into the time-dependent terms.

2.9.1 Long Term Deflection Multiplier

Deflection estimation procedure in ACI Code (2002) is simple where long-term deflections are calculated from instantaneous deflection by using multiplier. ACI Code specifies that additional long-term deflections Δ_i due to combined effects of creep and shrinkage shall be calculated by multiplying the immediate deflection Δ_i by the factor

$$\lambda = \frac{\xi}{1 + 50\rho'} \quad (2.27)$$

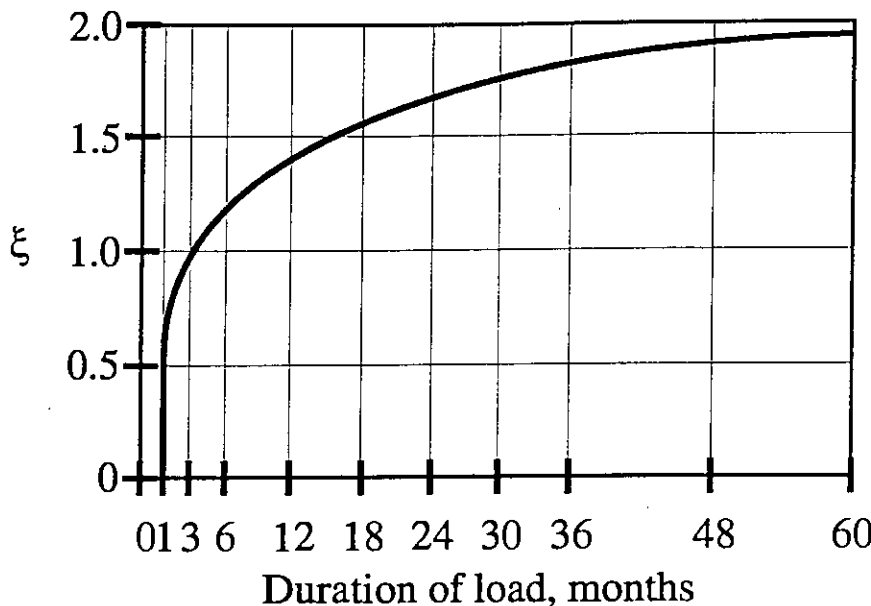


Figure 2.10 Multiplier for long term deflection (Adapted from ACI Code 2002)

where, $\rho' = \frac{A'_s}{bd}$ and ξ is a time-dependent coefficient that varies from 0.0 to 2.0 as

shown in Fig 2.10. In Eqn. (2.26) the quantity $\frac{1}{(1+50\rho')}$ is a reduction factor that is

essentially a section property, reflecting the beneficial effect of compression reinforcement A'_s in reducing long-term deflections, whereas ξ is a material property depending on creep and shrinkage characteristics. For simple and continuous span, the value of ρ' used in Eqn. (2.27) should be that at the mid section, according to the ACI Code, or that at the support for cantilevers.

Values of ξ given in the ACI Code and Commentary are satisfactory for ordinary beams and one-way slabs, but many result in underestimation of time-dependent deflections of two-way slabs, for which Branson (1977) has suggested a five-year value of $\xi=3.0$.

Based on long term test conducted at Cornell University (1984), plus correlation with results of six other experimental programs, the following modified is recommended:

$$\lambda = \frac{\mu\xi}{1+50\mu\rho'} \quad (2.28)$$

in which, $\mu = 1.4 - f'_c/10,000$; $0.4 \leq \mu \leq 1.0$

2.10 RESTRAINT CRACKING

In two-way reinforced concrete slabs built monolithically with supporting column and wall elements, in plane shortening due to shrinkage and thermal effects is restraint. The restraint is provided by a combination of factors, including embedded reinforcement, attachment to structural supports, and lower shrinkage rates of previously placed adjacent panels when slab panels are placed at different times. Nonlinear distribution of free shrinkage strains across the cross-section may also be a contributing factor.

Service load moments in two-way slabs are often of the same order of magnitude as the code-specified cracking moment, M_{cr} . Deflection calculations made using the code-specified modulus of rupture will often result in an uncracked section being used while cracking may actually be present due to a combination of flexural stress and restraint stress.

ACI 318-02 specifies the modulus of rupture for deflection calculations as $0.62\sqrt{f'_c}$ MPa ($7.5\sqrt{f'_c}$ psi). Laboratory test data, summarized in ACI 209R, indicate values ranging from 0.5 to $1.0\sqrt{f'_c}$ MPa (6 to $12\sqrt{f'_c}$ psi).

For slab sections with low reinforcement ratios, approaching minimum reinforcement, the difference between cracked and uncracked flexural stiffness is significant. It is important; therefore, to account for effects of any restraint cracking that may be present. Unfortunately, the extent of restraint cracking is difficult to predict. To account for restraint cracking in two-way slabs, Rangan (1976) suggested that column strip deflections be based on $(I_g + I_{cr})/2$. Good agreement was reported between calculated and filed measured deflections.

A more general approach was proposed by Scanlon and Murray (1982). They suggested that the effect of restrain cracking be included by introducing a restraint stress, f_{res} , that effectively reduces the modulus of rupture for calculating M_{cr} , i.e.

$$M_{cr} = \frac{f_e I_g}{y_t} \quad (2.29)$$

where, $f_e = f_r - f_{res}$

A value of $0.33\sqrt{f'_c}$ MPa ($4\sqrt{f'_c}$ psi), or about half of the value specified in ACI 318, was proposed for reduced effective modulus of rupture. This approach was investigated by Tam and Scanlon (1986) and has produced good correlation between calculated deflection and reported mean field-measured deflections [Jokinen and Scanlon 1985; Graham and Scanlon 1986 (b)]. Ghali (1989) has also used the idea of reduced modulus of rupture and demonstrates the calculation of restraint stress due to reinforcement in the presence of uniform shrinkage.

An additional consideration is that the moments used in design for strength are based on some redistribution of moments. The distribution of design moments does not reflect the high peaks of moment adjacent to columns that occur in uncracked slabs. Deflection calculations based on moment distributions used for design, therefore, tend to under-predict the effects of cracking. For slab system in which significant restraint to in-plane deformations may be present, it is recommended by ACI Committee 435 (1991) that a reduced effective modulus of $0.33\sqrt{f'_c}$ MPa ($4\sqrt{f'_c}$ psi) be used to compute the effective moment of inertia, I_e . A procedure for implementing this approach in finite element analysis is given by Tam and Scanlon (1986).

2.11 CONTROL OF DEFLECTION

Excessive deflections can lead to cracking of supporting walls and partitions, ill fitting of doors and windows, poor roof drainage, misalignment of sensitive machinery and equipment, or visually offensive sag. It is important to maintain control of deflections, so that members designed mainly for strength at prescribed overloads will also perform well in normal service.

In the past, deflection was achieved indirectly, by limiting service load stress in concrete and steel to conservatively low values. The resulting members were generally larger, and consequently stiffer, than those designed by current methods based on strength. In addition, stronger materials are now in general use, and this, too, tends to produce members of smaller cross section that are less stiff than before. Because of these changes in conditions of practice, deflection control is increasingly important.

There are presently two approaches. The first is direct and consist in setting suitable upper limits on the span-depth ratio. This is simple, and it is satisfactory in many cases where spans, load and load distributions, and member sizes and proportions fall in the usual ranges. Otherwise, it is essential to calculate deflections and to compare those predicted values with specific limitations that may be imposed by codes or by special requirements.

It will become clear, in the section that follow, that calculations can, at best, provide a guide to probable actual deflections. This is so because of uncertainties regarding material properties, effects of cracking, and load history for the member under consideration. The deflections of concern are generally those that occur during the normal service life of the member. In service, a member sustains the full dead load, plus some fraction or all of the specified service live load. Safety provision of the ACI Code and similar design specifications ensure that, under loads up to the full service load, stresses in both steel and concrete remain within the elastic ranges.

2.11.1 ACI Code provisions for deflection control

The direct approach of deflection control is providing the minimum slab thickness of two-way edge supported slab and the limitations have given satisfactory results. ACI Code (2002) contains three equations governing minimum slab thickness. These equations account for the relative stiffness of slabs and edge beams, the ratio of long to short panel side dimensions, and conditions of restraint along the edges.

ACI Code (2002) thickness: slab with beams on all sides

The parameter used to defined relative stiffness of the beam and slab spanning in the either direction is α . Then α_m is defined as the average value of α for all beams on the edges of a given panel. The relative stiffness α of the beam and slab spanning in either direction

$$\alpha = \frac{E_{cb} I_b}{E_{cs} I_s} \quad (2.30)$$

in which E_{cb} and E_{cs} are the moduli of elasticity of the beam and slab concrete (usually the same) and I_b and I_s are the moment of inertia of the effective beam and

the slab. Subscripted parameters α_1 and α_2 are used to identify α computed for the computation of l_1 and l_2 respectively.

According to ACI code (2002), for α_m equal to or less than 0.2, the minimum thickness of Table 2.2 shall apply.

For α_m greater than 0.2 but not greater than 2.0, the slab thickness must not be less than

$$h = \frac{l_n(0.8 + f_y / 200,000)}{36 + 5\beta(\alpha_m - 0.2)} \quad (2.31)$$

and not less than 5.0 in

For α_m greater than 2.0, the thickness must not be less than

$$h = \frac{l_n(0.8 + f_y / 200,000)}{36 + 9\beta} \quad (2.32)$$

and not less than 3.5 in.

where l_n = clear span in the long direction, in.

α_m = average value of α for all beams on edges of a panel

β = ratio of clear span in the long direction to clear span in the short direction

Table 2.2 Minimum thickness of slabs without interior beams (ACI 2002)

Yield stress f_y , Psi	Without drop panels			With drop panels		
	Exterior panels		Interior panels	Exterior panels		Interior panels
	Without edge beams	With edge beams		Without edge beams	With edge beams	
40,000	$l_n/33$	$l_n/36$	$l_n/36$	$l_n/36$	$l_n/40$	$l_n/40$
60,000	$l_n/30$	$l_n/33$	$l_n/33$	$l_n/33$	$l_n/36$	$l_n/36$
75,000	$l_n/28$	$l_n/31$	$l_n/31$	$l_n/31$	$l_n/34$	$l_n/34$

2.12 PERMISSIBLE DEFLECTION

To ensure the satisfactory performance in service, ACI Code (2002) imposes certain limits on calculated deflections. These limits are given in Table 2.3. Limits depend on whether or not the member supports or is attached to other nonstructural elements, and whether or not those nonstructural elements are likely to be damaged by large deflections. When long-term deflections are computed, that part of the deflection that occurs before attachment of the non-structural elements may be deducted. The last two limits of Table 2.2 may be exceeded under certain conditions, according to the ACI Code.

Table 2.3 Maximum allowable computed deflections (ACI 2002)

Types of member	Deflection to be considered	Deflection limitations
Flats roofs not supporting or attached to non structural elements likely to be damaged by large deflections	Immediate deflection due to live load L	$\frac{l}{180}$
Floors not supporting or attached to nonstructural elements likely to be damaged by large deflections	Immediate deflection due to live load L	$\frac{l}{360}$
Roof or floor construction supporting or attached to nonstructural element likely to be damaged by large deflections.	The part of the total deflection which occurs after attachment of the nonstructural elements, the sum of long-time deflection due to all sustained loads, and the immediate deflection due to any additional live load	$\frac{l}{480}$
Roof or floor construction supporting or attached to nonstructural elements not likely to be damaged by large deflections		$\frac{l}{240}$

2.13 ARTIFICIAL NEURAL NETWORK

2.13.1 Introduction to artificial neural network

An Artificial Neural Network (ANN) is an information processing paradigm that is inspired by the way biological nervous systems, such as the brain, process information. The key element of this paradigm is the novel structure of the information processing system. It is composed of a large number of highly interconnected processing elements (neurons) working in union to solve specific problems. Neural networks "learn" from examples, just like children learn to recognize dogs from examples of dogs, and exhibit some structural capability for generalization. An ANN is configured for a specific application, such as pattern recognition or data classification, through a learning process. Learning in biological systems involves adjustments to the synaptic connections that exist between the neurons.

Neural networks normally have great potential for parallelism, since the computations of the components are independent of each other. Neural networks are a form of multiprocessor computer system, with

- simple processing elements
- a high degree of interconnection
- simple scalar messages
- adaptive interaction between elements

A biological neuron may have as many as 10,000 different inputs, and may send its output (the presence or absence of a short-duration spike) to many other neurons. Neurons are wired up in a 3-dimensional pattern. Real brains, however, are orders of magnitude more complex than any artificial neural network so far considered.

2.13.2 Artificial neural networks

Artificial neural networks are relatively crude electronic networks of "neurons" based on the neural structure of the brain (Goharian and Grossman, 2003). They process records one at a time, and "learn" by comparing their classification of the record (which, at the outset, is largely arbitrary) with the known actual classification of the record. The errors from the initial classification of the first record is fed back into the

network, and used to modify the networks algorithm the second time around, and so on for much iteration.

The commonest type of artificial neural network consists of three groups, or layers, of units: a layer of "input" units is connected to a layer of "hidden" units, which is connected to a layer of "output" units. (see Fig. 2.11). The activity of the input units represents the raw information that is fed into the network. The activity of each hidden unit is determined by the activities of the input units and the weights on the connections between the input and the hidden units. The behavior of the output units depends on the activity of the hidden units and the weights between the hidden and output units.

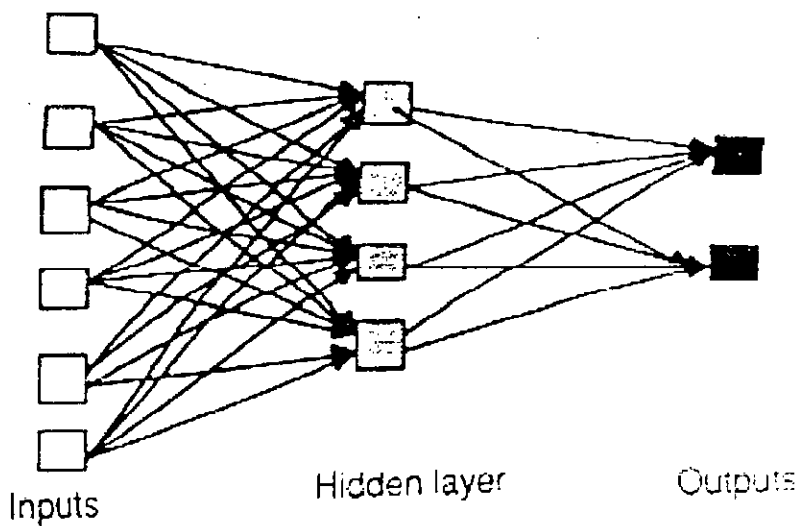


Figure 2.11 An example of a simple feed forward network

Artificial neural networks are biologically inspired in the sense that neural network configurations and algorithms are usually constructed with the natural counterpart in mind (Patodi, 2001). The tremendous processing power of human brain is basically the result of the massively parallel processing units called neurons. A human brain functions with hundreds of thousands of such biological neurons, which are interconnected by a highly complex network. Every neuron consists of a cell body, axon and dendrites. Dendrites extend from the cell body to the other neurons where they receive signals at a connection point called the synapse. These inputs are communicated to cell body where all such inputs are essentially summed up. If the

resulting sum exceeds a specified threshold value, the cell fires and a signal is sent down the axon. Using this model, an artificial neuron is developed which performs the basic characteristics of the biological neuron.

ANNs consist of small processing units called nodes, which operate in parallel, and these nodes are densely interconnected by elements called weights. The information to be stored is fed at the input and small values are assigned to the weights. The weights are modified until the output of the network is satisfactory. The artificial neurons can be arranged in a network in a variety of ways by changing the type of connectivity, the number of neurons and the number of layers. In a multi layer arrangement, the input and the output layers are separated by a number of hidden layers. A multi layer feed forward network can map even complicated relationships between the input and the desired output.

2.13.3 Structures of neural network

A neural network comprises the **neuron** and weight building blocks (Stephen Wolfram, 2002). The behavior of the network depends largely on the interaction between these building blocks. There are three types of neuron layers: input, hidden and output layers. Two layers of neuron communicate via a weight connection network. There are four types of weighted connections: feed forward, feedback, lateral, and time-delayed connections, as shown in the Fig.2.12.

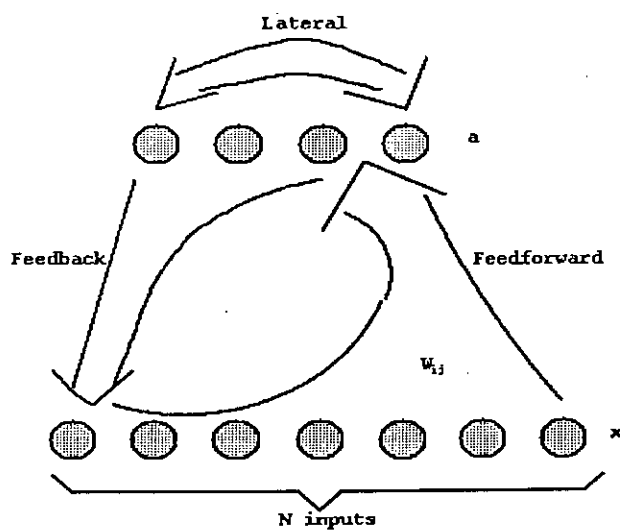


Figure 2.12 Structure of weight connection

1. *Feed forward connections*: For all the neural models, data from neurons of a lower layer are propagated forward to neurons of an upper layer via feed forward connections networks.
2. *Feedback Connections*: Feedback networks bring data from neurons of an upper layer back to neurons of a lower layer.
3. *Lateral Connections*: One typical example of a lateral network is the winners-takes-all circuit, which serves the important role of selecting the winner. In the feature map example, by allowing neurons to interact via the lateral network, a certain topological ordering relationship can be preserved. Another example is the *lateral orthogonalization network*, which forces the network to extract orthogonal components.
4. *Time-delayed Connections*: Delay elements may be incorporated into the connections to yield temporal dynamics models. They are more suitable for temporal pattern recognitions.

The synaptic connections may be fully or locally interconnected. Also, a neural network may be either a single layer feedback model or a multiplayer feed-forward model. It is possible to cascade several single layer feedback neural nets to form a larger net.

2.13.4 The iterative learning process of ANN

A key feature of neural networks is an iterative learning process in which data cases (rows) are presented to the network one at a time, and the weights associated with the input values are adjusted each time (Goharian and Grossman, 2003). After all cases are presented, the process often starts over again. During this learning phase, the network learns by adjusting the weights so as to be able to predict the correct class level of input samples. Neural network learning is also referred to as "connectionist learning," due to connections between the units. Advantages of neural networks include their high tolerance to noisy data, as well as their ability to classify patterns on which they have not been trained. The most popular neural network algorithm is back-propagation algorithm proposed in the 1980's. Once a network has been structured for a particular application, that network is ready to be trained. To start

this process, the initial weights are chosen randomly. Then the training, or learning, begins.

The network processes the records in the training data one at a time, using the weights and functions in the hidden layers, and then compares the resulting outputs against the desired outputs. Errors are then propagated back through the system, causing the system to adjust the weights for application to the next record to be processed. This process occurs over and over as the weights are continually tweaked. During the training of a network the same set of data is processed many times as the connection weights are continually refined.

Note that some networks never learn. This could be because the input data do not contain the specific information from which the desired output is derived. Networks also don't converge if there is not enough data to enable complete learning. Ideally, there should be enough data so that part of the data can be held back as a validation set.

The number of layers and the number of processing elements per layer are important decisions. These parameters to a feed forward, back-propagation topology are also the most ethereal - they are the "art" of the network designer. There is no quantifiable, best answer to the layout of the network for any particular application. There are only general rules picked up over time and followed by most researchers and engineers applying this architecture to their problems.

Rule One: As the complexity in the relationship between the input data and the desired output increases, the number of the processing elements in the hidden layer should also increase.

Rule Two: If the process being modeled is separable into multiple stages, then additional hidden layer(s) may be required. If the process is not separable into stages, then additional layers may simply enable memorization of the training set, and not a true general solution effective with other data.

Rule Three: The amount of training data available sets an upper bound for the number of processing elements in the hidden layer(s). To calculate this upper bound, use the number of cases in the training data set and divide that number by the sum of the number of nodes in the input and output layers in the network. Then divide that result again by a scaling factor between five and ten. Larger scaling factors are used for relatively less noisy data. If you use too many artificial neurons the training set will be memorized. If that happens, generalization of the data will not occur, making the network useless on new data sets.

2.13.5 Feed forward back-propagation

It is an abbreviation for 'back propagation of error', which is the most widely used learning method for neural networks today. It has pretty much success on practical applications and is relatively easy to apply (Goharian and Grossman, 2003). It is for the training of layered (i.e., nodes are grouped in layers) feed forward (i.e., the arcs joining nodes are unidirectional, and there are no cycles) nets.

Back-propagation needs a teacher that knows the correct output for any input ("supervised learning") and uses gradient descent on the error (as provided by the teacher) to train the weights. The activation function is (usually) a sigmoidal (i.e., bounded above and below, but differentiable) function of a weighted sum of the nodes inputs. The use of a gradient descent algorithm to train its weights makes it slow to train; but being a feed forward algorithm, it is quite rapid during the recall phase.

The feed forward, back-propagation architecture was developed in the early 1970's by several independent sources. This independent co-development was the result of a proliferation of articles and talks at various conferences, which stimulated the entire industry. Currently, this synergistically developed back-propagation architecture is the most popular, effective, and easy-to-learn model for complex, multi-layered networks. Its greatest strength is in non-linear solutions to ill-defined problems. The typical back-propagation network has an input layer, an output layer, and at least one hidden layer. There is no theoretical limit on the number of hidden layers but typically there are just one or two. Some work has been done which indicates that a

maximum of five layers (one input layer, three hidden layers and an output layer) are required to solve problems of any complexity. Each layer is fully connected to the succeeding layer.

As noted above, the training process normally uses some variant of the Delta Rule, which starts with the calculated difference between the actual outputs and the desired outputs. Using this error, connection weights are increased in proportion to the error times a scaling factor for global accuracy. Doing this for an individual node means that the inputs, the output, and the desired output all have to be present at the same processing element. The complex part of this learning mechanism is for the system to determine which input contributed the most to an incorrect output and how does that element get changed to correct the error. An inactive node would not contribute to the error and would have no need to change its weights. To solve this problem, training inputs are applied to the input layer of the network, and desired outputs are compared at the output layer. During the learning process, a forward sweep is made through the network, and the output of each element is computed layer by layer. The difference between the output of the final layer and the desired output is back-propagated to the previous layer(s), usually modified by the derivative of the transfer function, and the connection weights are normally adjusted using the Delta Rule. This process proceeds for the previous layer(s) until the input layer is reached.

2.13.6 Use of neural network

Neural networks cannot do anything that cannot be done using traditional computing techniques, but they can do some things, which would otherwise be very difficult. In particular, they can form a model from their training data (or possibly input data) alone (Haykin 1999). This is particularly useful with sensory data, or with data from a complex (e.g. chemical, manufacturing, or commercial) process.

Neural Networks are interesting for quite a lot of very dissimilar people:

- Computer scientists want to find out about the properties of non-symbolic information processing with neural nets and about learning systems in general.

- Engineers of many kinds want to exploit the capabilities of neural networks on many areas (e.g. signal processing) to solve their application problems.
- Cognitive scientists view neural networks as a possible apparatus to describe models of thinking and conscience (High-level brain function).
- Neuro-physiologists use neural networks to describe and explore medium-level brain function (e.g. memory, sensory system, motorics).
- Physicists use neural networks to model phenomena in statistical mechanics and for a lot of other tasks.
- Biologists use Neural Networks to interpret nucleotide sequences.

2.14 CONCLUSION

In this chapter the behavior of column supported slab has been discussed from serviceability point of view. The deflection calculation methods of slab by analytical and numerical approaches have been discussed for elastic and cracked conditions. Long-term deflection calculation using ACI multiplier approaches are presented. Deflection due to creep and shrinkage are explained. Restrained shrinkage cracking, deflection control and permissible deflection are discussed. In this chapter, development and details of Artificial Neural Network (ANN) have been discussed. Structures of Artificial Neural Network, the iterative learning processes are explained. Neural Network models, feed forward and back-propagation techniques have been discussed. Some uses of Neural Network have also been presented.

CHAPTER 3

NONLINEAR FINITE ELEMENT ANALYSIS

3.1 INTRODUCTION

In Chapter 2, different elastic and nonlinear analysis methods of deflection calculation have been discussed. As mentioned before, deflection calculation of slab is a nonlinear problem, even in service load range. Hossain (1999) proposed a secant stiffness based FE module incorporating ACI/Branson's equation in a general-purpose finite element package FE-77(Hitching, 1999). In this chapter, Hossain's(1999) nonlinear FE module is presented for calculation of immediate deflection of slab. The main aim of this chapter is to calculate immediate deflection of some experimental slabs using Hossain's (1999) nonlinear FE module. The chapter starts with explaining the incorporation of Branson's equation in the FE model and then its validation against experimental results.

3.2 INCORPORATION OF BRANSON'S EQUATION

A program module based on global plate stiffness approach has been developed by Hossain (1999) to incorporate the different short and long-term models for predicting deflection of reinforced concrete slabs. The module act as an integral part of the FE package FE-77 (1999) and calculates modified elastic properties to represent cracking, creep and shrinkage for each element on the basis of stresses of FE solution, which are then fed back into the assembly module of the FE package. Hossain and Vollum (2002) found good correlation in the analysis of the real full scale 7 storied building at Cardington using this FE module employing EC2 (1992) and CEB-FIP Model Code 1990 (MC-90, 1990) where creep and shrinkage deflection have been dealt with more rigorously along with the effect of construction load. Deflection estimation procedure in ACI Code (2002) is simpler than these codes where long-term deflections are calculated from instantaneous deflection using multiplier. Branson's crack model (1977) which is also adopted in the ACI Code (2002) has been used in the current work to calculate instantaneous deflection.

Within the FE program, elastic moments in two principal directions for each element are calculated in the first run which is then used to calculate the effective moment of inertia in two principal directions using Branson's (1977) equation:

$$I_{el} = \left(\frac{M_{cr}}{M_1} \right)^3 I_g + \left[1 - \left(\frac{M_{cr}}{M_1} \right)^3 \right] I_{cr1} \quad (3.1)$$

$$I_{e2} = \left(\frac{M_{cr}}{M_2} \right)^3 I_g + \left[1 - \left(\frac{M_{cr}}{M_2} \right)^3 \right] I_{cr2}$$

where, I_g and I_{cr} are the gross and cracked moment of inertia of slab element. M_{cr} is the moment at which cracks occur M_1 and M_2 are the principal moments.

3.3 INCORPORATION OF ACI METHOD

The effective moment of inertia adopted by the ACI Building Code (2002) was discussed in Section 2.8.1. The method uses the ratio of the section cracking moment to the applied moment to interpolate between uncracked and fully cracked states. In the present work, the ratio of modulus of rupture to principal tensile stress at the face of the section i.e. (f_r / σ_1) or (f_r / σ_2) is used instead of (M_{cr} / M) in Eqn. (3.1). The following equations are used to calculate the effective moment of inertia in the major and minor principal directions, respectively:

$$I_{el} = \left(\frac{f_r}{\sigma_1} \right)^3 I_g + \left[1 - \left(\frac{f_r}{\sigma_1} \right)^3 \right] I_{cr1} \quad (3.2)$$

$$I_{e2} = \left(\frac{f_r}{\sigma_2} \right)^3 I_g + \left[1 - \left(\frac{f_r}{\sigma_2} \right)^3 \right] I_{cr2}$$

where σ_1 and σ_2 are the two principal stresses at the surface of slab and I_{cr} is the moment of inertia of the fully cracked transformed section. The depth of neutral axis and the second moment of area fully cracked section are calculated considering both tension and compression steel. The depth of neutral axis of a fully cracked section, considering both tension and compression steel, is given by:

$$c_n = \frac{-a_2 + \sqrt{a_2^2 - 4a_1a_3}}{2a_1} \quad (3.3)$$

where

$$a_1 = b/2$$

$$a_2 = nA_s + (n-1)A_{sp}$$

$$a_3 = -nA_s d - (n-1)A_{sp} d'$$

The second moment of area around the neutral axis is:

$$I_{cr} = \frac{bc_n^3}{3} + nA_s(d - c_n)^2 + (n-1)A_{sp}(d' - c_n)^2 \quad (3.4)$$

The modification factor

For the ACI method, the modification factors, to account for cracking are calculated in the major and minor principal directions:

$$\alpha_n = \frac{I_{cl}}{I_g}$$

$$\alpha_t = \frac{I_{t2}}{I_g} \quad (3.5)$$

where α_n and α_t are the modification factors for major and minor principal directions, respectively.

3.4 FORMATION OF [E] MATRICES

In the FE analysis, initially the 6×6 elasticity matrices for all the elements are defined as anisotropic, so that they can have different values in orthogonal directions. These are then modified for each element using the modification matrices α_n and α_t to incorporate cracking, by using Eqn. (3.5). The modified matrix in the principal directions is thus follows:

$$[E'] = \begin{bmatrix} \frac{\alpha_n E_c}{(1-\alpha_n\alpha_t\nu^2)} & \frac{\alpha_n\nu\alpha_t E_c}{(1-\alpha_n\alpha_t\nu^2)} & 0 \\ \frac{\alpha_t\nu\alpha_n E_c}{(1-\alpha_n\alpha_t\nu^2)} & \frac{\alpha_t E_c}{(1-\alpha_n\alpha_t\nu^2)} & 0 \\ 0 & 0 & \frac{E_c\sqrt{\alpha_n\alpha_t}}{2(1+\nu\sqrt{\alpha_n\alpha_t})} \end{bmatrix} \quad (3.6)$$

These $[E']$ matrices are then transformed into global directions using:

$$[E] = [C_2]' [E'] [C_2] \quad (3.7)$$

where $[C_2]$ are transformation matrices.

A set of $3 \times 3 [E]$ matrices for all the elements are obtained in the global direction. The global $[E]$ matrices are then adjusted so that they can be used in the FE package (Hitchings, 1994). These $[E]$ matrices for all the elements are written in a file, which is subsequently read by the FE package in the next run and it modifies the global stiffness accordingly. As the material elasticity, and hence the structural stiffness is modified, there will be redistribution of stresses. Hossain's module has the capability of continuing until a state of equilibrium between stress redistribution and material properties is reached. However, in the current work, effect of stress redistribution has been ignored and FE analyses are carried out only once with modified elastic properties.

3.5 SEQUENCE OF ANALYSIS

A flow chart describing the incorporation of the ACI / Branson's model is shown in Fig. 3.I. First the analysis is carried out on the slab with gross concrete section (without reinforcement) using QD09 (general shell and plate bending element with nine nodes) elements. The FE solution gives deflections and stress at all nodes. Stresses are calculated in principal directions from x-y directional stresses. Gross moment of inertia I_g and cracked moment of inertia I_{cr} are calculated for two principal directions. Effective moments of inertias are calculated using σ/σ_c ratios in both principals direction. Factors to modify the $[E']$ matrices in the principal directions are calculated comparing effective moment of inertia and corresponding gross moment of inertia. The modified $[E']$ matrixes are then transformed to global x-y direction from principal directions. With the modified set of $[E']$ matrices, the FE package gives the desired solution of stresses and deflections. The incorporation of the ACI model to calculate the effective moment of inertia is presented in section 3.3. Once modification factors are calculated using Eqn. (3.5), modified $[E']$ matrices are formed in the principal directions and then transformed into global x-y directions as described in section 3.4.

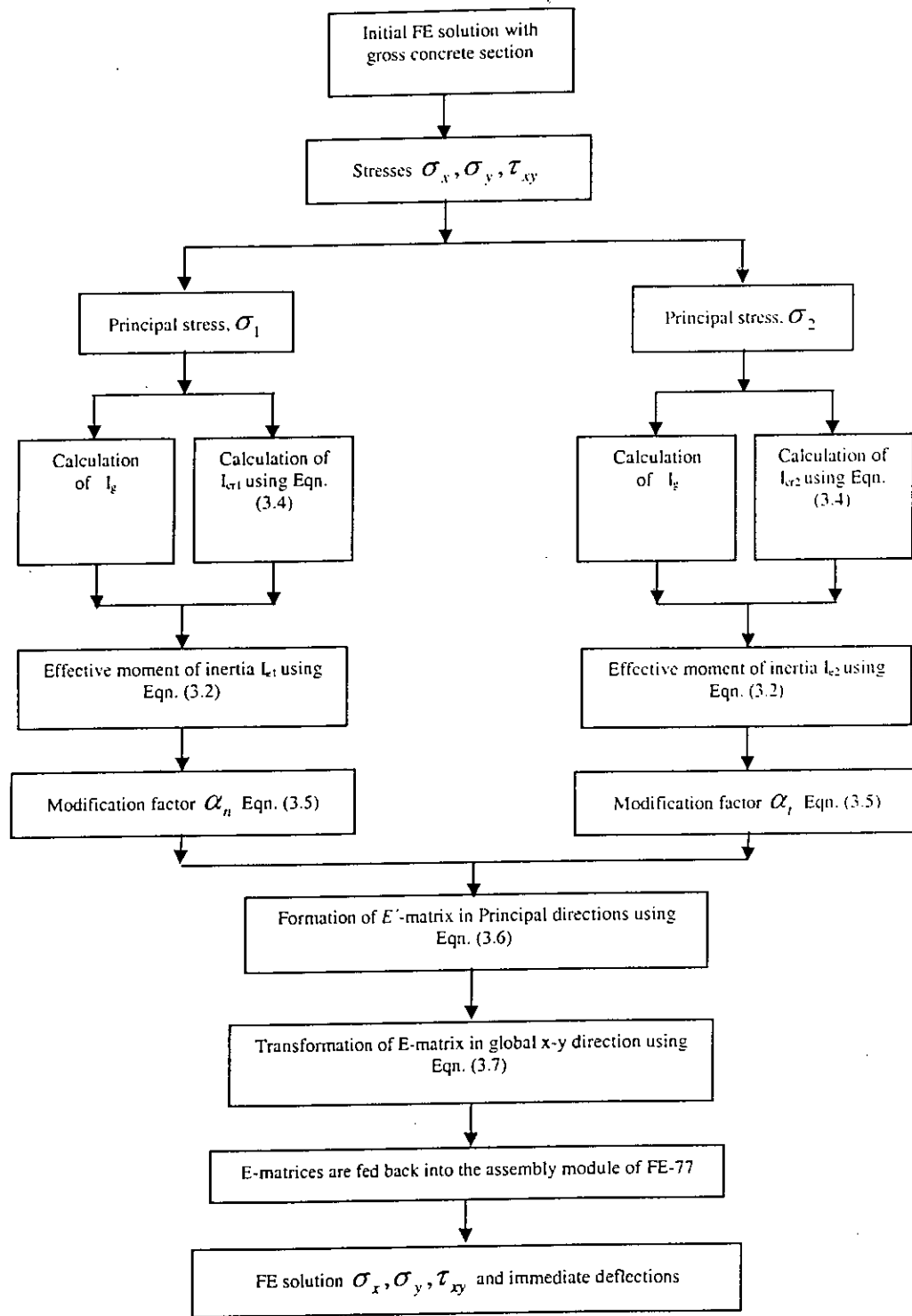


Figure 3.1 Flow chart showing the sequence of calculation

3.6 COMPARISON OF EXPERIMENTAL RESULTS WITH FE ANALYSIS

In this section, FE analysis results are verified with available experimental results. McNeice corner supported slab, McNeice one way slab and Shukla abd Mittal slabs have been analysed for this purpose.

3.6.1 McNeice corner supported slab

McNeice slab (McNeice, 1967) has been widely used as a benchmark of modeling of slabs. It was 914 mm (36 in) square and 44.45 mm (1.75 in.) thick slab and reinforced with an isotropic mesh giving a reinforcement ratio $100A_s/bh = 0.85$. It was supported at four corners and loaded by central point load. All the materials properties and details are taken from Jorfeit & McNeice (1971); as modulus of rupture is not specified; it is assumed to be $0.62\sqrt{f'_c}$ N/mm² ($7.5\sqrt{f'_c}$ psi), according to ACI Code (2002). Details of the material properties, slab dimension, reinforcement and the finite element mesh used in the present analysis are shown in the Fig.3.2.

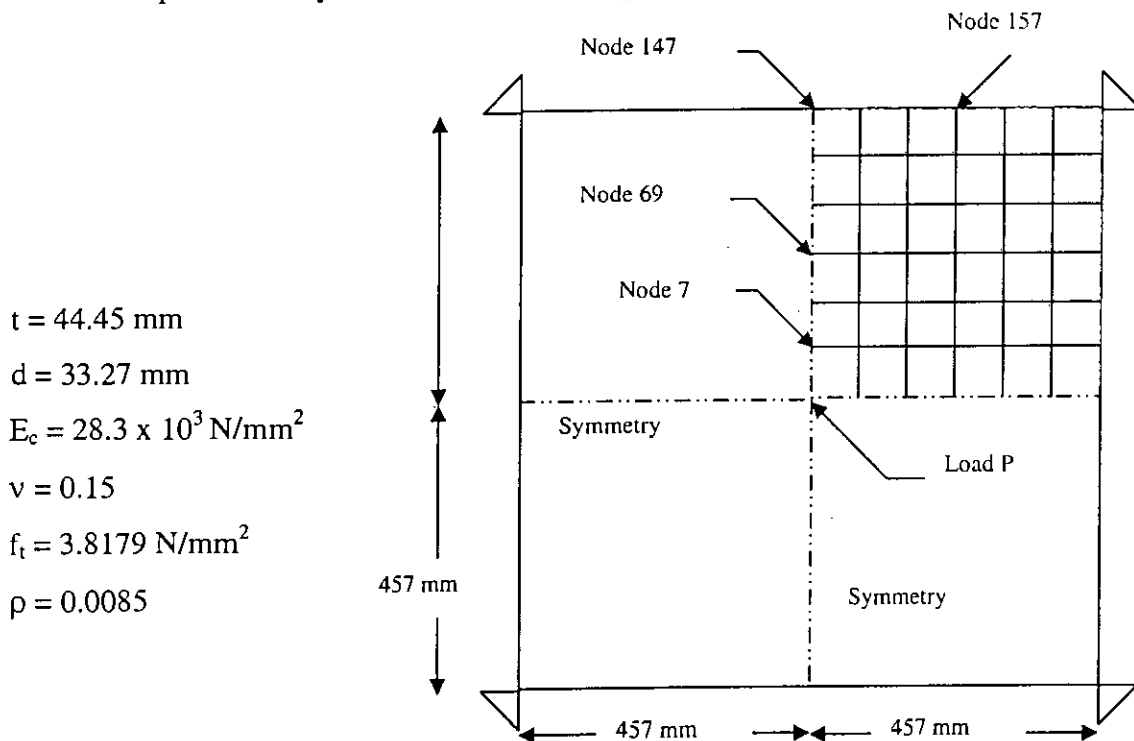


Figure3.2 Details of corner supported slab tested by McNeice: adapted from Jorfeit & McNeice (1971)

Load versus immediate deflections curves for four different nodes (node 7, node 69, node 147 and node 157) of experimental and FE results are presented in Figs 3.3 to 3.6. The FE analysis deflections are similar to the experimental deflection for all four nodes of McNeice corner supported slab.

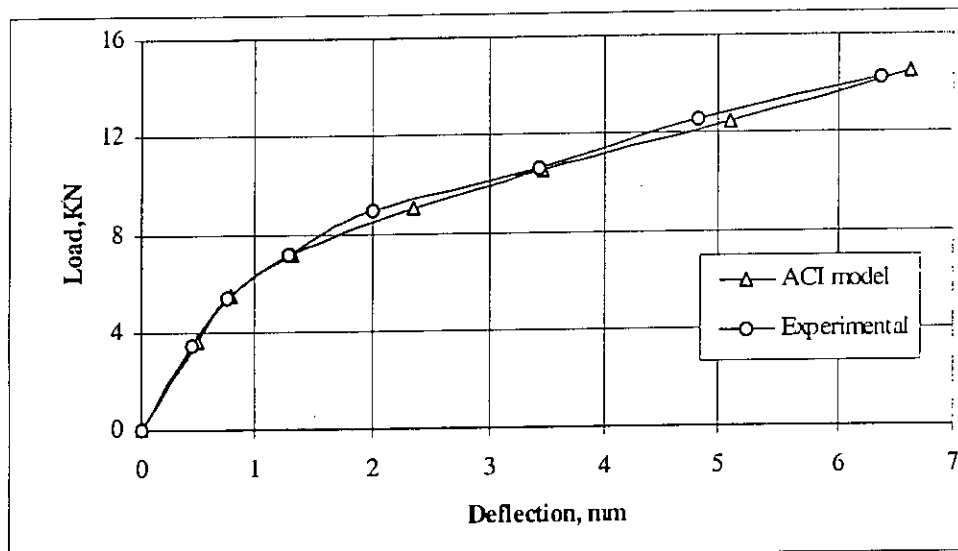


Figure 3.3 Load versus deflection curve for the corner supported slab at Node 7

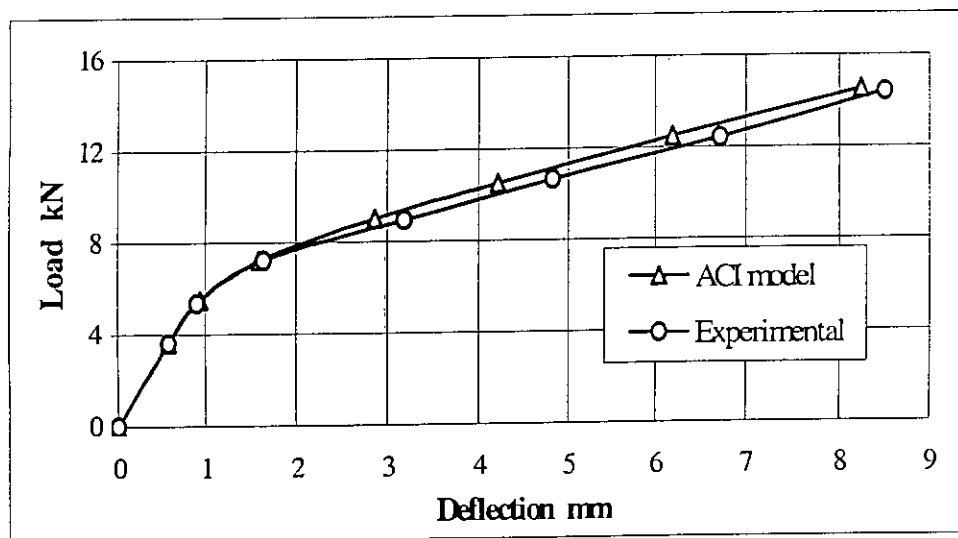


Figure 3.4 Load versus deflection curve for the corner supported slab at Node 69

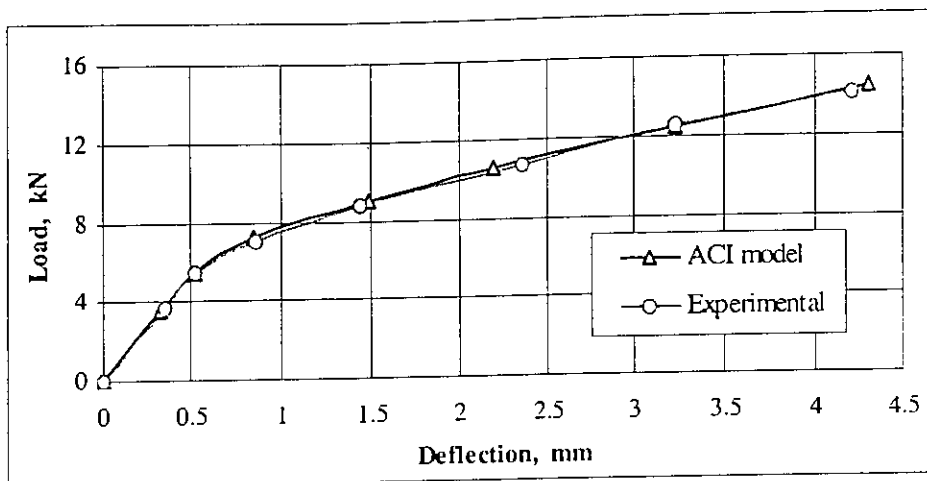


Figure 3.5 Load versus deflection curve for the corner supported slab at Node 147

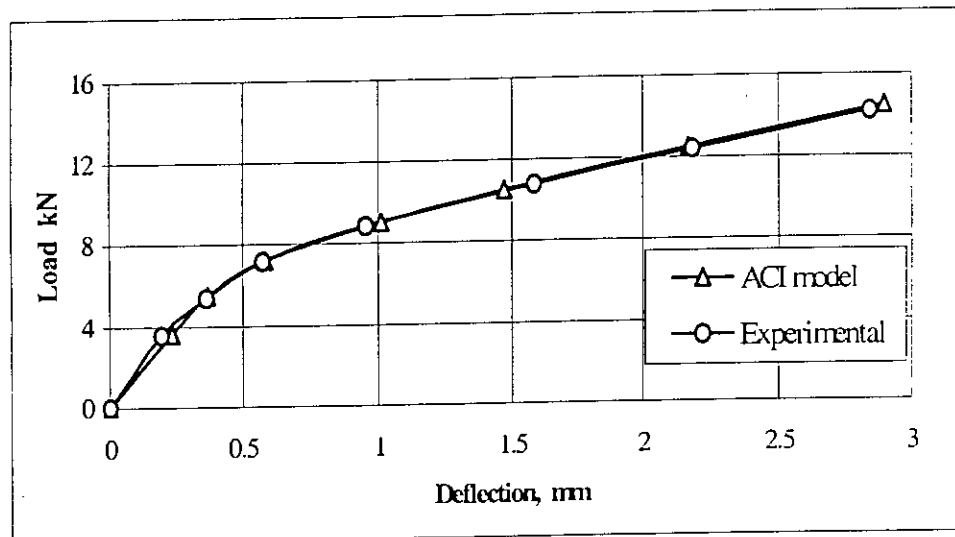


Figure 3.6 Load versus deflection curve for the corner supported slab at Node 157

3.6.2 McNeice one-way slab

A one way slab 304.8 mm wide and 44.5 mm thick, simply supported with a span of 863 mm reinforced with 0.8 percent steel as was tested by McNeice(1967). Details of the material properties and slab dimensions are shown in Fig.3.7. Half the slab was modeled by nonlinear FE analysis. Central deflections have been calculated with FE-analysis employing ACI model and compared with the experimental results shown in Fig.3.8. The FE analysis results have shown good agreement with the experimental results upto lower level of loading.

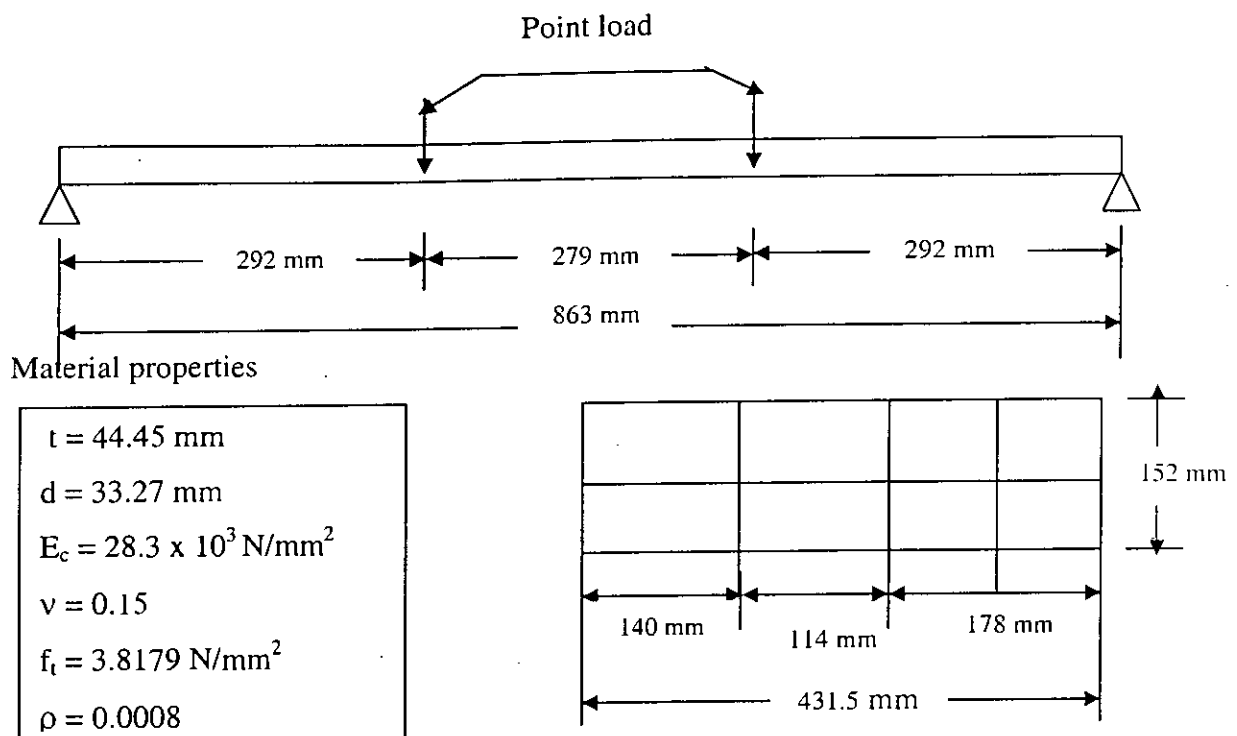


Figure 3.7 Details of simply supported one-way slab tested by McNeice: adapted from Jorfeit & McNeice (1971)

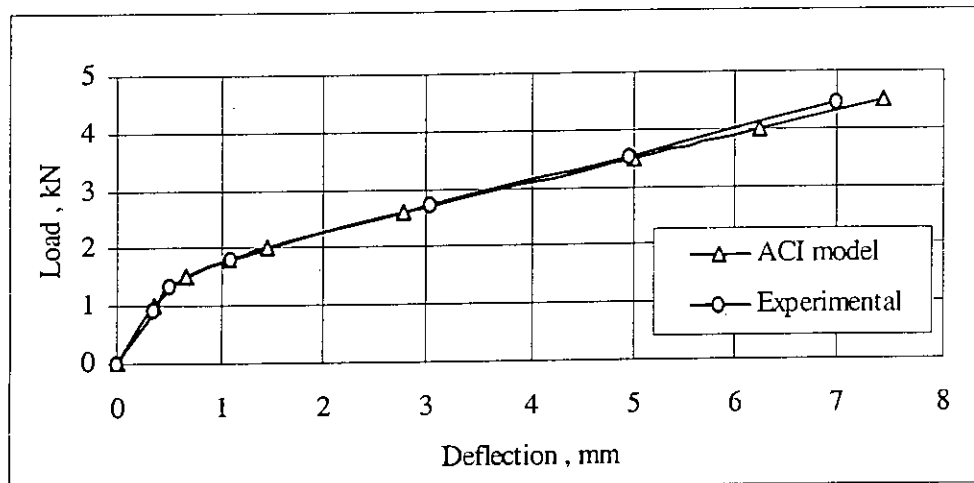


Figure 3.8 Load versus deflection curves for center point of the simply supported one-way slab tested by McNeice

3.6.3 Shukla and Mittal slabs

Shukla and Mittals (1976) carried out a series of tests on two-way edge-supported slabs. All the slabs were 214 cm square and 8 cm thick. The slabs were supported on

reinforced concrete walls with center-to-center span of 183 cm each way. Their corners were held down by means of 40 mm diameter steel rods anchored to the floor. Loads were applied to the test slab in increments of 2 tons each through an inverted waffle-tree system, which transferred load at 16 equidistant point of the slab. Three slabs (S-8, S-11, and S-12) from this series have been analyzed here. S-8 and S-11 were isotropically reinforced with 10 mm bars to provide 5.64 and 4.36 cm²/m steel in each direction respectively. Slab S-12 is reinforced with 10mm and 6 mm bars to make an orthotropic slab with 5.24 and 1.35 cm²/m steel in two directions. The amount of top steel is not specified by the authors and it is assumed to have same amount of steel as bottom layer. Three slabs differ in concrete strength, which were 15.9 (S-8), 22.0 (S-11), 19.1 (S-12) N/mm². Moduli of rupture and elasticity were not reported and hence have been estimated using ACI equations (in N/mm²)

$$E_c = 4733\sqrt{f'_c} \quad (3.9)$$

$$f_r = 0.62\sqrt{f'_c} \quad (3.10)$$

Details of slab dimensions and FE mesh are shown in Fig. 3.9.

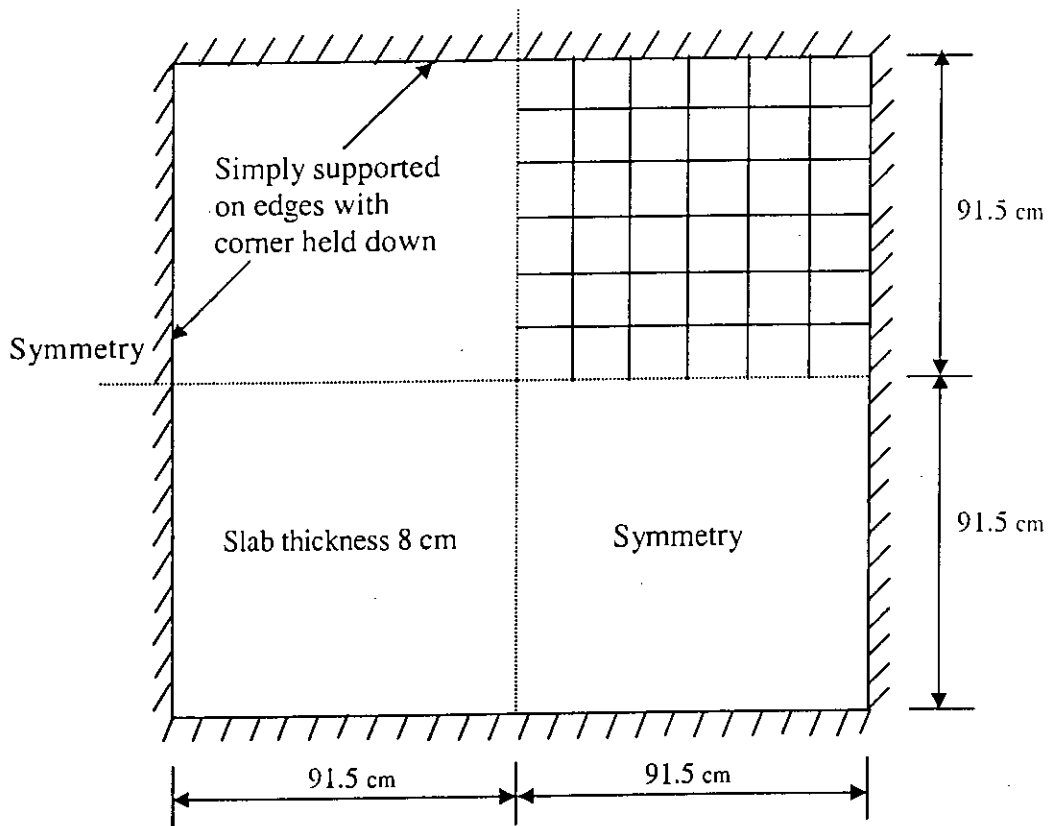


Figure 3.9 Details of edge-supported two-way slabs tested by Shukla and Mittal (1976)

FE deflections along with experimental results for the central nodes of S-8, S-11 and S-12 slabs are presented in Figs. 3.10 to 3.12. The FE results have shown good agreement with experimental deflections for slab S-8. But for slab S-11 and S-12, FE results are higher than the experimental deflection.

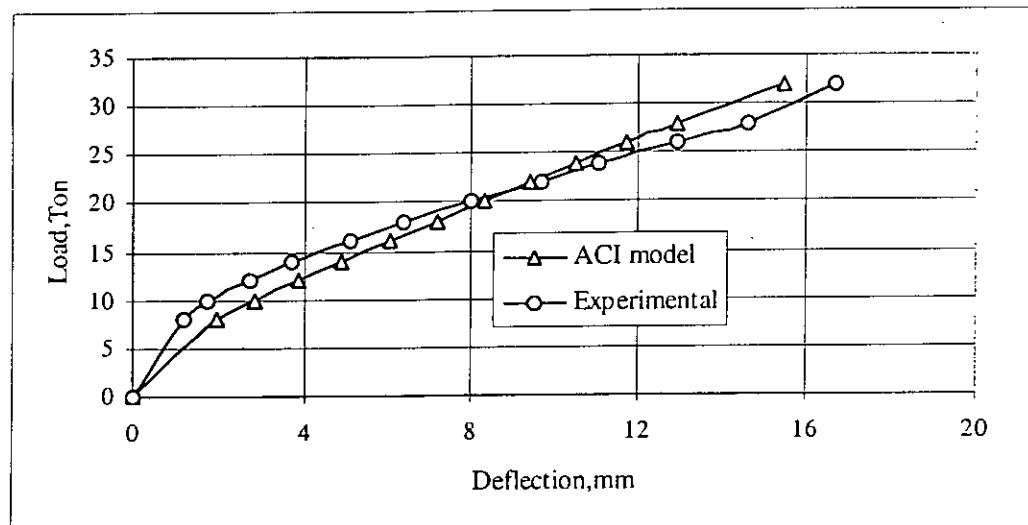


Figure 3.10 Load versus deflections curves for the edge supported Shukla and Mittal slab S-8

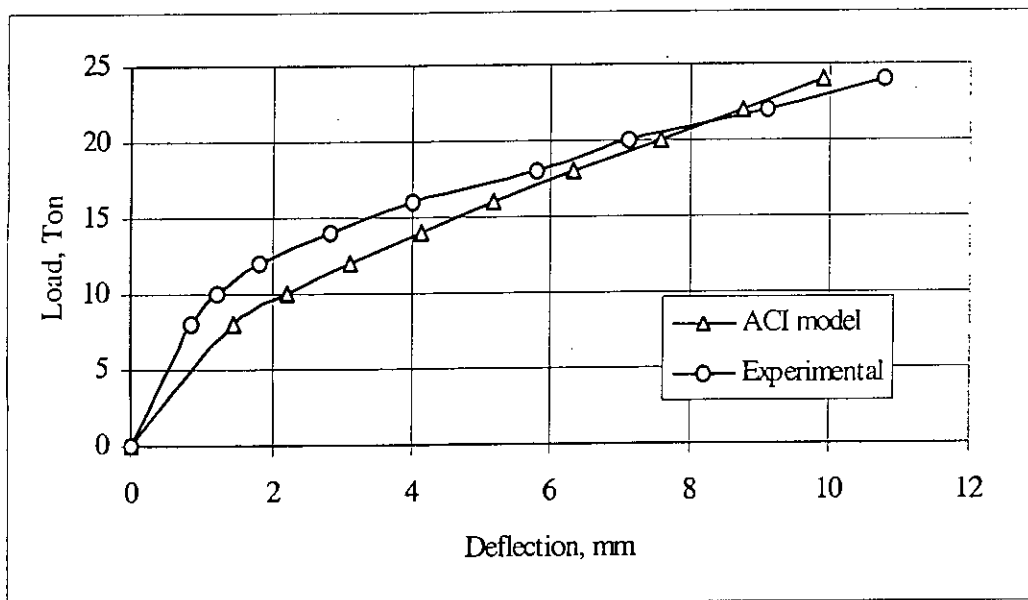


Figure 3.11 Load versus deflections curves for the edge supported Shukla and Mittal slab S-11

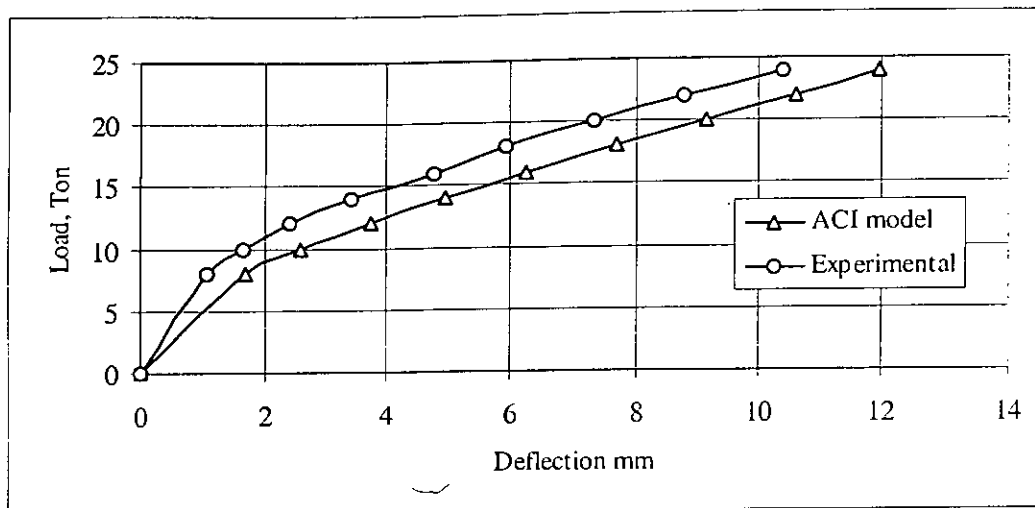


Figure3.12 Load versus deflections curves for the edge supported Shukla and Mittal slab S-12

3.7 CONCLUSION

Deflection calculation by nonlinear FE analysis using Hossain's (1999) module incorporating ACI/Branson crack model has been discussed in this chapter. At first, the incorporation of ACI/Branson crack model into the FE module has been discussed. Then the immediate deflection obtained from non linear FE analysis have been compared with the experimental results of McNeice(1971) corner supported slab, McNeice (1967) one way slab and Shukla and Mittal (1976) edge supported two-way slab. Good correlations have been observed for FE analysis results with experimental results. In the next chapter, the long-term deflection of Cardington slab will be studied using nonlinear FE analysis and ACI multiplier.

CHAPTER 4

LONG-TERM DEFLECTION CALCULATION: CARDINGTON ECBP BUILDING

4.1 INTRODUCTION

In Chapter 3, short-term deflection of reinforced concrete slab has been calculated using Hossain's (1999) nonlinear FE module which incorporates Branson /ACI crack model. The short-term deflection prediction of the different experimental slabs has been validated in Chapter 3. Long-term deflection of concrete slab mainly depends on the effect of creep and shrinkage of concrete. The calculation of long-term deflections of reinforced concrete slabs is a complex problem even in a controlled environment under constant loading. It is more difficult to predict long-term deflections in real buildings because many of the factors (including material properties, position of reinforcement, slab thickness and loading) that influence deflections can only be estimated at the time of design. In addition, there are considerable difficulties in estimating deflections for a realistic load time history. The researchers have been faced with the problem as there is lack of accurate and well-documented data on deflections in real buildings to calibrate their models. In 1998, a seven storied in-situ reinforced concrete building was constructed under European Concrete Building Project (ECBP) at the Cardington Large Building Testing Facilities (Fig. 4.1) to measure the deflection of flat plate slab. Hossain (1999) and Hossain & Vollum(2002) predicted deflection of Cardington slabs correctly using MC-90 approach where the effect of creep and shrinkage were rigorously dealt with. In this current chapter, short-term and long-term deflections of Cardington slab will be calculated using Branson/ACI crack model with ACI long-term multiplier curve and compared with test result.



Figure 4.1: Cardington ECPB building

4.2 Description of the Cardington ECBP Building

The Cardington test building is a seven-storey in-situ reinforced concrete building of flat plate construction. Construction of ECPB building started on January 12, 1998 and was completed on in just 14 weeks. The gird is 7.5 m square and the slab is 250 mm thick. The floor plan and grid for deflection measurements are shown in the Fig. 4.2. The slabs were cast in a single day. The floors were designed by different designers using different methods and also different reinforcement arrangements were adapted. The slabs with different material properties and applied peak loads as adopted from Hossain and Vollum (2002) are shown in the Table 4.1. The deflections of flat slabs in different floors in a typical commercial building over a minimum period of two years were measured. The experimental deflection values were presented in Vollum, Moss and Hossain (2002).

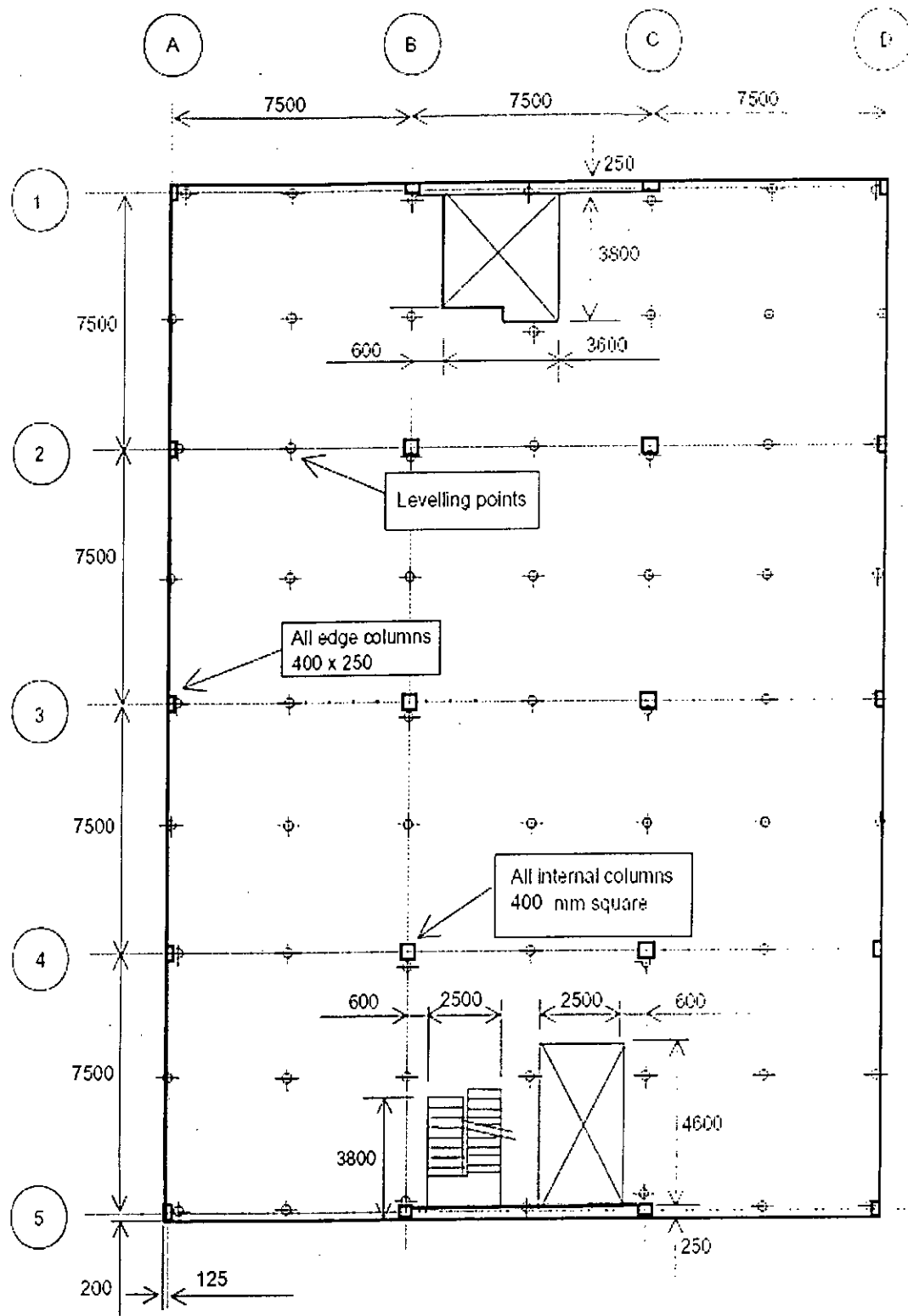


Figure 4.2: Plan of Cardington in situ concrete building and deflection measurement grid
(All dimension in mm) (Adapted from Hossain and Vollum (2002))

4.2.1 Material properties

The specified characteristic concrete cube strength was 37 MPa at all floors but in practice varied between 47 MPa and 55 MPa. A large number of tests were done to establish concrete properties at ages between 1 day and 2 years. The mean material properties during striking and peak loading are presented in Table 4.1.

Table 4.1: Loading and concrete material properties used in the analysis. (Adapted from Hossain and Vollum , 2002)

Slab	Age at			Load Peak kN/m ²	Mean material properties						
	Striking days	Peak load days	Applied load: days		Striking			Peak load			
					f _c : MPa	f _{ct} : Mpa	E: GPa	f _c : MPa	f _{ct} : MPa	E: GPa	
1	2	24	395	8.32	23.67	2.46	24.00	63.60	4.49	33.15	
2	1	13	386	10.34	23.80	2.43	25.50	47.00	3.43	31.70	
3	2	12	393	10.74	24.75	2.68	27.00	45.30	3.62	33.00	
4	2	14	374	10.27	27.63	2.50	29.25	57.00	4.19	35.18	
5	2	13	359	10.73	27.00	2.53	26.25	42.30	3.26	31.35	
6	3	19	337	10.14	18.50	2.00	23.25	33.00	3.06	31.86	

4.2.2 Loading

All the slabs were struck very early (at 2 or 3 days) and subsequently carried their self-weight. The slabs were back-propped before the next slab was cast. The back props were placed in position but not tightened so that the back props were theoretically only loaded when additional loads were applied. As a result, the magnitudes of the construction load were relatively low. One of the main aims of the Cardington project is to determine long-term slab deflections under loading representative of that in an office building. The majority of long-term laboratory tests to measure deflections have been carried out under constant loading in controlled conditions. The loading on a slab is dependent on construction method and building use. Figure 4.3 shows the load history of the third floor in the Cardington in-situ concrete building where the slab experienced a short-term peak load of 10.74 kN/m² at twelve days after casting when the fourth floor was poured. An additional short-term load of 8.75 kN/m² was applied at 27 days when the fifth floor slab was cast. Subsequently dead load of 3 kN/m² was applied at 393 days. The imposed load of

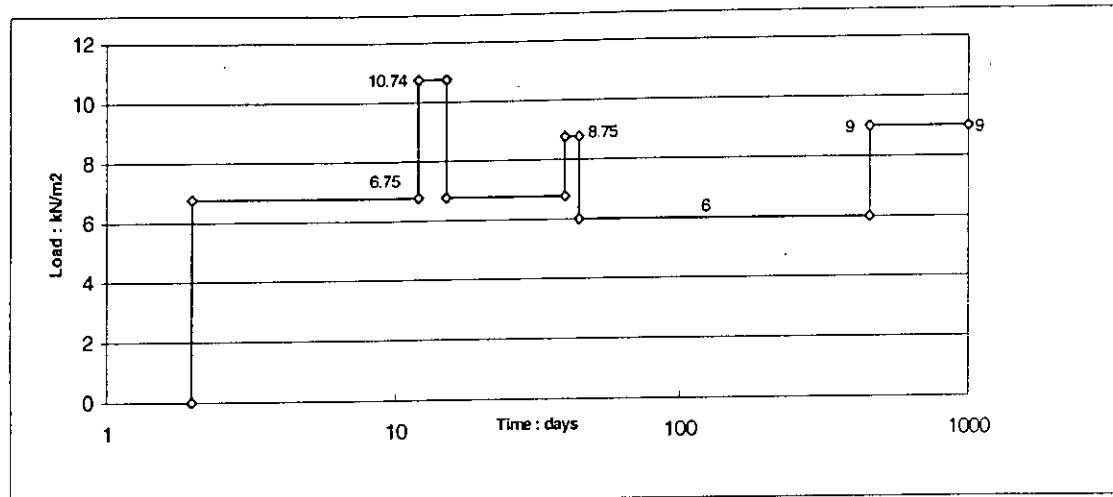


Figure 4.3 Diagrammatic representation of the load history for floor 3 in Cardington building. (Adapted from Hossain and Vollum, 2002)

3kN/m² includes allowances of 1 kN/m² for raised floor, services and ceilings and 1 kN/m² for partitions. Service load were applied with sand bags, on the panels between grid-lines 2 and 4, as shown in Fig. 4.4 at floors 1 to 6. A load of 6.75 kN/m² includes self-weight of slab (6 kN/m²) and weight of formwork (0.75 kN/m²) at striking. Deflections were measured at 60 test points (Fig. 4.4) by precise levelling. The instrument used is a Wild NA2 automatic level with parallel plate micrometer that enables levels to be measured to 0.001 cm.

4.3 FINITE ELEMENT ANALYSIS AND DEFLECTION CALCULATION

Hossain's nonlinear FE module which utilizes Branson/ACI crack model has been used in the current study along with ACI long-term multiplier curve to estimate slab deflections in the Cardington in-situ building. The results are presented in the following sections. Even though the floors are not exactly symmetrical (Fig.. 4.2) due to the presence of different size of holes on each side, they are assumed to be symmetrical so that one quarter of the slab can be considered in the analysis (Fig. 4.5). The slabs are modelled with 9-noded generalized plate elements and the columns are modelled with 27-noded brick elements. The columns are assumed to have points of contraflexure at mid-height. All the columns are modelled with brick

elements neglecting the effect of cracking and reinforcement. The effect of creep in the column was also neglected.

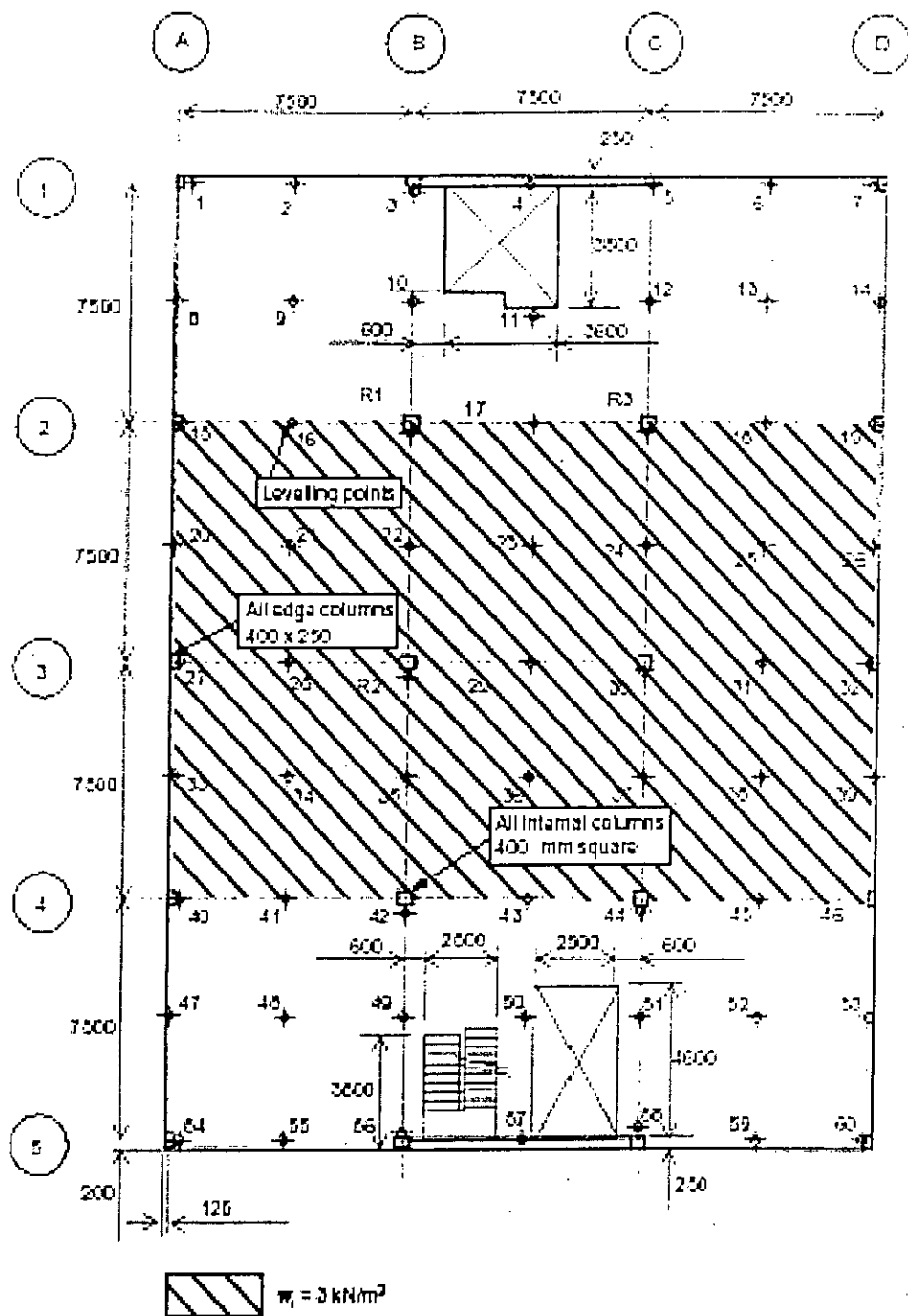


Figure 4.4: Loading pattern of Cardington building. (Adapted from Hossain and Vollum, 2002)

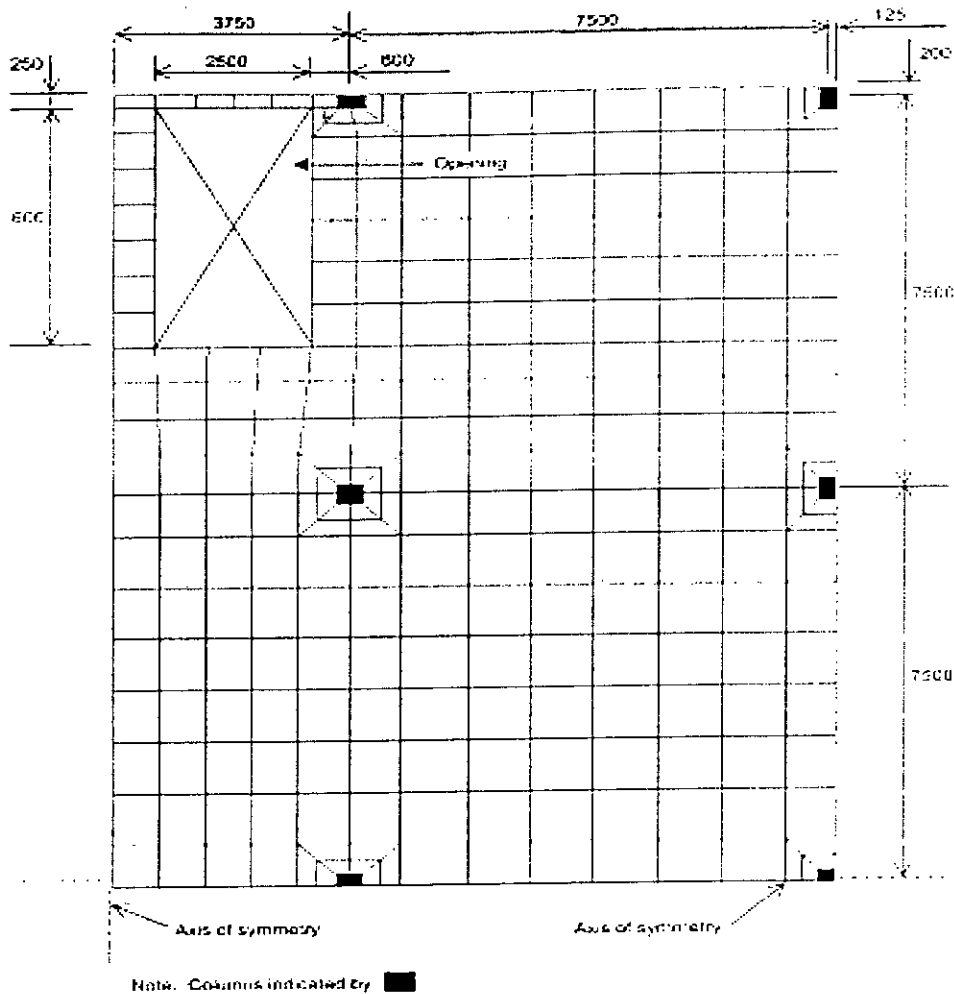


Figure 4.5 Finite element mesh of one quarter of the floor used in analysis (all dimensions are in mm)

The assumptions regarding the analysis of Cardington slabs are:

1. The thickness of all the slabs is 250 mm as specified.
2. The reinforcement assumed in the analysis is equivalent to that specified, although some adjustments were made to accommodate the chosen FE mesh.
3. The values made f_{ct} and E_c used in the analysis are based on control test.
4. Analyses are based on severest cracking.
5. Long-term deflections are calculated using ACI long-term multiplier curve.

On the basis of above assumptions, both the short-term and long-term deflection of Cardington slab 3, slab 4 and slab 6 have been calculated. The material properties and loading condition used in the analysis in different floors are described separately.

For short-term deflection calculation, materials properties (f_{ct} and E_c) used in the analysis are the mean material properties at striking (Table 4.1). The load used for short-term deflection calculation in the analysis is only for self weight and formwork.

For long-term deflection calculation, material properties (f_{ct} and E_c) are used in the NLFE analysis based on critical condition where cracking is severe. The severe cracking condition is based on the ratio of load to f_{ct} . The level of cracking will be critical when the ratio of load to modulus of rupture of concrete is the highest. The value of long-term deflection will be maximum for this critical cracking and the mean material properties used in the analysis based on this assumption. Unlike the approach shown in Nilson (1997), cracking in slab is considered in the FE analysis and the short-term cracked deflection due to peak load is taken from the NLFE analysis. The long-term deflection is calculated by using long-term deflection multiplier λ which depends on ξ , a time-dependant coefficient. Branson (1977) has suggested a five-year value of $\xi = 3.0$ for two-way slabs and ACI Code (2002) suggested that five-year value of $\xi = 2.0$ for ordinary beams and one-way slabs. The five-year value of ξ is taken as 2.0 and the intermediate values are picked from the ACI suggested graph (Fig.2.10). For the five-year value of $\xi = 3.0$ as suggested by Branson (1977), the intermediate values for long-term multiplier increased proportionately.

4.4 DEFLECTION CALCULATION OF CARDINGTON SLAB 3

4.4.1 Short-term deflection calculation

For short-term deflection calculation, the material properties used in the analysis is $f_{ct} = 2.68$ MPa and $E_c = 27.00$ GPa (mean material properties during striking) (Table 4.1). A sustained load of 6.75 kN/m 2 is used in the short-term analysis. This load includes 6 kN/m 2 for self-wt and 0.75 kN/m 2 for formwork. The age of the slab is 2 days when test deflection values are measured and in the FE model there is column only in the bottom of slab and no column above the slab for short-term deflection calculation. The experimental maximum, minimum and mean short-term deflections

and the estimated short-term deflections are presented in the Table 4.2, 4.3 and 4.4 for corner panel, edge panel and center panel respectively.

4.4.2 Long-term Deflection Calculation

For long-term deflection calculation, the material properties used in the analysis is $f_{ct} = 3.62 \text{ MPa}$ and $E_c = 33.00 \text{ GPa}$ (mean material properties during peak load) (Table 4.1). A load of 10.74 kN/m^2 was used in the long-term analysis as the ratio of peak load to f_{ct} 2.97 ($10.74/3.62 = 2.97$) is higher than the ratio of strike load to f_{ct} 2.52($6.75/2.68= 2.52$).

The experimental maximum, minimum and mean long-term deflection value and the estimated long-term deflection values are presented in the Table 4.2, 4.3 and 4.4 for corner panel, edge panel and center panel respectively.

Calculation of long-term deflection of corner panel for five-year value of $\xi=2.0$

Immediate cracked deflection for maximum load of 10.74 in corner panel of floor 3 is

$$\Delta_{d+I} = 11.724 \text{ mm (FE analysis)} \text{ (Table 4.2)}$$

The multiplier for 363 days is 1.4 obtained from ACI graph (Fig. 2.10) and the total deflection is calculated by multiplying the immediate deflection with 2.4 (1.4+1.0). The load used as sustained load in corner panel is 6.75 kN/m^2 as no sustain load in the corner panel.

The total deflection for sustained load (6.75 kN/m^2) at 363 days is

$$\Delta_{d363} = 11.724 \times \frac{6.75}{10.74} \times 2.4 = 17.68 \text{ mm}$$

The multiplier for 403 days, 789 days and 1825 days are also obtained similarly from ACI graph (Fig. 2.10)

$$\Delta_{d403} = 11.724 \times \frac{6.75}{10.74} \times 2.46 = 18.12 \text{ mm}$$

$$\Delta_{d789} = 11.724 \times \frac{6.75}{10.74} \times 2.7 = 19.89 \text{ mm}$$

10304

$$\Delta_{d1825} = 11.724 \times \frac{6.75}{10.74} \times 3.0 = 22.10 \text{ mm}$$

Calculation of long-term deflection of corner panel for five-year value of $\xi=3.0$

Immediate cracked deflection in corner panel of floor 3 for maximum load of 10.74 kN/m² is

$$\Delta_{d+l} = 11.724 \text{ mm (FE analysis) (Table 4.2)}$$

The multiplier value for 363 days is 3.1 obtained from multiplying the ξ value of 363 days for five-year value of $\xi=2.0$ with the ratio of 3/2 (1.4*3/2 =2.1) and the total deflection is calculated by multiplying the immediate deflection with 3.1 (2.1+1.0).

The total deflection for sustained load at 363 days is

$$\Delta_{d363} = 11.724 \times \frac{6.75}{10.74} \times 3.1 = 22.84 \text{ mm}$$

The multiplier for 403 days, 789 days and 1825 days are also obtained similarly. The load used as sustained load in corner panel is 6.75 kN/m² as there was no sustain load in corner panel.

$$\Delta_{d403} = 11.724 \times \frac{6.75}{10.74} \times 3.19 = 23.50 \text{ mm}$$

$$\Delta_{d789} = 11.724 \times \frac{6.75}{10.74} \times 3.55 = 26.16 \text{ mm}$$

$$\Delta_{d1825} = 11.724 \times \frac{6.75}{10.74} \times 4.0 = 29.47 \text{ mm}$$

The calculated short-term and long-term deflections are presented in Table 4.2 and in Fig. 4.6 for corner panel.

Table 4.2: Experimental and predicted deflection value of corner panel of Cardington slab 3.

Short-term deflection (at striking):

Day	Deflection mm			Variation (%)	
	Experimental Value		Predicted value		
	Min.	Max.	Mean		
2	6.24	7.85	6.99	8.171	16.89

Long-term deflection (for sustained load):

Cracked deflection due to peak load mm
11.724

Day	Deflection mm					Variation (%)	
	Experimental Value			Predicted value			
	Min.	Max.	Mean	(max. $\xi=3$)	(max. $\xi=2$)	(max. $\xi=3$)	(max. $\xi=2$)
363	17.29	23.14	20.13	22.84	17.68	-13.46	12.17
403	17.29	24	20.52	23.51	18.13	-14.57	11.65
789	19.27	27.11	23.86	26.16	19.89	-9.64	16.64
1825	-	-	-	29.47	22.11	-	-

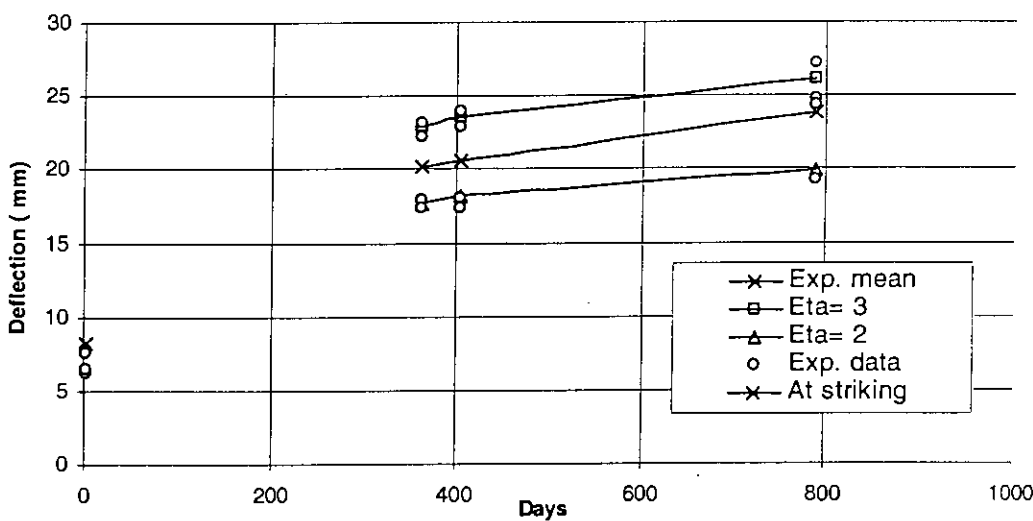


Figure 4.6 Experimental and predicted deflection curve of corner panel of Cardington slab 3

From the Table 4.2 and Fig.4.6, it can be seen that the experimental short-term deflection value is lower than the predicted value and predicted value is 16.89% higher than experimental mean short-term value. The experimental mean long-term deflection value is in between the predicted long-term deflection value using five-year value of $\xi= 3$ and using five-year value of $\xi=2$. The predicted long-term deflection using maximum value of $\xi= 3$ is 14.57% higher and using maximum value of $\xi= 2$ is 11.65% lower than experimental mean long-term deflection for 403 days.

Calculation of long-term deflection of edge panel for five-year value of $\xi=2.0$

The multiplier for 363 days is 1.4 obtained from ACI graph (Fig. 2.10) and the total deflection is calculated by multiplying the immediate deflection with 2.4 (1.4+1.0). The total deflection for sustained load (6.75 kN/m^2) is

$$\Delta_{d363} = 9.363 \times \frac{6.75}{10.74} \times 2.4 = 14.12 \text{ mm}$$

The multiplier for 403 days, 789 days and 1825 days are also obtained similarly from ACI graph (Fig.2.10).The load used as sustained load is 9.00 kN/m^2 for day 403, day 789 and day 1825 as the sustain load in edge and in centre panel after 393 days in slab 3 is 9.00 kN/m^2 (Fig. 4.4).

$$\Delta_{d403} = 9.363 \times \frac{9}{10.74} \times 2.46 = 19.30 \text{ mm}$$

$$\Delta_{d789} = 9.363 \times \frac{9}{10.74} \times 2.7 = 21.18 \text{ mm}$$

$$\Delta_{d1825} = 9.363 \times \frac{9}{10.74} \times 3.0 = 23.54 \text{ mm}$$

Calculation of long-term deflection of edge panel for five-year value of $\xi=3.0$

Immediate cracked deflection in corner panel of floor 3 for maximum load of 10.74 kN/m^2

$$\Delta_{d+1} = 9.363 \text{ mm (FE analysis)} \text{ (Table 4.3)}$$

The multiplier value for 363 days is 3.1 obtained from multiplying the ξ value of 363 days for five-year value of $\xi=2.0$ with the ratio of 3/2 ($1.4*3/2 =2.1$) and the total

deflection is calculated by multiplying the immediate deflection with 3.1 (2.1+1.0). The total deflection for sustained load (6.75 kN/m^2) at 363 days is

$$\Delta_{d363} = 9.363 \times \frac{6.75}{10.74} \times 3.1 = 18.24 \text{ mm}$$

The multiplier for 403 days, 789 days and 1825 days are also obtained similarly. The load used as sustained load is 9.00 kN/m^2 for day 403, day 789 and day 1825 as the sustain load in edge and in centre panel after 393 days in slab 3 is 9.00 kN/m^2 (Fig. 4.4)

$$\Delta_{d403} = 9.363 \times \frac{9}{10.74} \times 3.19 = 25.03 \text{ mm}$$

$$\Delta_{d789} = 9.363 \times \frac{9}{10.74} \times 3.55 = 27.85 \text{ mm}$$

$$\Delta_{d1825} = 9.363 \times \frac{9}{10.74} \times 4.0 = 31.38 \text{ mm}$$

The calculated short-term and long-term deflections are presented in Table 4.3 and in Fig. 4.7 for edge panel.

Table 4.3 Experimental and predicted deflection value of edge panel of Cardington slab 3.

Short-term deflection (at striking):

Day	Deflection mm			Variation (%)	
	Experimental Value		Predicted value		
	Min.	Max.			
2	5.05	5.89	5.347	6.524	22%

Long-term deflection (for sustained load):

Cracked deflection due to peak load mm
9.363

Day	Deflection mm						Variation (%)
	Experimental Value			Predicted value			
	Min.	Max.	Mean	(max. $\xi=3$)	(max. $\xi=2$)	(max. $\xi=3$)	(max. $\xi=2$)
363	15.95	18.19	17.09	18.24	14.12	-6.70	17.40
403	18.95	21.58	20.14	25.03	19.30	-24.28	4.17
789	23.93	26.37	24.94	27.85	21.18	-11.67	15.08
1825	-	-	-	31.38	23.54	-	-

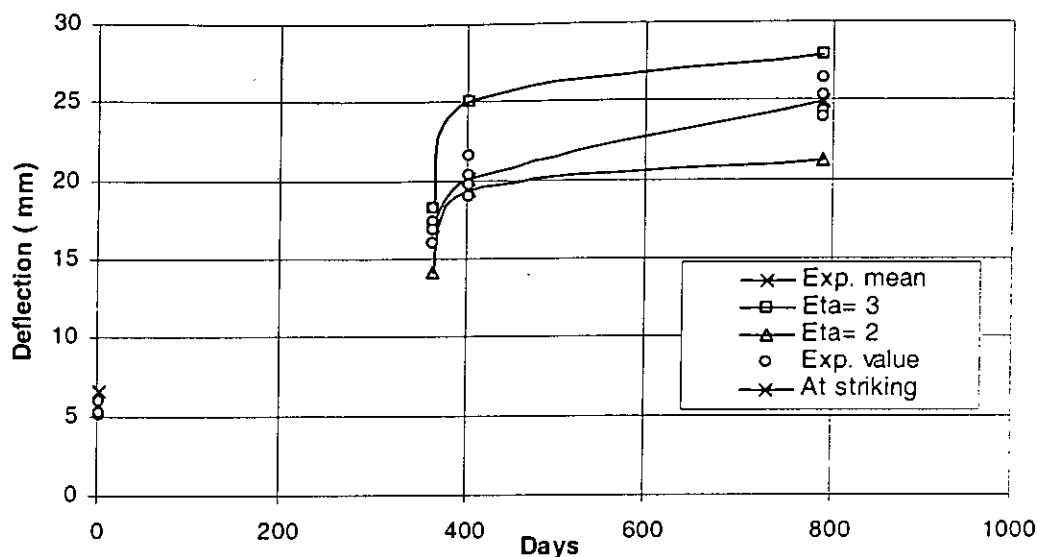


Figure 4.7 Experimental and predicted deflection curve of edge panel of Cardington slab 3

From the Table 4.3 and Fig. 4.7, it can be seen that for edge panel, the predicted short-term deflection is 22% higher than the mean experimental short-term deflection. The predicted long-term deflection using 5 year value of $\xi = 2$ show reasonable agreement to the experimental value at day 403 and the predicted long-term deflection using max. $\xi = 3$ are showing reasonable agreement to the experimental deflection value at day 789. The sudden increase in the deflection values in between 363 and 403 days due to the sustained load of 3 kN/m^2 applied in between that period.

Deflection of center panel

The calculated short-term and long-term deflections for center panel are presented in Table 4.4 and in Fig. 4.8.

Table 4.4 Experimental and predicted deflection value of center panel of Cardington slab 3.

Short-term deflection (at striking):

Day	Deflection mm			Variation (%)	
	Experimental Value				
	Min.	Max.	Mean		
2	3.35	3.70	3.525	4.298	17.98%

Long-term deflection (for sustained load):

Cracked deflection due to peak load mm
6.17

Day	Deflection mm						Variation (%)
	Experimental Value			Predicted value			
	Min.	Max.	mean	(max. $\xi = 3$)	(max. $\xi = 2$)	(max. $\xi = 3$)	(max. $\xi = 2$)
363	9.48	10.24	9.86	12.02	9.31	-21.91	5.58
403	11.74	12.5	12.12	16.49	12.72	-36.06	-4.95
789	15.00	16.06	15.53	18.35	13.96	-18.16	10.11
1825	-	-	-	20.68	15.51	-	-

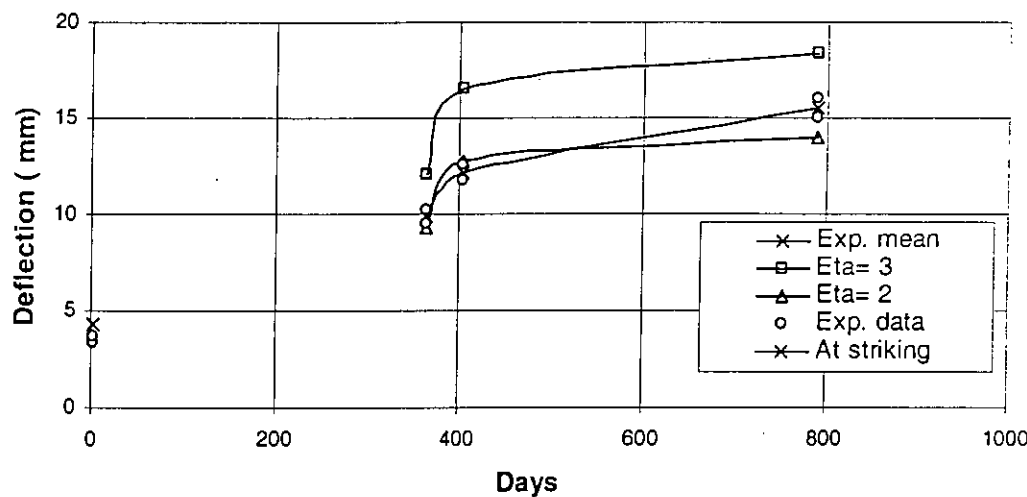


Figure 4.8 Experimental and predicted deflection curve of center panel of Cardington slab 3.

From the Table 4.4 and Fig. 4.8, the short-term predicted deflection is 17.98% higher than the experimental mean short-term deflection. The experimental long-term deflection values in different period showed good agreement with the predicted long-term deflection value using five-year value of $\xi=2.0$. The sudden increase in the deflection values in between 363 and 403 days due to the sustained load of 3 kN/m^2 applied in between that period.

From the above discussion, it is found that for corner panel, edge panel and center panel of Cardington slab 3, the experimental mean short-term deflection value is lower than the predicted short-term deflection value. For long-term deflection prediction, the designer will get conservative deflection value by using five-year value of $\xi=3.0$ as the predicted long-term deflection value is in between the five-year value of $\xi=3.0$ and five-year value of $\xi=2.0$.

4.5 DEFLECTION CALCULATION OF CARDINGTON SLAB 4

4.5.1 Short-term deflection calculation

For short-term deflection calculation, the material properties used in the analysis is $f_{ct}=2.50 \text{ MPa}$ and $E_c = 29.25 \text{ GPa}$ (mean material properties during striking) (Table 4.1). The sustain load and the FE model used in the analysis is as the same as slab 3 for short-term deflection calculation. The experimental maximum, minimum and mean short-term deflections and the estimated short-term deflections are presented in the Table 4.5, 4.6 and 4.7 for corner panel, edge panel and center panel respectively.

4.5.2 Long-term deflection calculation

For long-term deflection calculation, the material properties used in the analysis is $f_{ct}=3.8 \text{ MPa}$ and $E_c = 35.15 \text{ GPa}$ (mean material properties during peak load) (Table 4.1). A load of 10.27 kN/m^2 was used in the long-term analysis. The value of f_{ct} reduced to 3.8 ($10.27/2.7 = 3.8$) as the ratio of peak load to f_{ct} 2.45 ($10.27/4.19 = 2.45$) is lower than the ratio of strike load to f_{ct} 2.7 ($6.75/2.50 = 2.7$). The experimental maximum, minimum and mean long-term deflections and the estimated long-term deflections are presented in the Table 4.5, 4.6 and 4.7 for corner panel, edge panel

and center panel. The long-term deflections for corner, edge and center panel of slab 4 are calculated following the same procedure as shown in the slab 3.

Deflection of corner panel

The calculated short-term and long-term deflections for corner panel are presented in Table 4.5 and in Fig. 4.9.

Table 4.5 Experimental and predicted deflection value of corner panel of Cardington slab 4.

Short-term deflection (at striking):

Day	Deflection mm			Variation (%)	
	Experimental Value		Predicted value		
	Min.	Max.			
2	9.245	10.48	9.905	8.466	14.52%

Long-term deflection (for sustained load):

Cracked deflection due to peak load mm
9.975

Day	Deflection mm						Variation (%)
	Experimental Value			Predicted value			
	Min.	Max.	Mean	(max. $\xi=3$)	(max. $\xi=2$)	(max. $\xi=3$)	(max. $\xi=2$)
351	20.03	23.03	21.62	20.33	15.73	5.97	27.24
391	19.6	23.25	21.58	20.81	16.06	3.57	25.58
776	21.28	25.22	23.33	23.08	17.57	1.07	24.69
876	22.13	26.4	24.43	23.47	17.83	3.93	27.02
1825	-	-	-	26.22	19.66	-	-

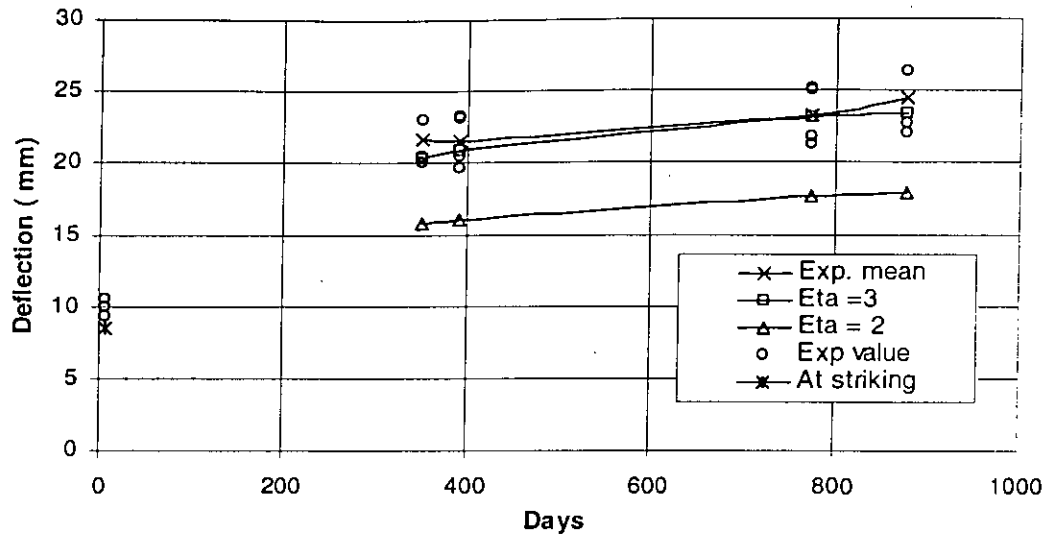


Figure 4.9 Experimental and predicted deflection curve of corner panel of Cardington slab 4

From the Table 4.5 and Fig. 4.9, it can be seen that the mean experimental short-term deflection value is 14.52% higher than the predicted value. The experimental mean long-term deflection value is closer to the predicted long-term deflection value using five-year value of $\xi=3$. The predicted long-term deflection using maximum value of $\xi=3$ is 1% to 6% higher than experimental mean long-term deflection in different period.

Deflection of edge panel

The calculated short-term and long-term deflections for edge panel are presented in Table 4.6 and in Fig. 4.10.

Table 4.6 Experimental and predicted deflection value of edge panel of Cardington slab 4

Short-term deflection (at striking):

Day	Deflection mm				Variation (%)	
	Experimental Value			Predicted value		
	Min.	Max.	Mean			
2	4.15	4.79	4.463	6.658	49.18%	

Long-term deflection (for sustained load):

Cracked deflection due to peak load mm
8.124

Day	Deflection mm						Variation (%)	
	Experimental Value			Predicted value				
	Min	Max	Mean	(max $\xi=3$)	(max $\xi=2$)	(max $\xi=3$)	(max $\xi=2$)	
351	12.85	14.70	13.85	16.55	12.81	-19.49	7.51	
391	14.53	17.36	16.12	16.95	13.08	-5.15	18.86	
776	17.97	21.06	19.57	25.06	19.08	-28.05	2.50	
876	22.38	18.94	20.65	25.48	19.36	-23.39	6.25	
1825	-	-	-	28.48	21.35	-	-	

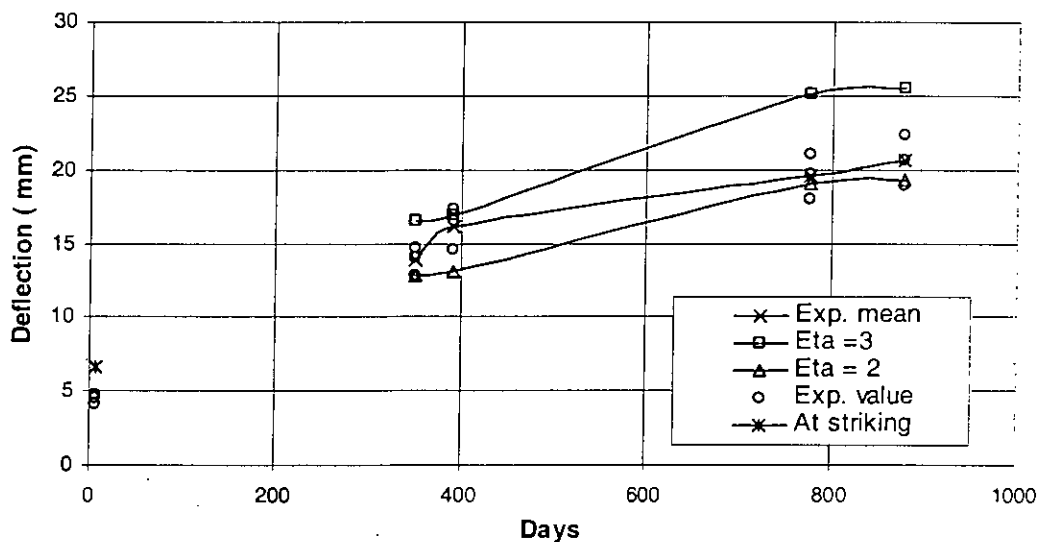


Figure 4.10 Experimental and predicted deflection curve of edge panel Cardington slab 4

From the Table 4.6 and Fig. 4.10, it can be seen that for edge panel, the predicted short-term deflection is much higher (49.18%) than the mean experimental short-term deflection. The predicted long-term deflection using 5 year value of $\xi=2$ show reasonable agreement to the experimental value in longer period (day 776 and day 876) and the predicted long-term deflection using max. $\xi=3$ are showing reasonable agreement to the experimental deflection value in shorter period (day 351 and day

391). The sudden increase in the deflection values in between 351 and 391 days due to the sustained load of 3 kN/m^2 applied in between that period.

Deflection of center panel

The calculated short-term and long-term deflections for center panel are presented in Table 4.7 and in Fig. 4.11.

Table 4.7 Experimental and predicted deflection value of center panel of Cardington slab 4

Short-term deflection (at striking):

Day	Deflection mm			Variation (%)	
	Experimental Value		Predicted value		
	Min.	Max.			
2	2.39	3.23	2.81	4.399	
				56.55%	

Long-term deflection (for sustained load):

Cracked deflection due to peak load mm
5.677

Day	Deflection mm					Variation (%)	
	Experimental Value			Predicted value			
	Min	Max	Mean	(max $\xi=3$)	(max $\xi=2$)	(max $\xi=3$)	(max $\xi=2$)
351	7.79	8.18	7.99	11.57	8.95	-44.81	-12,02
391	9.92	10.21	10.07	11.84	9.14	-17.58	9.24
776	11.82	13.29	12.55	17.51	13.33	-39.52	-6.22
876	12.16	13.89	13.03	17.81	13.53	-36.68	-3.84
1825	-	-	-	19.89	14.92	-	-

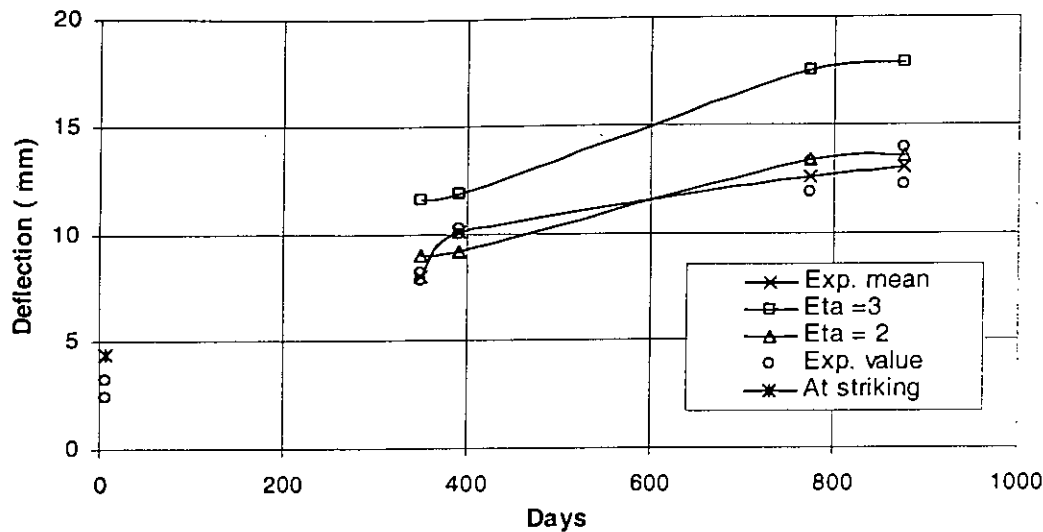


Figure 4.11 Experimental and predicted deflection curve of center panel of Cardington slab 4

From the Table 4.7 and Fig. 4.11, it can be seen that for center panel, the predicted short-term deflection is much higher (56.55%) than the mean experimental short-term deflection. The predicted long-term deflection using 5 year value of $\xi=2$ show reasonable agreement to the experimental value and the variation of the predicted value is 4% to 12% with experimental mean value.

From the above discussion, it is found that for corner panel, edge panel and center panel of Cardington slab 4, the predicted short-term deflection value is much higher than the experimental mean short-term deflection. For long-term deflection prediction the predicted value shows good agreement in corner panel by using five-year value of $\xi=3.0$ whereas by using five-year value of $\xi=2.0$ the prediction is reasonable agreement with the predicted long-term deflection value for edge and center panel

4.6 DEFLECTION CALCULATION OF CARDINGTON SLAB 6

4.6.1 Short-term deflection calculation

For short-term deflection calculation, the material properties used in the analysis is $f_{ct}=2.00$ MPa and $E_c=23.25$ GPa (mean material properties during striking) (Table

4.1). The sustain load and the FE model used in the analysis is as the same as slab 3 for short-term deflection calculation. The experimental maximum, minimum and mean short-term deflection value and the estimated short-term deflection value are presented in the Table 4.8, 4.9 and 4.10 for corner panel, edge panel and center panel respectively.

4.6.2 Long-term deflection calculation

For long-term deflection calculation, the material properties used in the analysis is $f_{ct} = 3.06 \text{ MPa}$ and $E_c = 31.86 \text{ GPa}$ (mean material properties during peak load) (Table 4.1). A load of 10.14 kN/m^2 was used in the long-term analysis. The ratio of peak load to f_{ct} 3.31 ($10.14/3.06 = 3.31$) is lower than the ratio of strike load to f_{ct} 3.375($6.75/2.00 = 3.37$). The experimental maximum, minimum and mean long-term deflection value and the estimated long-term deflection values are presented in the Table 4.8, 4.8 and 4.9 for corner panel, edge panel and center panel. The long-term deflection for corner, edge and center panel of slab 6 is calculated following the same procedure as shown in the slab 3.

Deflection of corner panel

The calculated short-term and long-term deflections are presented in Table 4.8 and in Fig. 4.12 for corner panel.

Table 4.8 Experimental and predicted deflection value of corner panel of Cardington slab 6

Short-term deflection (at striking):

Day	Deflection mm			Variation (%)	
	Experimental Value		Predicted value		
	Min.	Max.			
3	8.60	9.24	8.96	12.639	41.12%

Long-term deflection (for sustained load):

Cracked deflection due to peak load mm
12.802

Day	Deflection mm						
	Experimental Value			Predicted value		Variation (%)	
	Min	Max	Mean	(max $\xi=3$)	(max $\xi=2$)	(max $\xi=3$)	(max $\xi=2$)
323	25.43	26.92	26.17	24.76	19.35	5.41	26.07
340	24.48	26.38	25.43	26.16	20.28	-2.87	20.25
749	26.45	27.97	27.21	29.61	22.58	-8.82	17.02
1825	-	-	-	34.09	25.57	-	-

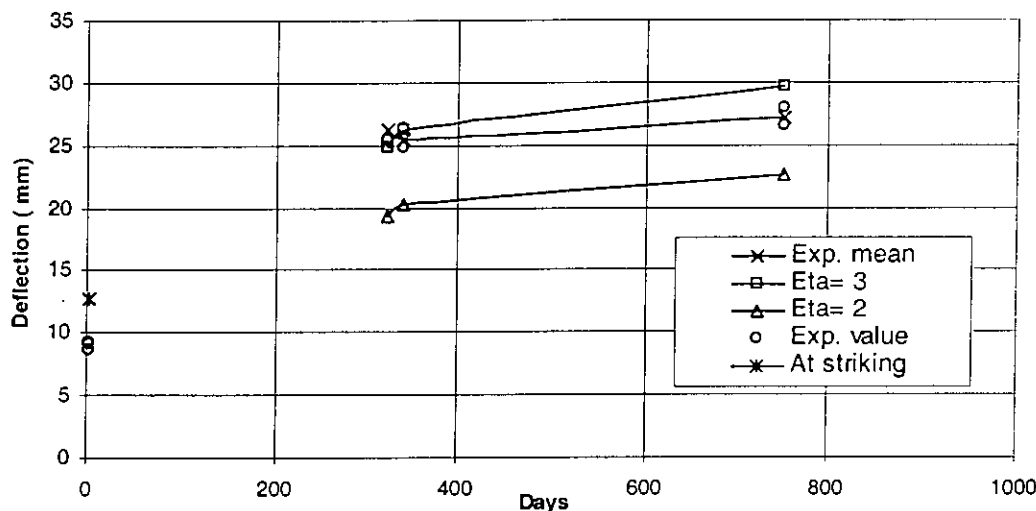


Figure 4.12 Experimental and predicted deflection curve of corner panel of Cardington slab 6

From the Table 4.8 and Fig. 4.12, it can be seen that the predicted short-term deflection is 41.12% higher than experimental mean short-term deflection value is. The experimental mean long-term deflection value is closer to the predicted long-term deflection value using five-year value of $\xi=3$. The predicted long-term deflection using maximum value of $\xi=3$ varied 3% to 9% with the mean experimental long-term deflection in different period.

Deflection of corner panel

The calculated short-term and long-term deflections for edge panel are presented in Table 4.9 and in Fig. 4.13.

Table 4.9 Experimental and predicted deflection value of edge panel of Cardington slab 6

Short-term deflection (at striking):

Day	Deflection mm			Variation (%)	
	Experimental Value		Predicted value		
	Min.	Max.	Mean		
3	6.20	6.53	6.40	9.077	41.82%

Long-term deflection (for sustained load):

Cracked deflection due to peak load mm
9.675

Day	Deflection mm					Variation (%)	
	Experimental Value			Predicted value			
	Min	Max	Mean	(max $\xi=3$)	(max $\xi=2$)	(max $\xi=3$)	(max $\xi=2$)
323	17.23	19.94	18.58	18.71	14.62	-0.67	21.33
340	20.13	22.75	21.44	26.36	20.44	-22.95	4.66
749	25.49	27.19	26.34	29.84	22.76	-13.29	13.59
1825	-	-	-	34.35	25.76	-	-

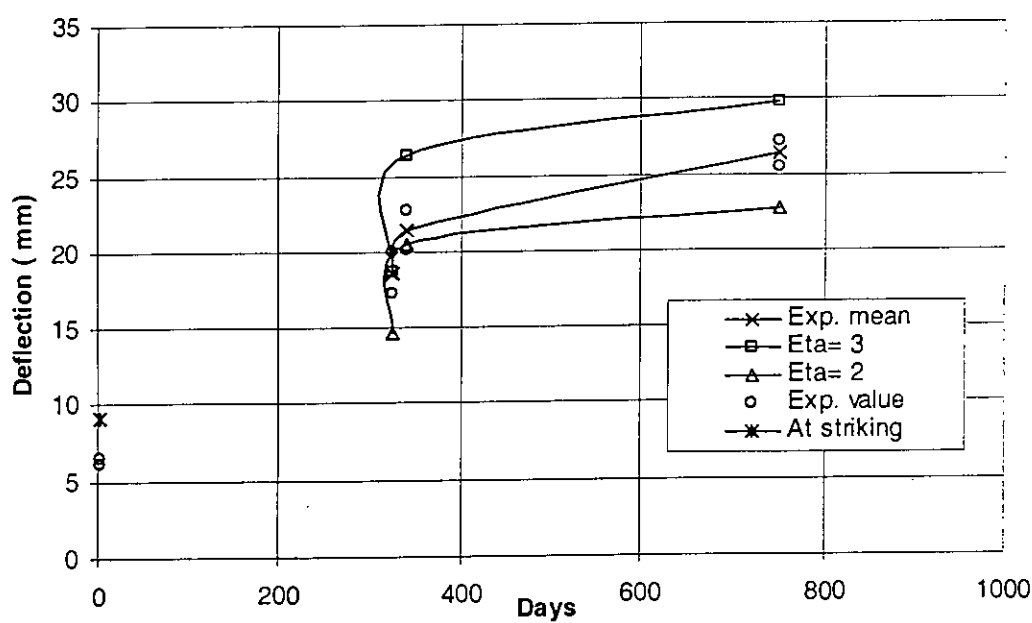


Figure 4.13 Experimental and predicted deflection curve of edge panel of Cardington slab 6

From the Table 4.9 and Fig. 4.13, it can be seen that for edge panel, the predicted short-term deflection is much higher (41.82%) than the mean experimental short-term deflection. The mean experimental deflection value is in between the predicted long-term deflection using 5 year value of $\xi= 2$ and 5 year value of $\xi= 3$. The sudden increase in the deflection values in between 351 and 391 days due to the sustained load of 3 kN/m^2 applied in between that period.

Deflection of center panel

The calculated short-term and long-term deflections are presented in Table 4.10 and in Fig. 4.14 for center panel.

Table 4.10 Experimental and predicted deflection value of center panel of Cardington slab 6

Short-term deflection (at striking):

Day	Deflection mm				Variation (%)	
	Experimental Value			Predicted value		
	Min.	Max.	Mean			
3	-	-	2.96	4.624	56.21%	

Long-term deflection (for sustained load):

Cracked deflection due to peak load mm
5.617

Day	Deflection mm						Variation (%)
	Experimental Value			Predicted value			
	Min	Max	Mean	(max $\xi= 3$)	(max $\xi= 2$)	(max $\xi= 3$)	(max $\xi= 2$)
323	-	-	8.57	10.86	8.49	-26.72	0.93
340	-	-	10.63	15.31	11.87	-44.03	-11.67
749	-	-	13.58	17.32	13.21	-27.54	2.72
1825	-	-	-	19.94	14.96	-	-

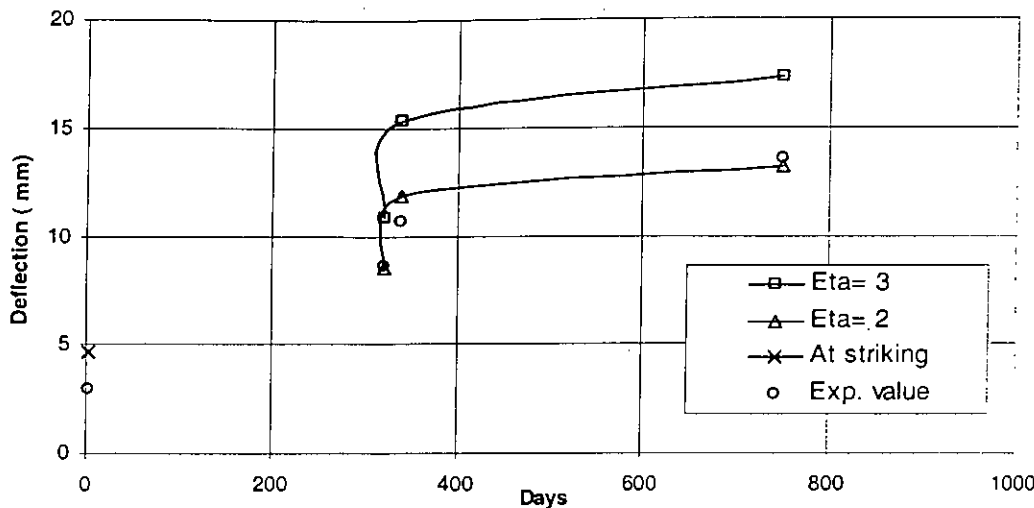


Figure 4.14 Experimental and predicted deflection curve of center panel of Cardington slab 6

From the Table 4.10 and Fig. 4.14, it can be seen that for center panel, the predicted short-term deflection is much higher (56.21%) than the mean experimental short-term deflection. Both the predicted long-term deflection value using 5 year value of $\xi = 3.0$ and using $\xi = 2.0$ are higher than the experimental value.

From the above discussion, it is found that for corner panel, edge panel and center panel of Cardington slab 6, the predicted short-term deflection value is much higher than the experimental mean short-term deflection. For long-term deflection prediction the predicted value shows good agreement in corner panel by using five-year value of $\xi = 3.0$ whereas by using five-year value of $\xi = 2.0$ the prediction is reasonable agreement with the predicted long-term deflection value for edge and center panel.

4.7 CONCLUSION

In this chapter, short-term and long-term deflections of Cardington ECBP building have been determined by using nonlinear FE analysis with ACI long-term multiplier of $\xi = 3.0$ and $\xi = 2.0$ and compared with the experimental short-term and long-term deflection. Short-term deflection prediction shows higher deflection value than the

experimental one. As for long-term predicted deflections of slab 3, slab 4 and slab 6, the prediction for corner edge and center panel using five-year value of $\xi=3.0$ gives conservative results with the experimental values.

The prediction of Cardington slab deflection using MC90 model with total load history by Hossain and Vollum (2002) showed good prediction but the procedure is much more complicated. Deflection prediction by using ACI (2002) suggested multiplier is much simpler than MC90 and predicted deflections are reasonable. But to predict long-term deflection using ACI suggested method, the multiplier should be used on the cracked deflection, not the elastic deflection. The calculation of cracked deflection is also difficult as nonlinear FE analysis is required to model cracking. Hence a simplified tool will be helpful to the designer to calculate cracked deflection of flat plate slab easily and quickly. In this regard, a simplified tool using Artificial Neural Network to calculate deflection will be described in the next chapter.

CHAPTER 5

DEFLECTION ESTIMATION OF FLAT PLATE SLAB BY ARTIFICIAL NEURAL NETWORK

5.1 INTRODUCTION

In Chapter 4, short- and long-term deflections of Cardington test slab were determined by Hossain's nonlinear FE analysis and the nonlinear FE analysis has been validated using Cardington test results. Deflection calculation is a nonlinear and complex problem and very time consuming to solve. From designer's point of view, a rather simple deflection prediction tool which can reasonably estimate the deflection considering the effect of nonlinear behavior would be very useful in order to satisfy serviceability conditions. Artificial Neural Network (ANN) program is capable of predicting result after adequate training with of a large number of known input-output data. With an aim to develop a tool that can predict deflection of flat plate slab, an Artificial Neural Network program (Siddique ,2007) has been trained in the current work.

In this Chapter, a large number of flat plate slabs with varying geometric, material and loading parameters have been analyzed with Hossain's nonlinear FE model and elastic deflection and cracked deflection are determined. Then the ANN program is trained by using these results. The predicted results are compared with FE results and the software is also validated with Cardington test results.

5.2 DATABASE DEVELOPMENT FOR TRAINING THE ANN

To predict the deflection of flat plat slab using Siddique's(2007) Artificial Neural Network (ANN) program, a large number of input data (geometric, material and loading parameters) and output (deflection) are required to train the ANN simulator. A flat plate slab of 3x3 panels was considered to be analyzed to prepare the database. The flat plate slab has same span length both for interior and exterior panel in one direction. The columns used in the model are of same size for all the panels. The flat

plate slab has columns below and above the slab. To calculate the deflection of flat plate slab, 3 types of panels i.e. corner panel, edge panel and center panel are considered and the deflection of the central point of the 3 panels are calculated using Hossain's nonlinear FE model. Both the elastic deflection and cracked deflection are calculated. In the nonlinear FE analysis plate element is used for modeling of slab and the brick element for modeling of column. Before selecting the final mesh size for plate element and brick element in the FE model, the sensitivity of the mesh for both plate element and brick element has been studied and the mesh size used for FE analysis has been finalized. Then a large number of nonlinear FE analyses have been performed varying span length, column size, slab thickness, load and concrete strength and the deflection values for corner, edge and center panel are picked from the output of the FE analysis. All the deflection values along with the input values were picked to prepare the database. The database having input and output values for flat plate slab is used to train the ANN simulator.

3 types of files i.e. data file, mesh file and property file are required for Hossain's (1999) nonlinear FE analysis to calculate deflection. Data files includes the finite element meshing, loading, support condition, element size and thickness; property file includes the properties of concrete, properties of reinforcement, Poisson's ratio, modular ratio; and the mesh file includes the top and bottom reinforcement in the slab in both directions. For reducing the time required to prepare a large number of input files, the automation of these files has been done which will be discussed later in the following sections.

5.2.1 The automated data file

In nonlinear FE analysis, the generation of the FE mesh, support condition, element definition, loading, material elasticity is done by numerical input in the data file. In the thesis work, flat plate slab analysis is done for 3 by 3 panels. To reduce the analysis run time and to reduce the complexity of FE mesh, one quarter of the total slab is modeled in the thesis work (Fig. 5.1). The columns supporting the slab are same in size for all the panels and are pinned at mid-height in the analysis. For creating FE mesh, the first step is to generate nodes of the FE mesh. In this work,

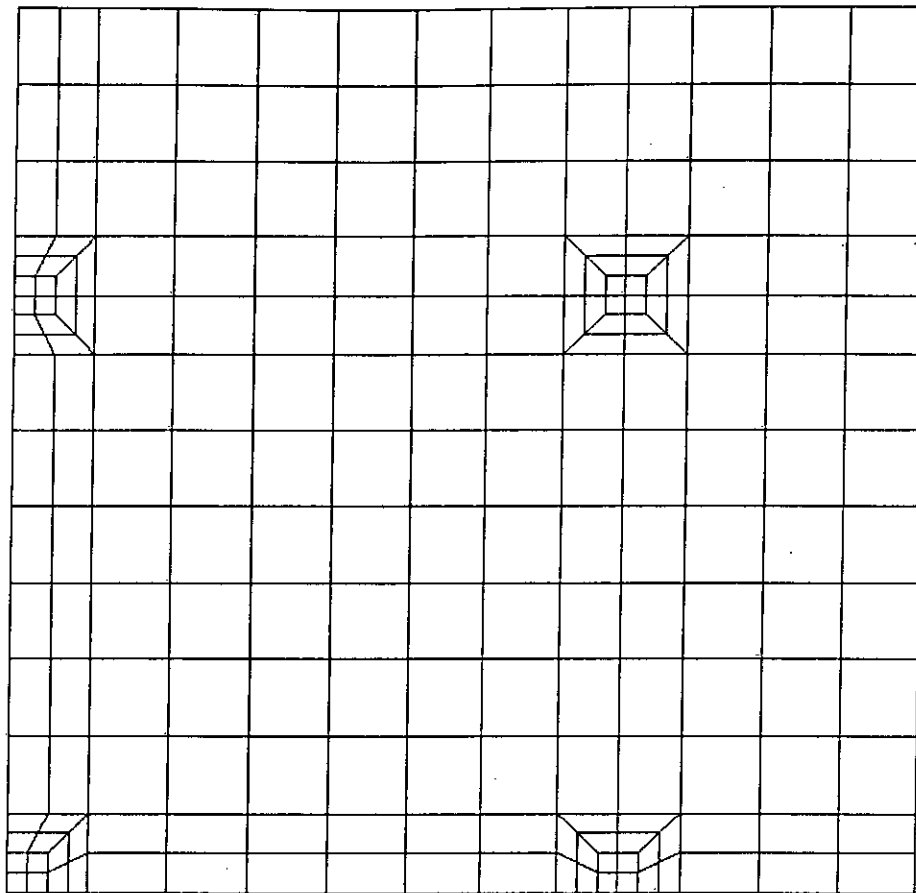


Figure 5.1 The finite element mesh for 3x3 panel (1/4th slab)

generation of the nodes is automated by using MS Excel. The automated nodes have the value of X coordinate, Y coordinate, Z coordinate and thickness for each node. Total 88 nodes have been created of which 40 nodes are created for modeling slab and 44 elements for modeling column. Then the material elasticity matrix is provided in the data file. Two types of element are used for modeling the FE mesh, 9-noded generalized plate element for modeling of slab and the 27-noded brick element for modeling of column. The elements are generated between the nodes as per number of element between the nodes defined and the finite element mesh is created. The slab mesh near the column support is finer than the slab mesh far from the column. The number of plate and brick element remains same for all types of analysis in the thesis work. The total numbers of elements used in the analysis are 313 including 217 plate elements and 96 brick elements in the analysis. The columns used in the analysis are fixed in three degrees of translation (X, Y, Z) at mid height in central point as the

3
D

< >

point of contra flexure lies in the mid height of column. Then the support condition and loading are to be given in the data file. Thus the required FE model is created by the data file.

5.2.2 The automated mesh file

The mesh file incorporates the effect of reinforcement in the deflection calculation of the slab. The reinforcement of the finite element mesh of flat plate slab is calculated by Equivalent Frame Method. The sample calculation of detail design of interior panel of a 3x 3 panel flat plate slab is presented in Appendix A. The design calculation of flat plate slab is performed by MS Excel presented in the Appendix B. The reinforcement required as per design in the column strip and the middle strip of the slab for interior and exterior panel in both directions was calculated by MS Excel. In FE mesh, reinforcement is provided in top and bottom of the element in both directions for each plate element. There are total 217 nos of plate element used in the analysis and reinforcement required in every plate element is assigned as per design to that particular plate element by MS Excel. The reinforcement in column strip and in middle strip is provided for critical moment from moment distribution. The minimum reinforcement required from ACI Code ($0.002bt$) is provided where the reinforcement required from moment is less than minimum reinforcement. In the location of the slab where no reinforcement required from design (top reinforcement in the middle strip) a nominal value of reinforcement is provided. In this way the reinforcement is provided in every plate element to prepare the mesh file. To generate the mesh file, the inputs are span length in both directions, column size in directions, floor height, concrete strength and steel strength. The MS Excel calculates the required reinforcement as per the logic and assigns the reinforcement in the plate elements. Thus the mesh file is automated.

5.2.3 The property file

The property file incorporates the effect of material property in the slab. In the property file, the modulus of elasticity of concrete E_c , modulus of rupture of concrete f_r , modular ratio n , slab thickness, number of plate and brick elements, and Poisson's ratio ν are provided.

5.3 SENSITIVITY ANALYSIS

In the nonlinear FE model of flat plate slab, plate element has been used for slab and brick element has been used for column in the thesis work. To study the sensitivity of the mesh of brick and plate elements, different mesh sizes are used and the mesh size to be used for subsequent analysis has been finalized.

5.3.1 Sensitivity of the plate elements

9-noded generalized plate element is used for modeling of slab. The plate element mesh size has an influence in the deflection calculation of the of flat plate slab. To study the impact of mesh size of the plate element, three different plate element meshes were studied while the no of the brick element remains the same (96 brick element) in all three meshes. Three types of mesh were used in the analysis to study the effect of the plate elements.

Mesh 1: Total elements no 244 including 148 plate elements and 96 brick elements.

Mesh 2: Total elements no 313 including 217 plate elements and 96 brick elements.

Mesh 3: Total elements no 400 including 304 plate elements and 96 brick elements.

The mesh size in the column strip remains the same in all three meshes. In the middle strip, the mesh size are gradually finer having plate element 148 in Mesh 1, plate element 217 in Mesh 2 and plate element 304 in Mesh 3 respectively. The values of deflection of different locations are given the Table 5.1. The difference of deflections in edge panel, corner panel and center panel in the elastic analysis and cracked analysis between Mesh 1 and Mesh 2 lies in the range of 4% -5% and between Mesh 2 and Mesh 3 lies in the range of 1%. Hence the Mesh 2 (no of plate element 217) is adopted for further study.

Table 5.1: Elastic and cracked deflection of different mesh size (same no of brick element)

	Elastic Deflection mm			Cracked deflection mm		
	Panel	Mesh 1	Mesh 2	Mesh 3	Mesh 1	Mesh 2
Corner	7.783	8.0802	8.1701	10.23	10.73	10.82
Edge	6.582	6.8848	6.9763	8.992	9.566	9.656
Center	5.072	5.3827	5.4766	7.48	8.077	8.144

5.3.2 Sensitivity of the brick elements:

The column size has an influence in the deflection of the flat plate slab. 27-noded brick elements are used in the column modeling. To study the effect of column mesh, three different column meshes have been used while the number of the plate element remains the same (304 plate Element).in all three meshes. Three types of mesh have been studied.

Mesh 4: Total elements no 368 including 304 plate elements and 64 brick elements.

Mesh 5: Total elements no 400 including 304 plate elements and 96 brick elements.

Mesh 6: Total elements no 432 including 304 plate elements and 128 brick elements.

The mesh size in the plate element remains the same and the brick mesh size reduced by increasing the no of element along the height of the column. The values of deflection of different locations are given the Table 5.2. The difference of deflections in edge panel, corner panel and center panel in the elastic analysis and cracked analysis between mesh 4 and mesh 5 lies in the range of 4% -5% and between mesh 5 and mesh 6 lies in the range of 1%. Hence the mesh 5 (no of brick element 96) is selected for further study.

Table 5.2: Elastic and cracked deflection of different mesh size (same no of plate element)

panel	Elastic Deflection mm			Cracked deflection mm		
	Mesh 4	Mesh 5	Mesh 6	Mesh 4	Mesh 5	Mesh 6
Corner	8.0965	8.1701	8.2104	10.726	10.82	10.871
Edge	6.9127	6.9763	7.0142	9.511	9.656	9.706
Center	5.4226	5.4766	5.5312	8.064	8.144	8.1932

5.4 INPUT PARAMETERS FOR DATABASE DEVELOPMENT

In order to train the neural network successfully to predict deflections, a large number of slabs with varying geometric, material and loading parameters were analyzed using the FE program. The varying parameters are span lengths in both directions, column sizes in directions, load, slab thickness, concrete strength and steel area. They are presented in the following sections.

5.4.1 Span length

The analysis has been performed for the span length of 8400 mm, 6900 mm, 5400 mm and 4200 mm in both directions. The panel sizes used in analysis for 3 x 3 panel flat plate are

- 8400 mm x 8400 mm,
- 8400 mm x 6900 mm,
- 8400 mm x 5400 mm
- 8400 mm x 4200 mm
- 6900 mm x 6900 mm
- 6900 mm x 5400 mm
- 6900 mm x 4200 mm
- 5400 mm x 5400 mm
- 5400 mm x 4200 mm
- 4200 mm x 4200 mm

5.4.2 Column size

Column size used in the analysis varies from 300 mm to 600 mm with an interval of 100 mm in size. The column sizes are 600mm by 600mm, 500mm by 500 mm, 400 mm by 400 mm and 300 mm by 300 mm. The columns supporting the slab have same cross sectional area for exterior and interior panel of the flat plate slab.

5.4.3 Slab thickness

In the current work, slab thickness was calculated as per ACI code (2002). Minimum thickness was restricted to 125mm (5 inch). Thicknesses were also used in the analysis for the value of 0.8t, 1.1t and 1.2t, where t is the ACI slab thickness.

5.4.4 Loading

The slabs are designed by USD method and dead load and live load have been considered in this analysis. The self-weight of slab and 1.0 kN/m² of floor finish load

are treated as total dead load. Total 2.4 kN/m^2 load is considered as random partitioned wall. The live load varied from 1.9 kN/m^2 to 4.79 kN/m^2 for design and analysis. For FE analysis, the total load includes constant floor finish and partition wall load as mentioned above. FE analysis has been performed using total unfactored load.

5.4.5 Reinforcement

Calculations for required slab reinforcement have followed by Equivalent Frame Method as per sample design calculation presented in Appendix A. The minimum reinforcement has been taken equal to $0.002bt$ in which b = width of slab and t = slab thickness. Reinforcement was also increased up to 10% and 20% of that required from strength design.

5.4.6 Material properties

The material properties used in the analyses are concrete strength f'_c , modulus of elasticity of concrete E_c , modulus of rupture of concrete f_r , yield strength of steel f_y , Poisson's ratio ν and modular ratio n . The material properties used in the analyses are as follows:

- Modulus of elasticity of concrete $E_c = 4733 \sqrt{f'_c} \text{ N/mm}^2$
- Poisson's ratio $\nu = 0.18$
- Modulus of elasticity of steel $E_s = 200000 \text{ N/mm}^2$
- According to ACI Code (2002) modulus of rupture of concrete is taken $f_r = 0.62\sqrt{f'_c} \text{ N/mm}^2$ and $f_r = 0.33\sqrt{f'_c} \text{ N/mm}^2$. The lower value indicates tensile strength reduced due to effect of restrained shrinkages
- Yield strength of steel $f_y = 413.7 \text{ N/mm}^2$
- Concrete cylinder strength $f'_c = 17.24 \text{ N/mm}^2, 20.7 \text{ N/mm}^2, 24.14 \text{ N/mm}^2, 27.69 \text{ N/mm}^2$
- Modular ratio $n = \frac{E_s}{E_c}$

5.5 TRAINING OF THE ARTIFICIAL NEURAL NETWORK (ANN) SIMULATOR

The ANN used in the current work is basically a back propagation type of neural network. In this network, a set of input parameters are connected to a set of output parameters through a set of weights and hidden layers. The network is trained to recognize the correct input-output pattern by adjusting the weight values of the interconnecting weight matrix. For the current analysis, the program the Neural Network Simulator shown in Fig. 5.2 has 8 input nodes, 10 output nodes, 16 hidden layer nodes the learning rate is varied from 0.01 to 0.05, momentum of 0.5 is selected, maximum iteration is set to 200000, tolerance is chosen to be 5E-9. Random seed 1, coefficient function 0.5, weight Wmax 1 and Wmin -1 are selected. In Neural Network Simulator, first from **File** menu open **Load input data** or click the '**Open**' button shown at the bottom with **Training Data File** as shown in Fig.5.2 and then select the input file shown in Fig. 5.3. Both of the items can open the required training data file. Then from **File** menu open **Load Test Data** or click '**Open**' button shown at the bottom with **Test Data File**. Both of the items can open the required weight data file. Then from **File** menu open **Load Weight** or click '**Open**' button shown at the bottom with **Weight Data File**. Both of the items can open the required weight data file. Thus all the input data's are ready to train in ANN simulator. Before staring training, set the value the reading old weight to 0 for the first time and select **Apply** button at the right. For further run, to read the old weight file change the value of reading old file from 0 to 1 and select apply button.

To start the training of ANN simulator, select the submenu **Execute ANN** from the menu **Execute**. First start with learning rate 0.01, in this case residual error more and iteration was reached 200000. Then save the weight file by selection **save weight** from file menu select **read existing weight** and increase learning rate 0.01 to 0.05 from execute menu again execute. The residual error decreases rapidly with the

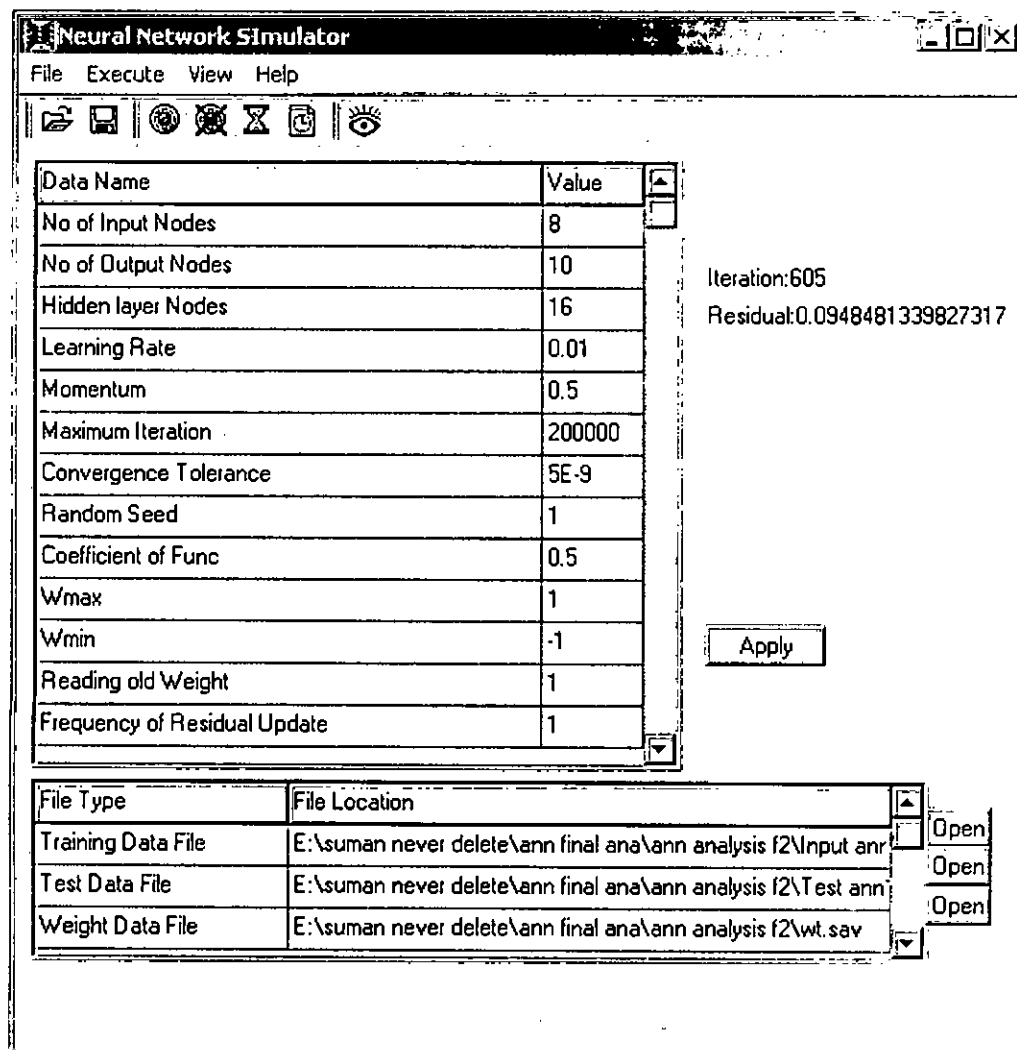


Figure 5.2 Neural Network Simulator

change of learning rate. After sufficient number of training when the residual becomes gradually diminished, the network becomes capable of predicting any new data within the trained range of input data or any data outside the range. When the amount of error i.e. the residual becomes very small, the network is ready for prediction.

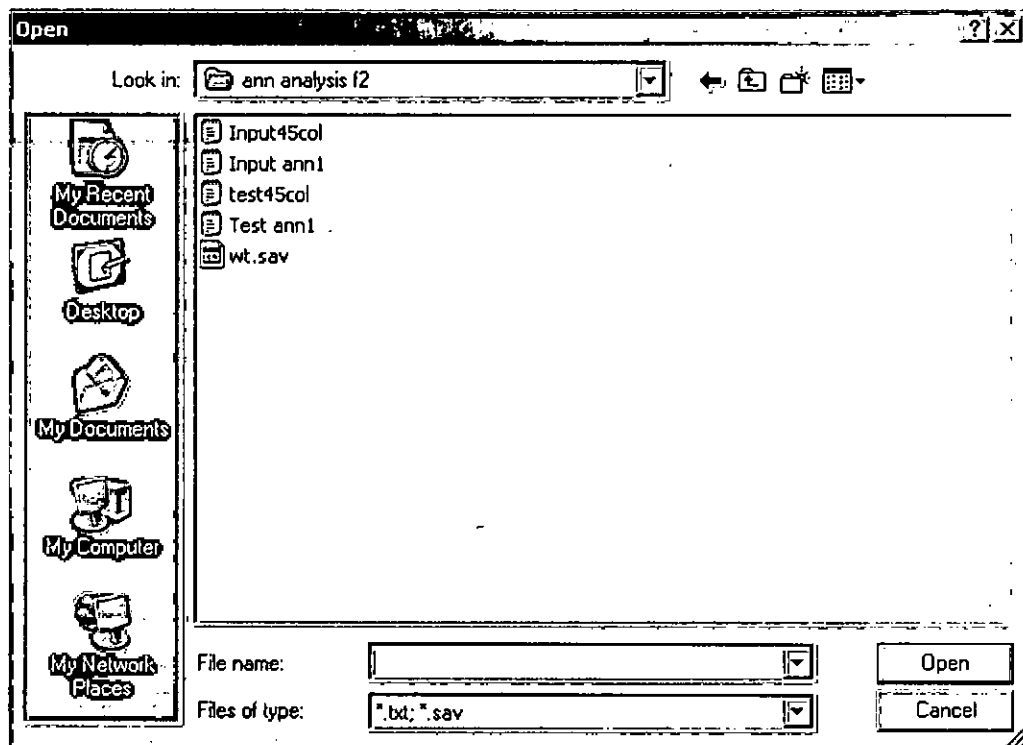


Figure 5.3 Opening dialogue box

5.6 USE OF NEURAL NETWORK SIMULATOR FOR PREDICTING DEFLECTION

To predict the result by ANN, open submenu **view results** from **View** menu. The window shows the results of the training of the ANN. It can show three types of training results. Firstly, it shows the error Residual versus Iteration, secondly, it can show the training data sets (Output column versus Input column) and thirdly, it can show a window for the single data prediction.

The third window as shown in Fig. 5.4 gives the predicted deflection value. In the Fig. 5.4 the left side indicates the input flat plate slab geometry, loading and material properties and the right side indicates predicted output values by the ANN program. In the input item, value of the input parameters span length (mm) in both x and y directions, column dimension (mm) in x and y direction, total service load in kN/m², slab thickness in mm, concrete strength in N/mm² and reinforcement in percentage (mm²/mm) are given as input and click calculate. Then the predictor will predict maximum stress, elastic deflection, cracked deflection for both $f_r = 7.5\sqrt{f'_c}$ psi

$(0.62\sqrt{f'_c} \text{ N/mm}^2)$ and $f_r = 4\sqrt{f'_c} \text{ psi}$ ($0.33\sqrt{f'_c} \text{ N/mm}^2$) of corner, edge and center panel. The lower value f_r indicates tensile strength reduced due to effect of restrained shrinkages.

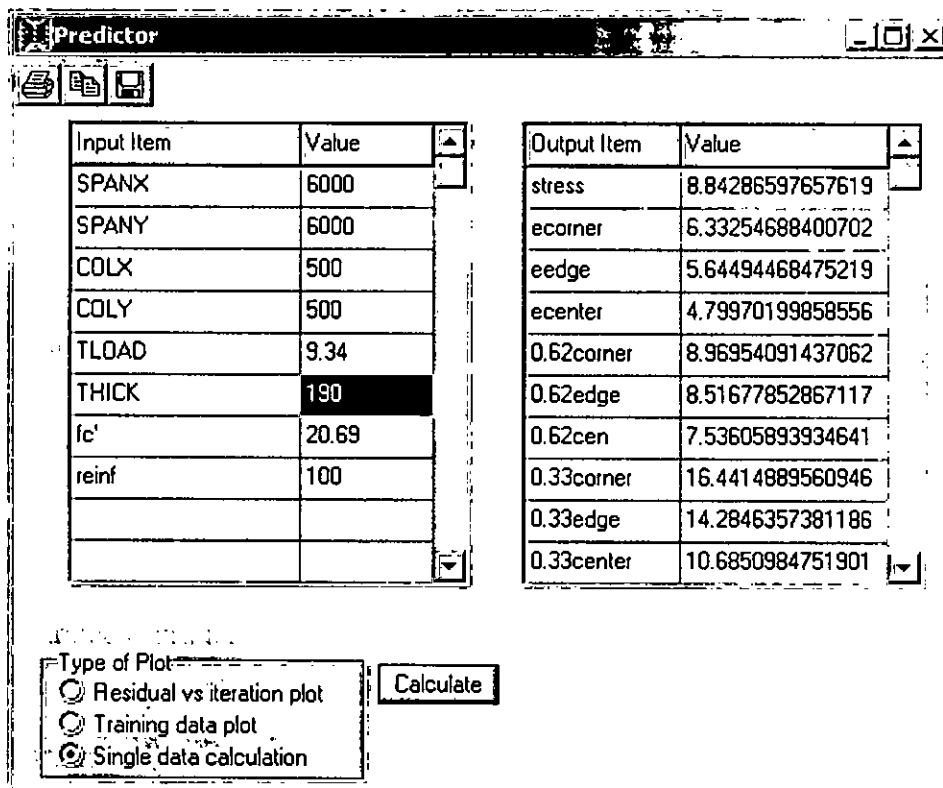


Figure 5.4 The neural network predictor to predict deflection and stress

5.7 VALIDATION OF ANN RESULTS WITH FE ANALYSIS

Once the ANN is trained, the slab deflection is predicted by ANN program. The predicted deflection then compared with the deflection of FE analysis. The comparison is shown in Table 5.3 where these predictions are reasonably good in comparison with the FE analysis. In most of the cases, the predicted value varies from 1% to 2% with the FE analysis value. It has been found that designers can easily predict stresses and deflections using this prediction tools without any rigorous calculations.

Table 5.3 Comparison of FE and ANN predicted deflection

Input							Output results										
Span		column size		Total load KN/m ²	Slab thickness (mm)	Concrete strength N/mm ²	Reinforcement	stress N/mm ²	Deflection			craked fr = 0.62 sqrt(f'c)			craked fr = 0.33 sqrt(f'c)		
x direction (mm)	y direction (mm)	x dirección (mm)	y dirección (mm)						elastic	Corner (mm)	Edge (mm)	center (mm)	Corner (mm)	Edge (mm)	center (mm)	Corner (mm)	Edge (mm)
8400	8400	600	600	12.45	265	20.69	100	13.119	12.689	11.015	9.037	21.963	17.784	13.481	34.262	28.226	21.000
								13.147	12.684	11.026	9.031	21.931	17.761	13.404	34.416	28.279	20.988
								-0.21%	0.04%	-0.10%	0.07%	0.15%	0.13%	0.57%	-0.45%	-0.19%	0.06%
8400	8400	300	300	12.45	265	20.69	100	22.093	18.713	13.924	7.316	35.191	24.128	9.492	47.229	33.464	15.413
								21.801	18.737	13.961	7.298	35.185	24.119	9.462	47.017	33.509	15.381
								1.32%	-0.13%	-0.27%	0.25%	0.02%	0.04%	0.32%	0.45%	-0.13%	0.21%
8400	6900	500	500	12.45	265	20.69	100	12.141	9.903	9.100	6.576	16.515	15.852	9.934	27.642	24.598	16.776
								12.253	9.869	9.089	6.501	16.786	15.930	9.765	27.598	24.676	16.706
								-0.92%	0.34%	0.12%	1.14%	-1.64%	-0.49%	1.70%	0.16%	-0.32%	0.42%
6900	6900	600	600	11.49	215	20.69	120	10.932	8.987	8.017	6.922	13.787	11.979	10.088	23.150	19.587	15.600
								10.938	8.948	8.011	6.966	13.793	11.811	10.038	23.251	19.672	15.409
								-0.05%	0.43%	0.07%	-0.64%	-0.04%	1.40%	0.50%	-0.44%	-0.43%	1.22%
6900	5400	600	600	13.40	215	20.69	100	10.204	6.869	6.589	5.518	11.420	11.311	8.239	20.501	16.809	15.828
								10.179	6.832	6.620	5.490	11.315	11.179	8.341	19.720	17.861	15.414
								0.25%	0.54%	-0.47%	0.51%	0.92%	1.17%	-1.24%	3.81%	-6.26%	2.62%
5400	4200	600	600	10.05	165	27.69	100	8.145	4.847	4.447	4.019	6.370	5.943	5.430	11.472	9.998	8.288
								8.259	4.843	4.458	4.015	6.234	6.029	5.295	11.701	9.798	8.133
								-1.40%	0.08%	-0.25%	0.10%	2.14%	-1.45%	2.49%	-2.00%	2.00%	1.87%
5400	4200	300	300	10.05	165	20.69	100	10.604	5.559	5.165	3.403	8.022	7.973	5.404	14.258	13.779	8.226
								10.578	5.507	5.103	3.378	8.073	8.144	5.398	14.221	13.796	8.177
								0.25%	0.94%	1.20%	0.73%	-0.64%	-2.14%	0.10%	0.26%	-0.12%	0.60%
4200	4200	300	300	9.33	125	20.69	100	11.405	5.688	4.899	3.907	8.334	7.312	6.004	14.210	11.651	8.379
								11.371	5.722	4.952	3.926	8.399	7.198	5.999	14.251	11.518	8.498
								0.30%	-0.60%	-1.08%	-0.49%	-0.78%	1.56%	0.08%	-0.29%	1.14%	-1.42%

5.8 VALIDATION OF ANN RESULTS WITH CARDINGTON TEST RESULT

In Chapter 4, the nonlinear FE analysis has been validated against Cardington test deflection results. The performance of ANN in predicting Cardington slab deflection has been studied in this chapter. The long-term deflection of Cardington slab 3 and slab 4 are predicted with ANN program and compared with test results. For comparing the ANN predicted deflection with the Cardington test results some assumptions are made. The assumptions are given below:

1. The external column size is larger in the ANN analysis than the actual Cardington slab where the edge columns were 400 mm x 250 mm.
2. In the real slab, there was punch in the slab, but in the ANN analysis punch is not considered.
3. In the Cardington test slab E_c and f_r value were measured and these value were presented in Table 4.1. In the ANN analysis, the value of E_c and f_r are calculated from value of concrete strength f'_c as per relationship described earlier. To compare the deflection value, the value of f'_c given as input of ANN analysis calculated from test f_r and the deflection values of ANN analysis are reduced to the ratio of calculated E_c to test E_c as the relationship between deflection and E_c is linear.

5.8.1 Validation of deflection of Cardington Slab 3 with ANN

To predict deflection by ANN simulator, the input values for Cardington slab 3 given in the simulator are SPANX = 7500 mm, SPANY=7500 mm, COLX=400 mm COLY=400 mm, Total load = 10.74 kN/m², Thick= 250 mm, f'_c = 34.09 MPa and Reinf. =100%. Some assumptions which are made to compare the ANN results with the test result are discussed above. The predicted values are reduced to the ratio of test E_c and calculated E_c from f'_c and then compared with test results.

Calculation of long-term deflection of corner panel for five-year value of $\xi=2.0$

Immediate predicted cracked deflection in corner panel of slab 3 for maximum load of 10.74 kN/m² ($f_r= 0.62 \sqrt{f'_c}$ N/mm²) is

$$\Delta_{d+l} = 10.83 \text{ mm (ANN prediction)}$$

$$E_c(\text{ANN analysis}) = 4733 \sqrt{34.09} \text{ MPa} = 27.63 \text{ GPa}$$

$$E_c(\text{Test}) = 33.00 \text{ GPa (Table 4.1)}$$

$$\Delta_{d+l} = 10.83 \times \frac{27.63}{33.00} = 9.067 \text{ mm (Modified from ANN value) (FE value = 11.72 mm)}$$

The multiplier for 363 days is 1.4 obtained from ACI multiplier graph (Fig 2.10) and the total deflection is calculated by multiplying the immediate deflection with 2.4 (1.4+1.0). The load used as sustained load in corner panel is 6.75 kN/m² as there was no sustain load in corner panel.

The total deflection for sustained load (6.75 kN/m²) is

$$\Delta_{d363} = 9.067 \times \frac{6.75}{10.74} \times 2.4 = 13.67 \text{ mm}$$

The multiplier for 403 days, 789 days and 1825 days are also obtained similarly from ACI graph (Fig. 2.10)

$$\Delta_{d403} = 9.067 \times \frac{6.75}{10.74} \times 2.46 = 14.01 \text{ mm}$$

$$\Delta_{d789} = 9.067 \times \frac{6.75}{10.74} \times 2.7 = 15.386 \text{ mm}$$

$$\Delta_{d1825} = 9.067 \times \frac{6.75}{10.74} \times 3.0 = 17.09 \text{ mm}$$

Calculation of long-term deflection of corner panel for five-year value of $\xi=3.0$

Immediate cracked deflection in corner panel of floor 3 for maximum load of 10.74 kN/m²

$$\Delta_{d+l} = 9.067 \text{ mm (modified ANN value)}$$

The multiplier value for 363 days is 3.1 which is obtained by multiplying the ξ value of 363 days for five-year value of $\xi=2.0$ with the ratio of 3/2 (1.4*3/2 = 2.1) and the total deflection is calculated by multiplying the immediate deflection with 3.1 (2.1+1.0). The total deflection for sustained load is

$$\Delta_{d363} = 9.067 \times \frac{6.75}{10.74} \times 3.1 = 17.66 \text{ mm}$$

The multiplier for 403 days, 789 days and 1825 days are also obtained similarly. The load used as sustained load in corner panel is 6.75 kN/m^2 as no sustain load in corner panel.

$$\Delta_{d403} = 9.067 \times \frac{6.75}{10.74} \times 3.19 = 18.17 \text{ mm}$$

$$\Delta_{d789} = 9.067 \times \frac{6.75}{10.74} \times 3.55 = 20.23 \text{ mm}$$

$$\Delta_{d1825} = 9.067 \times \frac{6.75}{10.74} \times 4.0 = 22.79 \text{ mm}$$

The predicted ANN long-term deflections and test deflections of corner panel of Cardington slab 3 are presented in Table 5.4 and in Fig. 5.5.

Table 5.4 Experimental and ANN predicted deflection of corner panel of Cardington slab 3

Cracked deflection due to peak load mm	
9.067	

Day	Deflection mm						Variation (%)
	Experimental Value			ANN Predicted value			
	Min.	Max.	Mean	(max. $\xi=3$)	(max. $\xi=2$)	(max. $\xi=3$)	(max. $\xi=2$)
363	17.29	23.14	20.13	17.66	13.67	12.27	32.09
403	17.29	24	20.52	18.18	14.01	11.40	31.72
789	19.27	27.11	23.86	20.23	15.38	15.52	35.54
1825	-	-	-	22.79	17.09	-	-

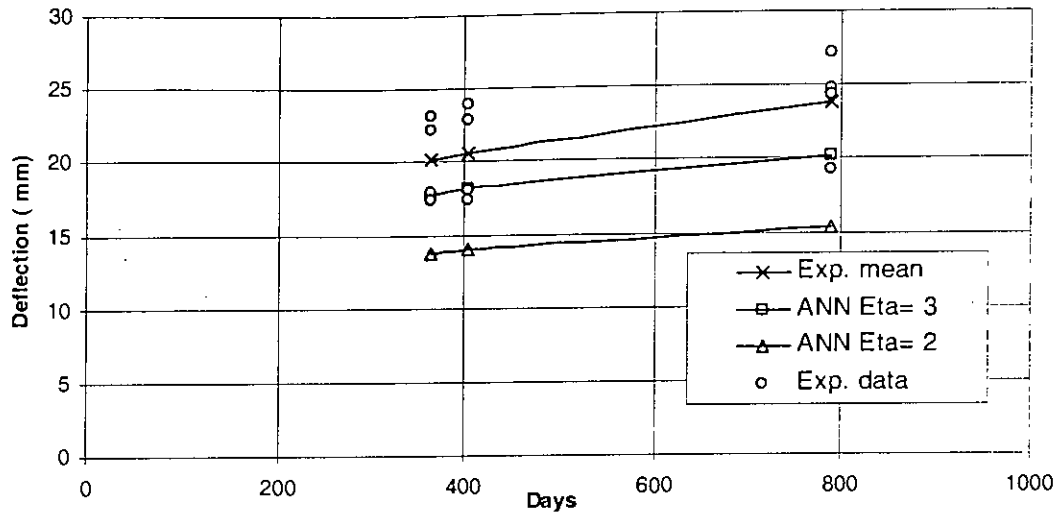


Figure 5.5 Defection versus time curve for experimental and ANN predicted deflection of corner panel of Cardington slab 3

From the Table 5.4 and Fig. 5.5, it is found that the ANN predicted deflections for both five-year value of $\xi = 3.0$ and $\xi = 2.0$ is smaller than the experimental mean deflection value. The larger column size in exterior panel, absence of punch in the slab in the modelling of the FE mesh could be the reason for lower value of predicted deflection than the experimental one.

Calculation of long- term deflection of edge panel

Immediate predicted cracked deflection for maximum load of 10.74 kN/m^2 in edge panel of slab 3 ($f_r = 0.62\sqrt{f'_c} \text{ N/mm}^2$)

$$\Delta_{d+l} = 9.22 \text{ mm (ANN value)}$$

$$\Delta_{d+l} = 9.22 \times \frac{27.63}{33.00} = 7.22 \text{ mm (Modified from ANN value) (FE value = 9.36 mm)}$$

The predicted deflections for edge panel are calculated for five-year value of $\xi = 2.0$ and $\xi = 3.0$ as the same procedure as described in the Chapter 4. The predicted ANN long-term deflection and experimental deflection for edge panel are presented in Table 5.5 and in Fig. 5.6

Table 5.5 Experimental and ANN predicted deflection of edge panel of Cardington slab 3

Cracked deflection due to peak load mm
7.724

Day	Deflection mm						Variation (%)
	Experimental Value			ANN Predicted value			
	Min.	Max.	Mean	(max. $\xi= 3$)	(max. $\xi= 2$)	(max. $\xi= 3$)	(max. $\xi= 2$)
363	15.96	18.19	17.09	15.04	11.64	12.02	31.91
403	18.85	21.58	20.14	20.63	15.91	-2.43	21.00
789	23.93	26.37	24.94	22.96	17.46	7.93	29.99
1825	-	-	-	25.87	19.41	-	-

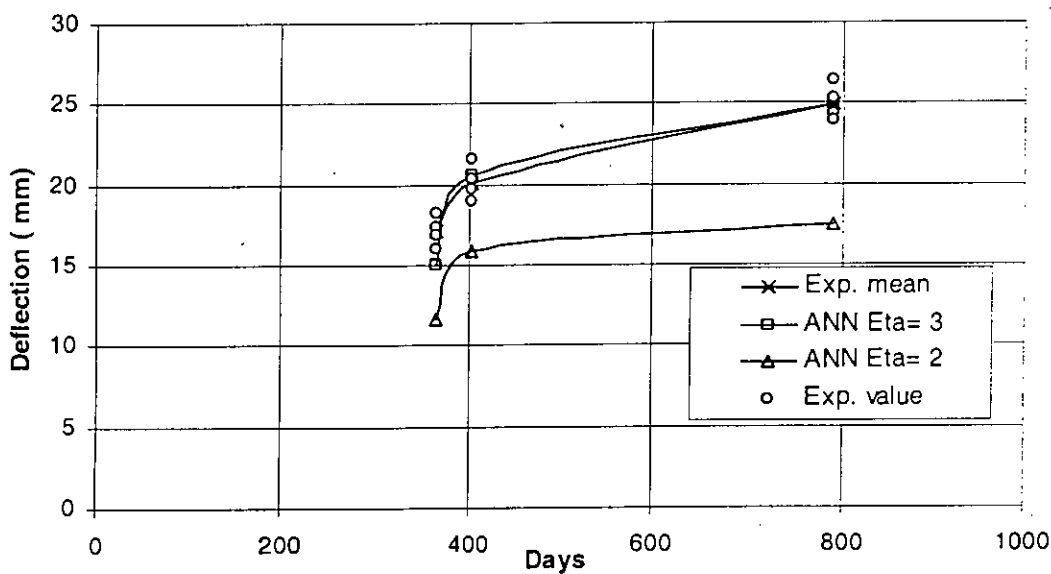


Figure 5.6 Defection versus time curve for Experimental and ANN predicted deflection of edge panel of Cardington slab 3

From the Table 5.5 and Figure 5.6, it is found that the ANN deflection for five-year value of $\xi=3.0$ is showing good agreement with the experimental mean deflection in spite of the larger column size in the exterior panel and absence of punch in the slab in the modelling of the FE mesh.

Calculation of long-term deflection of center panel

Immediate predicted cracked deflection in center panel of slab 3 for maximum load of 10.74 kN/m^2 ($f_r = 0.62\sqrt{f'_c} \text{ N/mm}^2$) is

$$\Delta_{d+l} = 6.37 \text{ mm (ANN value)}$$

$$\Delta_{d+l} = 6.37 \times \frac{27.63}{33.00} = 5.33 \text{ mm (Modified from ANN value) (FE value = 6.17 mm)}$$

The predicted ANN long-term deflection and experimental deflection for center panel of Cardington slab 3 are presented in Table 5.6 and in Fig. 5.7.

Table 5.6 Experimental and ANN predicted deflection of center panel of Cardington slab 3

Cracked deflection due to peak load mm	
5.33	

Day	Deflection mm						Variation (%)
	Experimental Value			Predicted value			
	Min.	Max.	mean	(max. $\xi=3$)	(max. $\xi=2$)	(max. $\xi=3$)	(max. $\xi=2$)
363	9.48	10.24	9.86	10.39	8.045	-5.37	18.45
403	11.74	12.5	12.12	14.25	10.99	-17.57	9.32
789	15.00	16.06	15.53	15.86	12.06	-2.12	22.34
1825	-	-	-	17.87	13.41	-	-

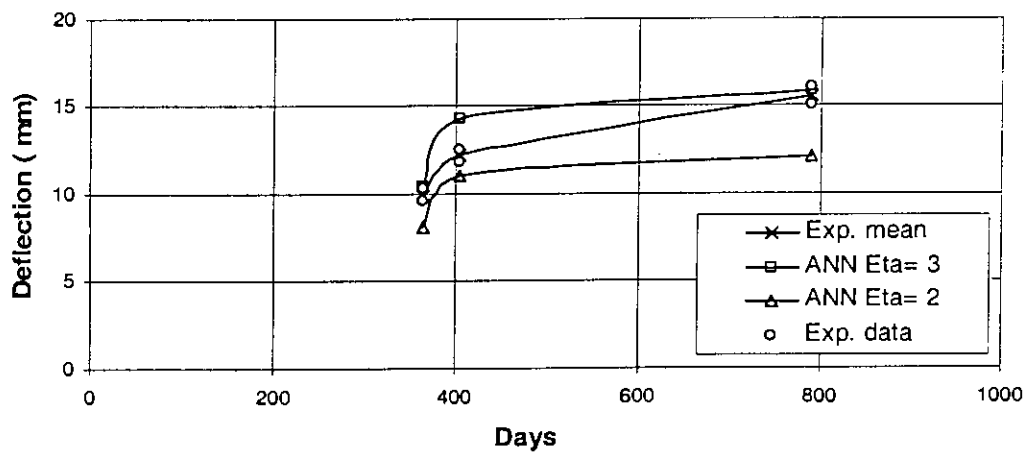


Figure 5.7 Deflection versus time curve for Experimental and ANN predicted deflection of center panel of Cardington slab 3

From the Table 5.6 and Figure 5.7, it is found that the experimental mean deflection value lies in between the ANN deflection value for five-year value of $\xi=3.0$ and $\xi=2$ and the ANN prediction using the five year value for $\xi=3.0$ giving good agreement with experimental mean value .

5.8.2 Validation of deflection of Cardington Slab 4 with ANN

Calculation of long-term deflection of corner panel

Immediate predicted cracked deflection in corner panel of Cardington slab 4 for maximum load of 10.74 kN/m^2 ($f_r = 0.62 \sqrt{f'_c} \text{ N/mm}^2$)

$$\Delta_{d+l} = 8.494 \text{ mm (ANN)}$$

$$E_c(\text{ANN analysis}) = 4733 \sqrt{45.67} \text{ MPa} = 31.98 \text{ GPa}$$

$$E_c(\text{Experimental}) = 35.18 \text{ GPa (Table 4.1)}$$

$$\Delta_{d+l} = 8.494 \times \frac{31.98}{35.18} = 7.721 \text{ mm (Modified from ANN value) (FE value = 9.975 mm)}$$

The predicted ANN long-term deflection and experimental deflection for corner panel of Cardington slab 4 are presented in Table 5.7 and in Fig. 5.8.

Table 5.7 Experimental and ANN predicted deflection of corner panel of Cardington slab 4.

Cracked deflection due to peak load mm	
7.721	

Day	Deflection mm					Variation (%)	
	Experimental Value			Predicted value			
	Min.	Max.	Mean	(max. $\xi=3$)	(max. $\xi=2$)	(max. $\xi=3$)	(max. $\xi=2$)
351	20.03	23.03	21.62	15.73	12.18	27.2	43.7
391	19.6	23.25	21.58	16.11	12.43	25.3	42.4
776	21.28	25.22	23.33	17.86	13.6	23.4	41.7
876	22.13	26.4	24.43	18.17	13.8	25.6	43.5
1825	-	-	-	20.30	15.22	-	-

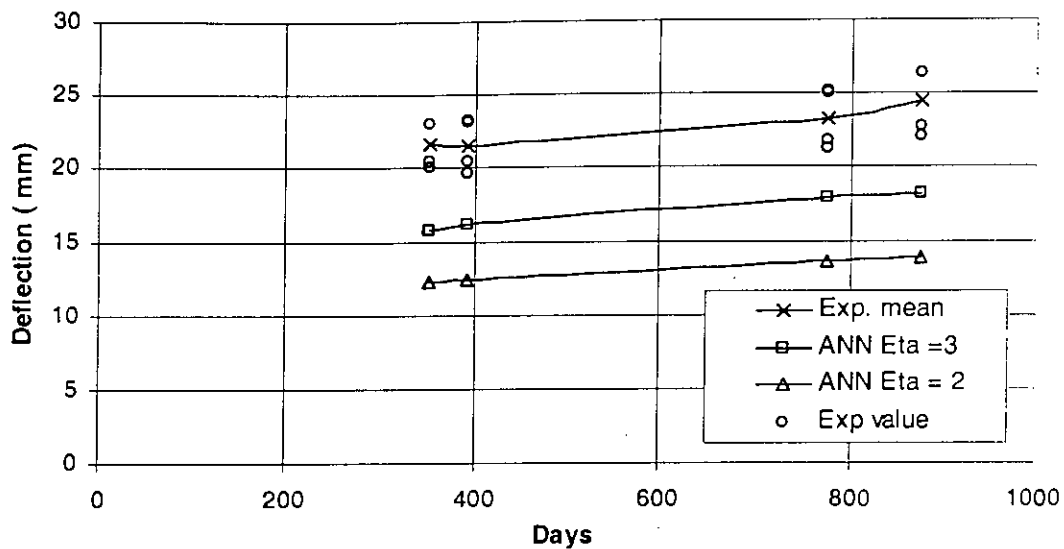


Figure 5.8 Deflection versus time curve for Experimental and ANN predicted deflection of corner panel of Cardington slab 4

From the Table 5.7 and Fig. 5.8, it is found that the ANN predicted deflection for both five-year value of $\xi = 3.0$ and $\xi = 2.0$ is smaller than the experimental mean deflection value. The larger column size in the exterior panel, absence of punch in the slab in the modelling of the FE mesh could be the reason for lower value of predicted deflection than the experimental results.

Calculation of long-term deflection of edge panel

Immediate predicted cracked deflection for $f_{ct} = (0.62\sqrt{f'_c} \text{ N/mm}^2)$ for maximum load of 10.74 kN/m^2 in edge panel of slab 4

$$\Delta_{d+I} = 6.742 \text{ mm (ANN)}$$

$$\Delta_{d+I} = 6.742 \times \frac{31.98}{35.18} = 6.129 \text{ mm (Modified from ANN value) (FE value = 8.124 mm)}$$

The predicted ANN long-term deflection and experimental deflection for edge panel of Cardington slab 4 are presented in Table 5.8 and in Fig. 5.9.

Table 5.8 Experimental and ANN predicted deflection of edge panel of Cardington slab 4.

Cracked deflection due to peak load mm	
6.129	

Day	Deflection mm					Variation (%)	
	Experimental Value			Predicted value			
	Min	Max	Mean	(max $\xi=3$)	(max $\xi=2$)	(max $\xi=3$)	(max $\xi=2$)
351	12.85	14.70	13.85	12.48	9.67	9.89	30.18
391	14.53	17.36	16.12	12.79	9.87	20.66	38.77
776	17.97	21.06	19.57	18.91	14.39	3.37	26.47
876	22.38	18.94	20.65	19.228	14.61	6.89	29.25
1825	-	-	-	21.483	16.11	-	-

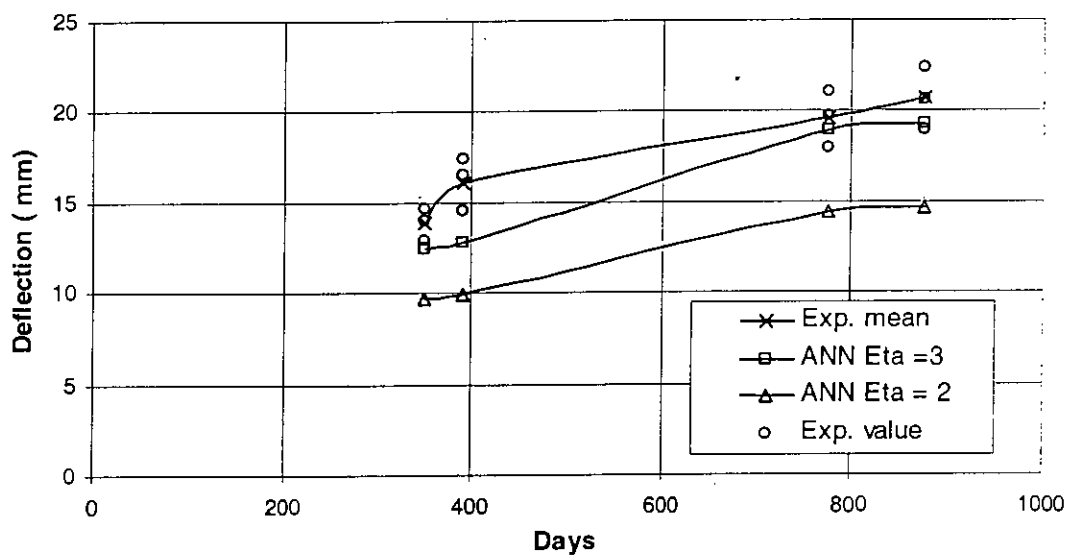


Figure 5.9 Deflection versus time curve for Experimental and ANN predicted deflection of edge panel of Cardington slab 4

From the Table 5.8 and Fig. 5.9, it is found that the ANN deflection value for five-year value of $\xi = 3.0$ is showing good agreement with the experimental mean deflection value in spite of the larger column size in the exterior panel and absence of punch in the slab in the modelling of the FE mesh.

Calculation of long-term deflection of center panel

Immediate predicted cracked deflection in center panel of Cardington slab 4 for maximum load of 10.74 kN/m^2 ($f_c = 0.62\sqrt{f'_c} \text{ N/mm}^2$)

$$\Delta_{d+l} = 5.361 \text{ mm (ANN)}$$

$$\Delta_{d+l} = 5.361 \times \frac{31.98}{35.18} = 4.87 \text{ mm (Modified from ANN value)}$$

The predicted ANN long-term deflection and experimental deflection in center panel of Cardington slab 4 are presented in Table 5.9 and in Fig. 5.10.

Table 5.9 Experimental and ANN predicted deflection of center panel of Cardington floor 4

Cracked deflection due to peak load mm
5.361

Day	Deflection mm						Variation (%)	
	Experimental Value			Predicted value				
	Min	Max	Mean	(max $\xi=3$)	(max $\xi=2$)	(max $\xi=3$)	(max $\xi=2$)	
351	7.79	8.18	7.99	9.93	7.69	-24.28	3.75	
391	9.92	10.21	10.07	10.17	7.85	-0.99	22.05	
776	11.82	13.29	12.55	15.03	11.45	-19.76	8.76	
876	12.16	13.89	13.03	15.29	11.62	-17.34	10.82	
1825	-	-	-	17.08	12.81	-	-	

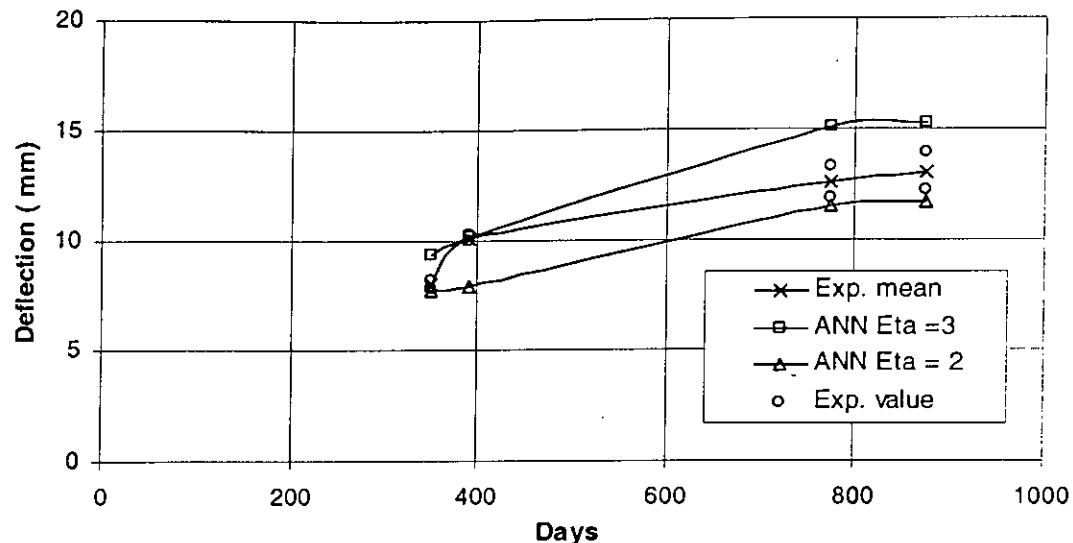


Figure 5.10 Deflection versus time curve for Experimental and ANN predicted deflection of center panel of Cardington slab 4

From the Table 5.9 and Fig. 5.10, it is found that the experimental mean deflection value lies in between the ANN deflection value for five-year value of $\xi=3.0$ and $\xi=2$ and the ANN value for $\xi=2.0$ giving good agreement with experimental mean value.

5.8.3 Discussion of ANN prediction with Cardington experimental results

From the above discussion, it can be concluded that the deflection prediction by ANN for Cardington slab 3 and 4 are giving reasonable good prediction. The difference of geometry of the ANN slab with the actual Cardington slab has more effect in the deflection of corner panel and the predicted deflection in corner panel is lesser than the experimental results. In the edge panel and in the center panel, the ANN prediction shows good performance. Thus the ANN simulator predicts reasonably good deflection value for the Cardington slab and the performance of the ANN has been validated.

5.9 Deflection prediction by ANN: Case study

To predict deflection of flat plate slab by ANN, the ANN simulator has been trained with the database containing known input-output obtained by nonlinear FE analysis.

After the training has been completed, ANN is capable of predicting deflection of flat plate slab. The use of the ANN to predict deflection is described in Section 5.6. Then the performance of ANN in predicting deflection has been validated with numerical and experimental results. The performance of the ANN in predicting deflection of flat plate slabs is reasonably good. Now three case studies will be described to demonstrate how a designer can predict deflection of a real building and then to select the slab thickness.

5.9.1 Case Study 1:

A 10 storied office building of 3x3 panel with flat plate floor system (no edge beam, dropped panel or column capital) having span length of 6000 mm in both direction and the column size is 500 mm by 500 mm for all columns. The loads considered are 1 kN/m² for floor finish, 1.44 kN/m² for random partition wall and 2.4 kN/m² for live load. Material strengths used are $f_y = 414 \text{ MPa}$, $f'_c = 20.69 \text{ MPa}$. For long-term deflection calculation, the long-term multiplier $\xi = 3$ will be used as per Branson.

Calculation of slab thickness

$$\text{Clear span} = 6000 - 500 = 5500 \text{ mm}$$

$$\text{Slab thickness} = \frac{5500}{30} = 183 \text{ mm} \approx 190 \text{ mm} \quad (\text{according to ACI Code2002})$$

$$\text{Self weight} = 4.5 \text{ kN/m}^2$$

$$\text{Floor finish} = 1 \text{ kN/m}^2$$

$$\text{Random partition wall} = 2.4 \text{ kN/m}^2$$

$$\text{Live load} = 2.9 \text{ kN/m}^2$$

$$\text{Total un-factored load} = 4.5 + 1 + 1.44 + 2.4 = 9.34 \text{ kN/m}^2$$

The eight inputs required to predict the short-term deflections are given to the ANN predictor as shown in Fig. 5.11.

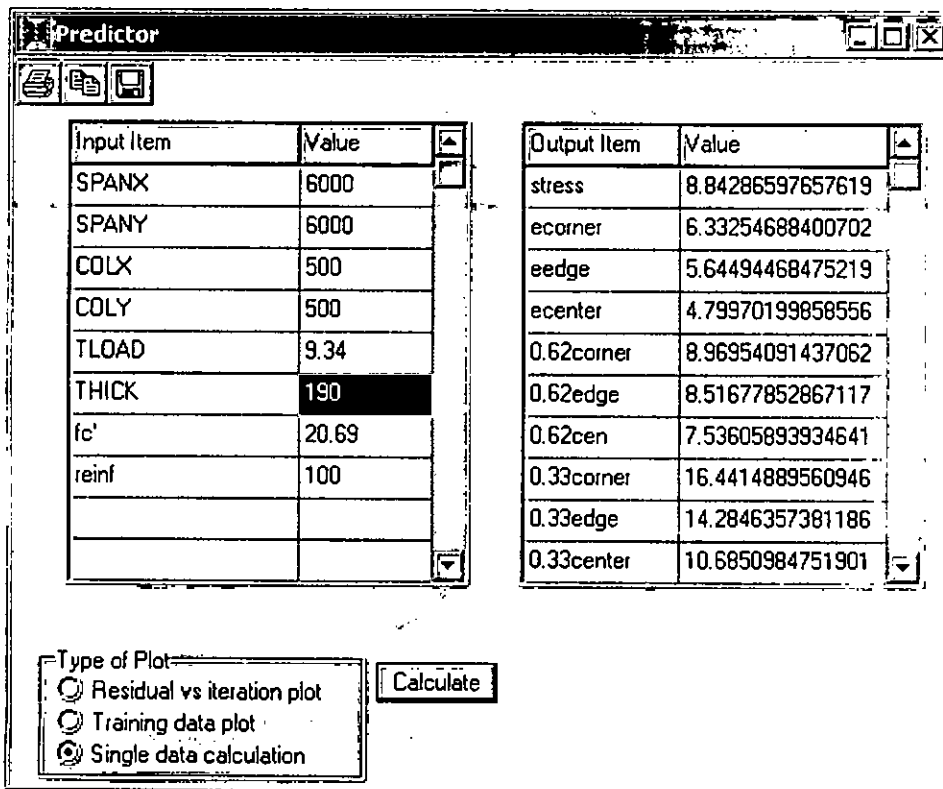


Figure 5. 11 Deflection predictions by ANN

Long term deflection calculation of corner panel

Immediate predicted deflection for dead and live load in corner panel for $0.62\sqrt{f_c'}$

MPa using ANN is

$$\Delta_{d+l} = 8.97 \text{ mm}$$

Using the long-term multiplier $\xi = 3$, the time dependent portion of dead load deflection is

$$\Delta_d = 8.97 \times \frac{6.94}{9.34} \times 3 = 19.99 \text{ mm}$$

The long-term deflection due to sustained portion of live load is

$$\Delta_{0.3l} = 8.97 \times \frac{6.94}{9.34} \times 3 = 2.76 \text{ mm}$$

The instantaneous deflection due to application of short-term portion of the live load is

$$\Delta_{0.7L} = 8.97 \times \frac{2.4}{9.34} \times 0.7 = 1.61 \text{ mm}$$

The total incremental deflection is $\Delta = 19.99 + 2.76 + 1.61 = 24.37 \text{ mm}$

The ACI Code limitation of incremental deflection is $\frac{span}{480} = 12.5 \text{ mm}$

The total deflection is $\Delta_{total} = 19.99 \times \frac{4}{3} + 2.76 + 1.61 = 31.03 \text{ mm}$

The ACI Code limitation of total deflection is $\frac{span}{240} = 25 \text{ mm}$

Both the incremental deflection and the total deflection exceed the allowable limit.

Hence the slab thickness is not adequate and needs to be increased.

5.9.2 Case Study 2:

A 10 storied office building of 3x3 panel with flat plate floor system (no edge beam, dropped panel or column capital) having span length of 6000 mm in both direction and the column size is 500 mm by 500 mm for all columns. The loads considered are 1 kN/m² for floor finish, 1.44 kN/m² for random partition wall and 2.4 kN/m² for live load. Materials strength used are f_y = 414 MPa, f'_c = 20.69 MPa. For long-term deflection calculation, the long-term multiplier ξ= 2 will be used as per ACI Code (2002).

Calculation of slab thickness

Clear span = 6000 - 500 = 5500 mm

Slab thickness = $\frac{5500}{30} = 183 \text{ mm} \approx 190 \text{ mm}$ (according to ACI Code 2002)

Self weight = 4.5 kN/m²

Floor finish = 1 kN/m²

Random partition wall = 2.4 kN/m²

Live load = 2.9 kN/m²

Total un-factored load = 4.5+1+1.44+2.4 = 9.34 kN/m²

Long term deflection calculation of corner panel

Immediate predicted deflection for dead and live load in corner panel for $0.62\sqrt{f'_c}$

MPa using ANN is

$\Delta_{d+l} = 8.97 \text{ mm}$

Using the long-term multiplier $\xi = 2$, the time dependent portion of dead load deflection is

$$\Delta_d = 8.97 \times \frac{6.94}{9.34} \times 2 = 13.33 \text{ mm}$$

The long-term deflection due to sustained portion of live load is

$$\Delta_{0.3l} = 8.97 \times \frac{6.94}{9.34} \times 2 = 2.07 \text{ mm}$$

The instantaneous deflection due to application of short-term portion of the live load is

$$\Delta_{0.7L} = 8.97 \times \frac{2.4}{9.34} \times 0.7 = 1.61 \text{ mm}$$

The total incremental deflection is $\Delta = 13.33 + 2.07 + 1.61 = 17.06 \text{ mm}$

The ACI Code limitation of incremental deflection is $\frac{\text{span}}{480} = 12.5 \text{ mm}$

The total deflection is $\Delta_{\text{total}} = 13.33 \times \frac{3}{2} + 2.76 + 1.61 = 23.68 \text{ mm}$

The ACI Code limitation of total deflection is $\frac{\text{span}}{240} = 25 \text{ mm}$

The incremental deflection exceeds the allowable limit. The total deflection is within the allowable limit. Hence the slab thickness is not adequate from incremental deflection point of view.

5.9.3 Case Study 3:

A 10 storied office building of 3x3 panel with flat plate floor system (no edge beam, dropped panel or column capital) having span length of 4500 mm in both direction and the column size is 400 mm by 400 mm for all columns. The loads considered are 1 kN/m² for floor finish, 1.44 kN/m² for random partition wall and 2.4 kN/m² for live load. Materials strength used are $f_y = 414 \text{ MPa}$; $f'_c = 20.69 \text{ MPa}$. For long term deflection calculation, the long-term multiplier $\xi = 2$ will be used as per ACI Code.

Calculation of slab thickness

Clear span = 4500 - 400 = 4100 mm

$$\text{Slab thickness} = \frac{4100}{30} = 137 \text{ mm} \approx 140 \text{ mm} \quad (\text{according to ACI Code})$$

Self Weight = 3.3 kN/m²

Floor finish = 1 kN/m²

Random partition wall = 1.44 kN/m²

Live load = 2.4 kN/m²

Total un-factored load = $3.3+1+1.44+2.4=8.14 \text{ kN/m}^2$;

Long term deflection calculation of corner panel

Immediate predicted deflection for dead and live load in corner panel for $0.62\sqrt{f_c}$

MPa using ANN is

$$\Delta_{d+l} = 4.88 \text{ mm}$$

Using the long-term multiplier $\xi = 2$, the time dependent portion of dead load deflection is

$$\Delta_d = 4.88 \times \frac{5.74}{8.14} \times 2 = 6.89 \text{ mm}$$

The long-term deflection due to sustained portion of live load is

$$\Delta_{0.3l} = 4.88 \times \frac{2.4}{8.14} \times 2 = 1.29 \text{ mm}$$

The instantaneous deflection due to application of short-term portion of the live load is

$$\Delta_{0.7L} = 4.88 \times \frac{2.4}{8.14} \times 0.7 = 1.00 \text{ mm}$$

The total incremental deflection is $\Delta = 6.89 + 1.29 + 1.00 = 9.18 \text{ mm}$

The ACI Code limitation of incremental deflection is $\frac{\text{span}}{480} = 9.375 \text{ mm}$

The total deflection is $\Delta_{total} = 6.89 \times \frac{3}{2} + 1.29 + 1.00 = 12.63 \text{ mm}$

The ACI Code limitation of total deflection is $\frac{\text{span}}{240} = 18.75 \text{ mm}$.

The incremental deflection and the total deflection is within the allowable limit. Hence the slab thickness is adequate.

Minimum thickness of flat plate slab as per ACI Code (Table 2.2) is very much simplified which mainly depends on span length. But from serviceability point of

view, there are a number of parameters e.g. column size, loading, material properties and long-term multiplier have significant effect on deflection of flat plate slab. The ACI Code specified thickness may not be adequate for all conditions. Hence, a designer should calculate deflection before selecting the slab thickness.

5.10 CONCLUSION

Deflection estimation of reinforced concrete member is a complicated problem for both immediate (short-term) deflection and time dependent (long-term) deflection. The immediate deflection should be calculated based on the properties of the cracked member as flat plate slabs are generally cracked even under service loads. It takes huge time to calculate short-term deflection by rigorous hand calculation or nonlinear FE analysis. On the other hand, the time dependent deflection of concrete due to creep and shrinkage is also difficult to determine. To solve this problem, a simplified method of predicting deflections of flat plate has been developed in this chapter. A database has been developed using the results of the FE package for training the ANN. Short-term deflection is obtained using the trained ANN program and the long-term deflection is calculated by using ACI multiplier. The study shows that in most of the cases, deflection prediction by ANN analysis is similar with FE results. The performance of ANN program has also been verified against experimental results of Cardington slabs and the performance of deflection prediction of flat plate slab is reasonably good. The trained network can easily be used to predict the short-term deflection of flat plate slab. A designer can predict short- term deflection for flat plate slab using only a small number of inputs value without any rigorous calculation. Long-term deflections can also be estimated easily using ACI long-term multiplier and the designer will be able to select the appropriate thickness of the flat plate slab.

CHAPTER 6

CONCLUSION AND RECOMMENDATION

6.1 INTRODUCTION

The main aim of this research work is to develop a tool for prediction of short-term as well as long-term deflections of flat plate slabs using Artificial Neural Network (ANN). In recent years, realistic estimation of slab deflections under service loads has become more important than ever due to increasing use of high strength materials and due to the use of ultimate limit state design that generally leads to thinner members. The current work starts with a literature review, which is presented in Chapter 2, where different methods of deflection calculation are discussed. A brief introduction to Neural Network and Artificial Neural Network are given in this chapter. In Chapter 3, performance of nonlinear FE analysis using ACI/Branson crack model is studied with experimental short-term deflection. In Chapter 4, the short-and long-term deflections of slabs of full scale Cardington ECBP building have been determined using ACI/Branson crack model along with ACI long-term multiplier. In Chapter 5, deflection prediction by ANN is discussed and performance of ANN against Cardington test results is also studied. The total work is summarized in the current chapter along with conclusions and recommendations for future works.

6.2 SUMMARIES AND CONCLUSION

6.2.1 Nonlinear FE analysis

Nonlinear Finite Element analysis has been discussed in Chapter-3 and Chapter-4. A nonlinear FE analysis involving Branson's model to reduce stiffness due to cracking has been employed. Following are the findings of the study:

- The results obtained from nonlinear FE analysis have been compared with the experimental results of McNeice's (1971) corner supported and one way slab and Shukla and Mittal's (1976) edge supported slab. FE results have shown good performance with experimental results.

- The short-term and long-term deflections determined using nonlinear FE analysis and ACI long term multiplier have been compared with the Cardington test results. Predicted short-term deflections are higher than the test values. For long term deflection, the designer will get conservative value by using the five year value of $\xi = 3.0$.
- Earlier studies [Hossain & Vollum(2002), Hossain (1999)] predicted deflection-time histories of Cardington slabs correctly using MC-90 approach where effect of creep and shrinkage are more rigorously dealt with. In the current study, a somewhat conservative prediction of deflection with time has been achieved using a much simpler ACI long-term multiplier approach.
- To get long-term deflection, the designer must multiply the short-term cracked deflection with ACI multiplier, not the elastic deflection as all the slabs are cracked even under service load as observed from analysis of Cardington slabs.

6.2.2 Deflection prediction by Artificial Neural Network

Deflection calculation using FE analysis, considering cracking is time consuming and may be proved difficult for the designer. In Chapter 5, deflection prediction for flat plate slab using ANN is discussed. The summaries of this Chapter are as follows:

- The results obtained from nonlinear FE analysis have been used to train the ANN program. Some results have been checked randomly and good correlations have been observed between FE analysis results and ANN results.
- The results obtained from ANN have also been compared with Cardington test results and performance of ANN is reasonably good in predicting the test deflections.
- The increase of reinforcement has a little effect on the deflection whereas the reduction of slab thickness as specified by ACI Code (2002) has a large effect on the deflection.

6.3 CONCLUSION

Deflection is an important parameter in slab design. Excessive deflections of reinforced concrete slabs can cause severe serviceability problems. The calculation of short-term and long-term deflections of flat plate slab using nonlinear FE method is difficult and time consuming. In the current work, a general purpose ANN prediction tool have been trained so that a designer can easily calculate short as well as long-term deflections using only a small number of inputs. Use of the ANN software has been demonstrated with example.

6.4 RECOMMENDATIONS FOR FUTURE WORK

The following recommendations are made for future works:

- The study can be extended for larger number of panels in both directions having different span length in each panel with different column size for interior and exterior panels of flat plate slabs.
- The long term deflection prediction using ACI multiplier can be incorporated in the ANN program itself.
- It is possible to develop ANN prediction for other structure related problems.

REFERENCES

- ACI Committee 435 (1991), *State-of-the-Art Report on Control of Two-way Slab Deflections*, American Concrete Institute, Michigan.
- ACI Committee 318-02 (2002), *Building Code Requirements for Structural Concrete (ACI 318-02) and Commentary (ACI 318R-02)*, American Concrete Institute, Michigan.
- Alam, M. R. (2003), *Computation of Deflections of Edge Supported Reinforced Concrete Slabs under Service Loads*, M. Sc. Engineering thesis, BUET, Dhaka.
- Bernal, D. and Leet, K. M. (1997), *Reinforced Concrete Design*, 3rd Edition, McGraw-Hill Book Co., New York.
- Branson, D. E. (1977), "Deformation of Concrete Structures," McGraw-Hill Book Co., New York.
- Breen, J. E., Ferguson, P. M. and Jirsa, J. O. (1988), *Reinforced Concrete Fundamentals*, 5th Edition, John Wiley and Sons, New York.
- CEB-FIP (1993), *CEB-FIP Model Code 1990-Design Code*, Comité Euro International de Béton (CEB), Lausanne.
- EC2 Editorial Group (1991), *Design of Concrete Structures, Part 1 General Rules and Rules for Building*, Eurocode-2.
- Fausett, L. (1994), *Fundamentals of Neural Networks*, Prentice – Hall, Englewood Cliffs, New Jersey.
- Ghali, A. (1989), "Prediction of Deflection of Two-Way Floor Systems," *ACI Structural Journal*, 86 (5), 551-562.
- Gilbert, R. I. (1999), "Deflection Calculation for Reinforced Concrete Structures- why we sometimes get it wrong," *ACI Structural Journal*, 96(6), 1027-1032.
- Goharian and Grossman (2003), *Neural Network Classification*, Illinois Institute of Technology.
- Graham, C.J. and Scanlon, A.(1986), "Long-term Multiplier for Estimating Two-Way Slab Deflections," *ACI Journal*, 83(6), 699-908.
- Haykin, S. (1999), *Neural Networks*, 2nd Edition, Prentice-Hall, Englewood Cliffs, New Jersey.
- Hitchings, D. (1999), *FE-77 User manual*, version 2.54, Aeronautics Dept., Imperial College, University of London.

- Hossain, T.R. and Vollum R.L. (2002), "Prediction of Slab Deflections and Validation against Cardington Data," *Structures & Building*, 152 (3), 235-248.
- Hossain, T.R. (1999), *Numerical Modeling of Deflections of Reinforced Concrete Flat Slabs under Service Loads*, PhD. thesis, University of London.
- Jeforiet, J.C. and McNeice, G. M. (1971), "Finite-Element Analysis of Reinforced Concrete Slabs," *Journal of the Structural Division, ASCE*, 97(3), 785-806.
- Jokinen, E.P. and Scanlon, A. (1987), "Field Measured Two-Way Slab Deflections" *Canadian Journal of Civil Engineering*, 14, 807-819.
- McNeice, G. M. (1967), *Elastic-Plastic Analysis of Flat Plates by Finite Element Method*, PhD. Thesis, University of London.
- Meyers, B.L. and Branson, D.E. (1972), "Design Aid for Predicting Creep and Shrinkage Properties of Concrete" *ACI Journal*, 69, 551-555.
- Nilson, A. H., Darwin D. and Dolan C.W. (2003), *Design of Concrete Structures*, 13th Edition, McGraw-Hill Book Co., New York.
- Nilson, A. H. (1997), *Design of Concrete Structures*, 12th Edition, McGraw-Hill Book Co., New York.
- Nilson, A.H. and Slate, F.O. (1984), "Performance of High-Strength Concrete Beams under Sustained Loads," *Research Report No.84-4*, Department of Structural Engineering, Cornell University.
- Nilson, A.H. and Walters, D. B. (1975), "Deflection of two-way floor systems by the equivalent frame method," *ACI Journal*, 72(5), 210-218.
- Patodi, S.C. (2001), *Application of Artificial Intelligence in Structural Engineering*, M.Sc. thesis, Applied Mechanics Dept. ,University of Baroda, Gujarat.
- Polak, M.A. (1996), "Effective Stiffness Model for Reinforced Concrete Slab," *Journal of Structural Engineering, ASCE*, 122(9), 1025-1030.
- Rangan, B. V. (1976), "Prediction of long-term deflections of flat plates slabs," *ACI Journal*, 73, 223-226.
- Scanlon, A. and Murry, D.W. (1982) "Practical Calculation of Two-way Slab Deflections," *International Design & Construction*, 4(11), 43-56.
- Scanlon, A. and Thompson, D. P. (1990), "Evaluation of ACI-318 Minimum Thickness Requirements for Control of Two-Way Slab Deflections," *ACI Structural Journal*, 87 (6), 657-661.

Shukla, S. N. and Mittal, M. K. (1976), "Short-term deflection in two-way reinforced concrete slabs after cracking," *ACI Structural Journal*, 73, 416-419.

Siddique, M.S.A. (2007), *Neural Network Simulator*, <http://203.208.166.84/sid/www.buet.ac.bd/ce>.

Stephen, W. (2002), *A new kind of science* (Wolfram Media, 2002), Stephen Wolfram, LLC.

Tam, K.S.S. and Scanlon, A. (1986), "Deflection of Two-Way Slabs subjected to Restraint Volume Change and Transverse Loads," *ACI Structural Journal*, 83(5), 737-774.

Uddin M.T. (2005), *Deflection estimation of edge supported reinforced concrete slabs using Artificial Neural Network*, M. Engineering thesis, BUET, Dhaka.

Vollum R.L, Moss R.M. and Hossain T.R. (2002), "Slab Deflections in the Cardington In-situ Concrete Frame Building," *Magazine of Concrete Research*, 54(1), 23-34.

Wang, C. K. and Salmon, C. G. (1998), *Reinforced Concrete Design*, 6th Edition, Wesley Educational Publishers, Inc, California.

Yu, W.W. and Winter, G. (1960), "Instantaneous and Long-Time deflection of reinforced Concrete Beams under Working Loads," *ACI Journal*, 57(1), 29-50.

Appendix -A

DESIGN OF FLAT PLATE

For the design of flat plate, equivalent frame method is used in the thesis work and a numerical example of the flat plate design followed in the thesis work is given below.

Design data

Span = 7.2 m x 7.2m(22 ft x 22 ft), 3 x 3 panel, no edge beam (as shown in Fig. A.1)

Column size = 450 x 450 mm(18 in x 18 in)

Floor finish = 1 kN/m² (20 psf)

Random partition wall = 2.4 kN/m² (50 psf)

Live load = 4.8 kN/m² (100 psf)

Floor to floor height = 3.66 m(12 ft)

f'c = 28 MPa (4000 psi)

f_y = 414 MPa (60000 psi)

$$1 \text{ kN/m}^2 = 20.88 \text{ psf}$$

$$1 \text{ MPa} = 145 \text{ psi}$$

$$1 \text{ kN/m}^2 = 20.88 \text{ psf}$$

$$1 \text{ m} = 3.28 \text{ ft}$$

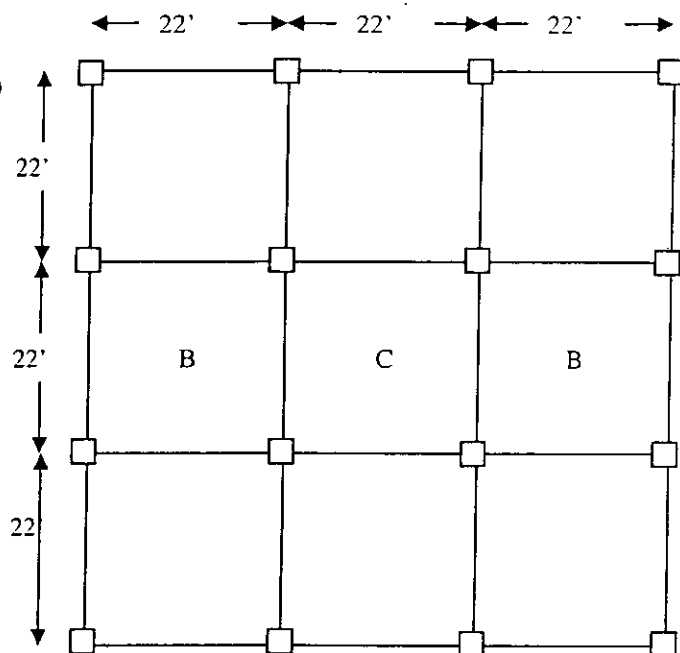


Figure A.1 Two-way flat plate slab

Design:

- **Slab thickness**

Minimum slab thickness h for a flat plate, according to ACI code

$$h = \frac{l_n(800 + 0.005f_y)}{36000}$$

$$h = \frac{20.5 \times 12(800 + 0.005 \times 60000)}{36000}$$

$$= 7.52 \text{ inch}$$

$$l_n = \text{max span} - \text{min col.size}$$

$$= 22 - 1.5 = 20.5 \text{ ft}$$

For flat plate with no edge beam, increase slab thickness by 10%

$$h = 7.52 \times 1.1 = 8.27 \text{ inch rounded to 8.5 inch}$$

Provide h = 8.5 inch

- Load calculation

Dead load $w_d = 8.5 * \frac{150}{12} + 20 = 106 + 20 = 126 \text{ psf}$

Live load $w_l = 100 \text{ psf}$

Factored design loads are

Factored DL = 1.4 $w_d = 1.4 \times 126 = 176 \text{ psf}$

Factored LL = 1.7 $w_l = 1.7 \times 100 = 170 \text{ psf}$

Total factored load = $176 + 170 = 346 \text{ psf}$

- Stiffness Calculation

Slab stiffness $K_s = \frac{4E_c I_s}{l_n}$
 $= \frac{4E_c \times 13510.75}{264}$
 $= 205 E_c$

Column stiffness $K_s = \frac{4E_c I_c}{l_c}$
 $= \frac{4E_c \times 8748}{144}$
 $= 243 E_c$

Torsional stiffness $K_t = \frac{9E_{cs} C}{l_2(1 - c_2/l_2)^3}$
 $= \frac{9E_{cs} \times 2590}{264(1 - 1.5/22)^3}$
 $= 109 E_c$

$I_s = \frac{22 \times 12 \times 8.5^3}{12} = 13510.75 \text{ in}^4$

$l_n = 22 \times 12 = 264 \text{ in}$

$I_c = \frac{18 \times 18^3}{12} = 8748 \text{ in}^4$

$l_c = 12 \times 12 = 144 \text{ in}$

l_2 = (span length in \perp direction) = 22 ft

c_2 = size of col in \perp direction = 18 in

- The equivalent column

For internal panel at each joint there are two columns and two torsional members

$$\frac{1}{K_{ec}} = \frac{1}{2 \times 243 E_c} + \frac{1}{2 \times 109 E_c}$$

From which $K_{ec} = 151 E_c$

- Distribution factor**

For panel B

$$\text{The distribution factor for slab} = \frac{205}{205 + 151} = 0.576$$

$$\text{The distribution factor for column} = 1 - 0.576 = 0.474$$

For panel C

$$\text{The distribution factor for slab} = \frac{205}{205 + 205 + 151} = 0.365$$

$$\text{The distribution factor for column} = 1 - 0.365 - 0.365 = 0.27$$

- Load cases**

$$\text{The ratio of LL to DL} = 100/126 = 0.79 > 0.75$$

So as per ACI code maximum positive and negative moment must be based on pattern loading. Three load cases is considered

- Full factored DL and LL = $176 + 170 = 346 \text{ psf}$ in all panel
- Full factored DL 176 psf in all spans and 0.75 factored LL = $0.75 \times 170 = 128 \text{ psf}$ in panel C
- Full factored DL 176 psf in all spans and 0.75 factored LL = $0.75 \times 170 = 128 \text{ psf}$ in first and second span

- Moment distribution**

$$\text{Load case a: Load} = 346 \text{ psf all panel, Fixed end moment} = \frac{346 \times 22^2 \times 22}{12} = 308 \text{ k-ft}$$

Table A.1 Moment distribution of load case a (k-ft) (1k-ft = 1.35 kN-m)

Panel	B			C			B		
Joint	1		2	2		3	3		4
DF	0.576		0.365	0.365		0.365	0.365		0.576
FEM	308		-308	308		-308	308		-308
COM	-177.3								173.3
			-88.6				88.6		
			32.4	32.4		-32.4	-32.4		
	16.2			-16.2		16.2			-16.2
	-9.3		5.9	5.9		-5.9	-5.9		9.3
	2.9			-2.9		2.9			-2.9
	-1.7		1.1	1.1		-1.1	-1.1		1.7
	0.5			-0.5		0.5			-0.5
	.3		0.2	0.2		-0.2	-0.2		
Final moments	139		-357	328		-328	357		-139

Load case b: 176 psf panel B and 346 psf panel C

$$\text{Fixed end moment} = \frac{176x22^2x22}{12000} = 157 \text{ k-ft}, \frac{346x22^2x22}{12000} = 304 \text{ k-ft.}$$

Table A.2 Moment distribution of load case b (k-ft) (1k-ft = 1.35 kN-m)

Panel	B			C			B		
Joint	1		2	2		3	3		4
DF	0.576		0.365	0.365		0.365	0.365		0.576
FEM	157		-157	270		-270	157		-157
COM	-90.4		-41.4	-41.4		41.4	41.4		90.4
	-20.7		-45.2	20.7		-20.7	45.2		20.7
	11.9		8.9	8.9		-8.9	-8.9		-11.9
	4.5		5.9	-4.5		4.5	-5.9		-4.5
	-2.6		-0.5	-0.5		0.5	0.5		2.6
Final moment	60		-229	253		-253	229		-60

Load case c: 304psf panel B (left) and C and 176 psf panel B (right)

$$\text{Fixed end moment} = \frac{304x22^2x22}{12000} = 270 \text{ k-ft}, \frac{176x22^2x22}{12000} = 157 \text{ k-ft}$$

Table A.3 Moment distribution of load case c (k-ft) (1k-ft = 1.35 kN-m)

Panel	B			C			B		
Joint	1		2	2		3	3		4
DF	0.576		0.365	0.365		0.365	0.365		0.576
FEM	270		-270	270		-270	157		-157
COM	-155.6					41.4	41.4		90.4
			-77.8	20.7			45.2		20.7
			20.9	20.9		-16.52	-16.5		-11.9
	10.44			-8.26		10.44	-5.9		-8.3
	-6		3.02	3.02		-1.6	-1.6		4.8
Final moment	119		-324	306		-236	219		-61

- **Design moment calculation**

Moment diagram for the two controlling cases are shown in the Figure A.2. According to the ACI code the critical section at interior supports may be taken as at the face of the supports but not greater than $0.175l_1$ from the column centerline. The former criterion controls here and the negative design moment is calculated by subtracting the area under the shear diagram between the centerline and the face of the support for load case a, from the negative moment at the support centerline. The shear diagram for load case a is given in the figure with adjusted design moments in Fig. A.2.

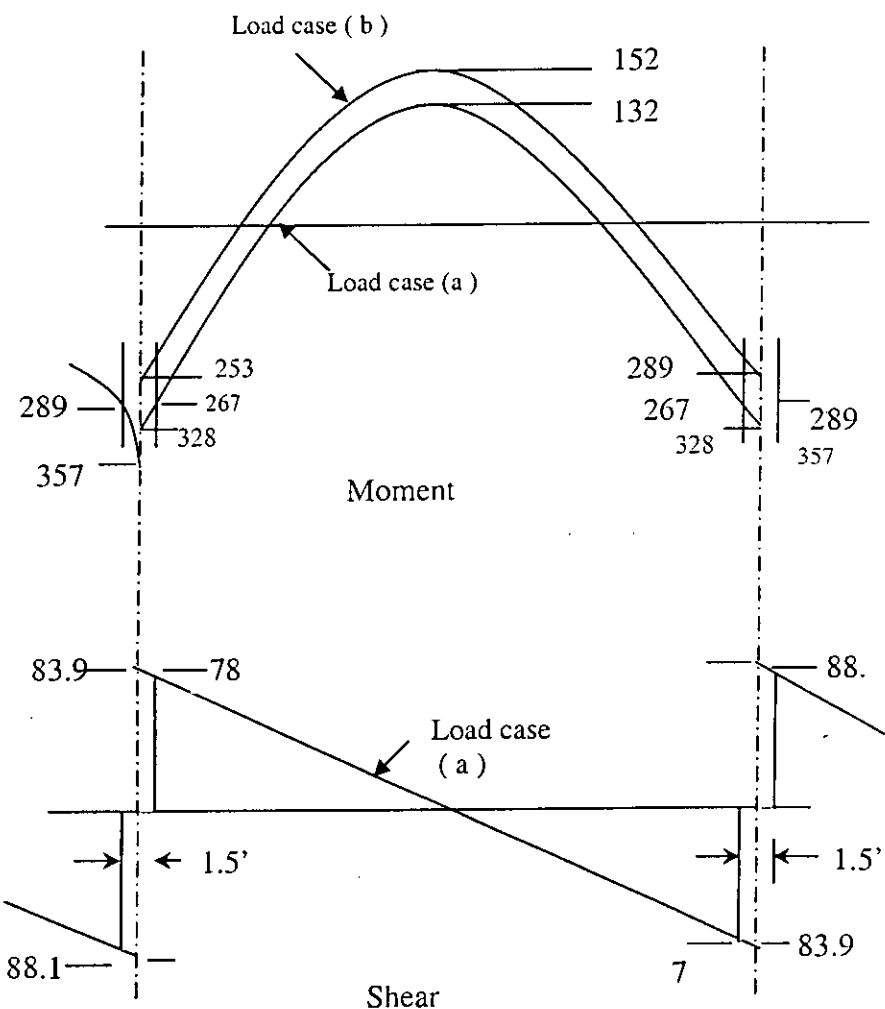


Figure A.2: Design moments and shear for flat plate floor (moments in k-ft and shear in kip) ($1 \text{ k-ft} = 1.35 \text{ kN-m}$, $1 \text{ kip} = 4.44 \text{ kN}$)

Panel C

Maximum Negative moment at panel C = 357 k-ft (load case A)

Shear at panel C = $0.346 \times 22 \times 22/2 = 83.9$ kip

Shear due to Unbalance moment = $(357-139)/22 = 9.93$ kip

Total shear = $83.9 + 9.93 = 93.8$ kip

Shear at column = $0.346 \times 18 \times 22/12/2 = 5.72$

Moments at the face of column = $93.8 - 5.72 = 88.12$ k-ft

Design negative moment = 357 k-ft (from case A) - $(93.8 + 88.12) * 18/12/2 = 289$ k-ft

Design positive moment = $(0.304 \times 22^2 \times 22/8) - 253$ (from case B)
 $= 405 - 253 = 152$ k-ft

- **Reinforcement Design**

According to the table 2.1, moment will be distributed laterally to the across the slab width which indicates 75 percent of the negative moment will be assigned to the column strip and 60 percent of the positive moments assigned to the column strip.

Column strip negative moment = $289 \times 0.75 = 216$ k-ft

Width of the strip = $22 \times 12/2 = 132$ inch

Effective depth = $8.5 - 1.5 = 7$ inch

Moments per unit width = $216 \times 12/132 = 19.82$ k-ft /ft

$$M_u = \phi \rho f_y d^2 \left(1 - 0.59 \frac{\rho f_y}{f'_c} \right) \text{ per unit width}$$

$$\text{Or } 19.82 \times 1000 = 0.9 \times \rho \times 60000 \times 7^2 \left(1 - 0.59 \times \frac{\rho \times 60000}{4000} \right)$$

$$\therefore \rho = 0.008$$

$$A_s = 0.008 \times 132 \times 7 = 7.48 \text{ in}^2$$

$$\text{No of bar provided} = 7.48 / 0.48 = 15.37 \approx 16 \text{ nos 20 mm bar}$$

$$\text{Reinforcement per unit width} = 16 \times 0.48 \times 12 / 132 = 0.70 \text{ in}^2 / \text{in}$$

Similarly

$$\text{Middle strip negative moment} = 289 \times 0.25 = 73 \text{ k-ft}$$

$$\text{Column strip negative moment} = 152 \times 0.6 = 91 \text{ k-ft}$$

Middle strip negative moment = $152 \times 0.4 = 61$ k-ft

And corresponding reinforcement for panel C given in the following Table

Table A.4 Design of flat plate reinforcement

	Location	M_u k-ft	b in	d in	$M_u \times 12/b$	ρ	A_s	A_s in ² /ft	A_s mm ² /mm
Column strip	Negative	216	132	7	19.64	0.008	7.38	0.70	1.48
	Positive	91	132	7	8.27	0.0032	2.97	0.28	0.42
Two half- middle strips	Negative	73	132	7	6.61	0.0026	2.36	0.23	0.34
	Positive	61	132	7	5.52	0.0021	2.02	0.23	0.34

Appendix -B

Q

FLAT PLATE DESIGN

CALCULATION

B-C-B

SLAB THICKNESS

LOAD

floor finish	20 psf
DL=	126 psf
LL=	100 psf
Factored Load	347 psf

SPAN

X dir	22 ft
Y dir	22 ft

COLUMN SIZE

X dir	18 in
Y dir	18 in

Floor height

fc=	4000 psi
fy=	60000 psi
fs=	20000 psi

CALCULATION

B-C-B

SLAB THICKNESS

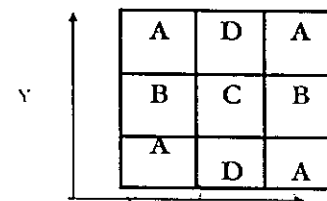
max span	22 ft
min col size	18 in
h =	7.52 in
no edge beam increase h 10 %	
h =	8.27 in
thickness	8.5 inch
d =	7 in

SLAB stiffness

Ks 205 in⁴

COLUMN stiffness

Kc	243 in ⁴
c	2589
Kt	109 in ⁴
1/Kec	0.006642
Kec	150.5596 in ⁴



EQUIVALENT FRAME METHOD

along x direction

Moment distribution

panel	B	C	B			
Joint	1	2	2	3	3	4
DF	0.576		0.366	0.366		0.576
FEM	308		-308	308		-308
C o m	-177.29					177.3
		-88.6			88.64	
		32.4	32.4		-32.4	-32.41
	16.2		-16.2		16.2	
	-9.3		5.9	5.9	-5.9	-5.92
	3.0		-3.0		3.0	-3.0
	-1.7		1.1	1.1	-1.1	-1.08
	0.5		-0.5		0.5	-0.5
	-0.3		0.2	0.2	-0.2	-0.20
						0.3
	139		-357	328	-328	357
						-139

Design moment calculation

Panel C

	shear	83.914	Negative moment	357	Positive moment
		9.9273			68.2351
final shear		93.841	88.119		289
shear at l/2		5.7214			152

Design moment calculation

Panel B

	shear	83.914	Negative moment	139	Positive moment
		9.9273			53.34412
final shear		73.986	68.265		85
shear at l/2		5.7214			176

1 k-ft = 1.356 KN-m

Moment distribution

panel Joint	B		D		B		4
	1	2	2	3	3		
DF	0.576		0.366	0.366		0.366	0.576
FEM	157		-157	270		-270	156.84
C o m	-90.37		-41.36	-41.36		41.36	41.36
	-20.68		-45.19	20.68		-20.68	45.19
	11.92		8.96	8.96		-8.96	-8.96
	4.48		5.96	-4.48		4.48	-5.96
	-2.58		-0.54	-0.54		0.54	0.54
							2.58
	60		-229	253		-253	229
							-60

design moment
negative 289 k ft positive 152 k ft

Int 0.75 int 0.6

design moment
negative 85 k ft positive 176 k ft

Int 1 int 0.6

$$1 \text{ k-ft} = 1.356 \text{ KN-m}$$

CALCULATION

A-D-A

SLAB THICKNESS

max span 22 ft

min col size 18 in

h = 7.52 in

no edge beam increase h 10 percent

h = 8.27 in

thickness 8.5 inch

d = 7 in

SLAB stiffness

Ks 205 in⁴

COLUMN stiffness

Kc 243 in⁴

c 2589

Kt 109 in⁴

1/Kec 0.011226

Kcc 89.07764 in⁴

along x direction

Moment distribution

panel	A		D		A		
Joint	1	2	2	3	3	4	
DF	0.697		0.411	0.411		0.411	0.697
FEM	154		-154	154		-154	154
Com	-107.2						107.2
			-53.6			53.60	
			22.0	22.0		-22.0	-22.01
	11.0			-11.0		11.0	
	-7.7		4.5	4.5		-4.5	-4.52
	2.3			-2.3		2.3	
	-1.6		0.9	0.9		-0.9	-0.93
	0.5			-0.5		0.5	
	-0.3		0.2	0.2		-0.2	-0.19
							0.3
	51		-180	168		-168	180
							-51

Design moment calculation Panel D

shear	41.9568 5.87793	Negative moment	180 34.80325	Positive moment
final shear	47.8347 2.86069		145	76
shear at H/2	44.974			

Design moment calculation Panel A

shear	41.9568 5.87793	Negative moment	51 25.98636	Positive moment
final shear	36.0788 2.86069		25	96
shear at H/2	33.2181			

design moment

negative 145 k ft positive 76 k ft

Int

145 K II

positive

76 k ft

design moment

negative 25 k ft positive 96 k ft

Int

1

int

116

$$1 \text{ k-ft} = 1.356 \text{ KN-m}$$

CALCULATION

D-C-D

SLAB THICKNESS

max span 22.00 ft

min col size 18 in

h = 7.52 in

no edge beam increase h 10 percent

h = 8.27 in

thickness 8.5 inch

d = 7 in

SLAB stiffness

Ks 205 in⁴

COLUMN stiffness

Kc 243 in⁴

c 2589

Kt 109 in⁴

1/Kec 0.006642

Kec 150.5596 in⁴

along Y direction

Moment distribution

panel Joint	D		C		D		4
	1	2	2	3	3		
DF	0.576		0.366	0.366		0.366	0.576
FEM	308		-308	308		-308	308
C o m	-177.29						177.3
		-88.6				88.64	
		32.4	32.4		-32.4	-32.41	
	16.2		-16.2		16.2		-16.2
	-9.3		5.9	5.9		-5.9	9.3
	3.0		-3.0		3.0		-3.0
	-1.7		1.1	1.1		-1.1	1.7
	0.5		-0.5		0.5		-0.5
	-0.3		0.2	0.2		-0.2	0.3
	139		-357	328		-328	357
							-139

Design moment calculation Panel C

shear	83.9135	Negative moment	357	Positive moment
	9.92732		68.2351	
final shear	93.8408	88.1194	289	152
shear at 11/2	5.72138			

Design moment calculation Panel D

shear	83.9135	Negative moment	139	Positive moment
	9.92732		53.34412	
final shear	73.9862	68.2648	85	176
shear at 11/2	5.72138			

Moment distribution

$$1 \text{ k-ft} = 1,356 \text{ KN-m}$$

design moment

negative 289 k ft positive 152 k ft

Int 0.75 int 0.6

design moment

negative 85 k ft positive 176 k ft

Int. J. Environ. Res. Public Health 2020, 17, 406

Moment distribution

1 k-ft = 1.356 KN-m

panel	D		C		D			
Joint	1	2	2		3	3	4	
DF	0.576		0.366	0.366		0.366	0.366	0.576
FEM	270		-270	270		-270	157	-157
C o m	-155.56		0.00	0.00		41.36	41.36	90.37
	0.00		-77.78	20.68		0.00	45.19	20.68
	0.00		20.87	20.87		-16.52	-16.52	-11.92
	10.44		0.00	-8.26		10.44	-5.96	-8.26
	-6.01		3.02	3.02		-1.64	-1.64	4.76
	119		-324	306		-236	219	-61

CALCULATION

A-B-A

SLAB THICKNESS

max span 22 ft

min col size 18 in

h = 7.52 in

no edge beam increase h 10 percent

h = 8.27 in

thickness 8.5 inch

d = 7 in

SLAB stiffness

Ks 205 in⁴

COLUMN stiffness

Kc 243 in⁴

c 2589

Kt 109 in⁴

1/Kec 0.011226

Kec 89.07764 in⁴

along Y direction

Moment distribution

1 k-ft = 1.356 KN-m

panel	A		B		A		
Joint	1	2	2	3	3	4	
DF	0.697		0.411	0.411		0.411	0.697
FEM	154		-154	154		-154	154
C o m	-107.2						107.2
		-53.6			53.60		
		22.0	22.0		-22.0	-22.01	
	11.0		-11.0		11.0		-11.0
	-7.7		4.5	4.5	-4.5	-4.52	7.7
	2.3		-2.3		2.3		-2.3
	-1.6		0.9	0.9	-0.9	-0.93	1.6
	0.5		-0.5		0.5		-0.5
	-0.3		0.2	0.2	-0.2	-0.19	0.3
	51		-180	168		-168	180
							-51

Design moment calculation Panel B

shear	41.9568	Negative moment	180	Positive moment
	5.87793		34.80325	
final shear	47.8347	44.974	145	76
shear at 11/2	2.86069			

Design moment calculation Panel A

shear	41.9568	Negative moment	51	Positive moment
	5.87793		25.98636	
final shear	36.0788	33.2181	25	96
shear at 11/2	2.86069			

Moment distribution

$$1 \text{ k-ft} = 1.356 \text{ KN-m}$$

design moment

negative 145 k ft positive 76 k ft

Int 0.75 int 0.6

design moment

negative 25 k ft positive 96 k ft

lot 1 int 0.6

Moment distribution

$$1 \text{ k-ft} = 1.356 \text{ KN-m}$$

as min	c	a		rho
2.02	0.0074	8.85	0.2627087	0.0079855
2.02	0.0031	8.85	0.1106782	0.00132182

2.02	0.0025	8.85	0.088398	0.0025549
2.02	0.0021	8.85	0.0738576	0.0021264

2.02	0.0029	8.85	0.1033807	0.0030000
2.02	0.0036	8.85	0.1277056	0.0037307

2.02	0.0000	8.85	0.000208	0.0000059
2.02	0.0024	8.85	0.0859322	0.0024820

INT. PANEL ALONG X DIR

as min	c	a		rho
1.01	0.0074	8.85	0.2627087	0.007985
1.01	0.0031	8.85	0.109462	0.003182

1.01	0.0026	8.85	0.0904368	0.002615
1.01	0.0021	8.85	0.0759429	0.002188

1.01	0.0016	8.85	0.0583797	0.001674
1.01	0.0039	8.85	0.1386518	0.004063

1.01	0.0000	8.85	0.001657	0.000047
1.01	0.0027	8.85	0.0958259	0.002775

EXT. PANEL ALONG X DIR

		Mu	b	d	Mu*12/b	rho	As	bar dia	no	no prov.	in2/ft	mm2/mm
column	negative	216	132	7	19.64	0.0080	7.38	0.48	15.372085	16	0.70	1.48
strip	positive	91	132	7	8.27	0.0032	2.97	0.31	9.5921887	10	0.28	0.60

two half middle strip	negative	73	132	7	6.61	0.0026	2.36	0.31	7.615207	8	0.23	0.48
	positive	61	132	7	5.52	0.0021	2.02	0.31	6.5148387	8	0.23	0.48

column	negative	85	132	7	7.73	0.0030	2.77	0.48	5.7750205	8	0.35	0.74
strip	positive	105	132	7	9.55	0.0037	3.45	0.31	11.119826	12	0.34	0.72

two half middle strip	negative	0.1710031	132	7	0.02	0.0000	2.02	0.31	6.5148387	8	0.23	0.48
	positive	71	132	7	6.42	0.0025	2.29	0.31	7.3979068	8	0.23	0.48

		Mu	b	d	Mu*12/b	rho	As	bar dia	no	no prov.	in2/ft	mm2/mm
column	negative	108	66	7	19.64	0.0080	3.69	0.48	7.6860426	8	0.70	1.48
strip	positive	45	66	7	8.18	0.0032	1.47	0.31	4.7418168	5	0.28	0.60

two half middle strip	negative	37	66	7	6.76	0.0026	1.21	0.31	3.8975521	4	0.23	0.48
	positive	31	66	7	5.68	0.0022	1.01	0.31	3.2602777	4	0.23	0.48

column	negative	24	66	7	4.36	0.0017	1.01	0.48	2.10375	4	0.35	0.74
strip	positive	57	66	7	10.36	0.0041	1.88	0.31	6.0548815	7	0.39	0.84

two half middle strip	negative	1	66	7	0.12	0.0000	1.01	0.31	3.2574194	4	0.23	0.48
	positive	39	66	7	7.16	0.0028	1.28	0.31	4.1357975	5	0.28	0.60

as min	c	a		rho
2.02	0.0074	8.85	0.2627087	0.007985
2.02	0.0031	8.85	0.1106782	0.003218

2.02	0.0025	8.85	0.088398	0.002555
2.02	0.0021	8.85	0.0738576	0.002126

2.02	0.0029	8.85	0.1033807	0.003000
2.02	0.0036	8.85	0.1277056	0.003731

2.02	0.0000	8.85	0.000208	0.000000
2.02	0.0024	8.85	0.0859322	0.002482

INT. PANEL ALONG Y DIR

as min	c	a		rho
1.01	0.0074	8.85	0.2627087	0.007985
1.01	0.0031	8.85	0.109462	0.003182

1.01	0.0026	8.85	0.0904368	0.002615
1.01	0.0021	8.85	0.0759429	0.002188

1.01	0.0016	8.85	0.0583797	0.001674
1.01	0.0039	8.85	0.1386518	0.004063

1.01	0.0000	8.85	0.001657	0.000047
1.01	0.0027	8.85	0.0958259	0.002775

EXT. PANEL ALONG Y DIR

Mu	b	d	Mu*12/b	rho	As	bar dia	no	no prov.	in2/ft	mm2/mm
----	---	---	---------	-----	----	---------	----	----------	--------	--------

column strip	negative	216	132	7	19.64	0.0080	7.38	0.48	15.372085	16	0.70	1.48
	positive	91	132	7	8.27	0.0032	2.97	0.31	9.5921887	10	0.28	0.60

two half middle strip	negative	73	132	7	6.61	0.0026	2.36	0.31	7.615207	8	0.23	0.48
	positive	61	132	7	5.52	0.0021	2.02	0.31	6.5148387	8	0.23	0.48

column strip	negative	85	132	7	7.73	0.0030	2.77	0.48	5.7750205	8	0.35	0.74
	positive	105	132	7	9.55	0.0037	3.45	0.31	11.119826	12	0.34	0.72

two half middle strip	negative	0	132	7	0.02	0.0000	2.02	0.31	6.5148387	8	0.23	0.48
	positive	71	132	7	6.42	0.0025	2.29	0.31	7.3979068	8	0.23	0.48

Mu	b	kl	Mu*12/b	rho	As	bar dia	no	no prov.	in2/ft	mm2/mm
----	---	----	---------	-----	----	---------	----	----------	--------	--------

column strip	negative	108	66	7	19.64	0.0080	3.69	0.48	7.6860426	8	0.70	1.48
	positive	45	66	7	8.18	0.0032	1.47	0.31	4.7418168	5	0.28	0.60

two half middle strip	negative	37	66	7	6.76	0.0026	1.21	0.31	3.8975521	4	0.23	0.48
	positive	31	66	7	5.68	0.0022	1.01	0.31	3.2602777	4	0.23	0.48

column strip	negative	24	66	7	4.36	0.0017	1.01	0.48	2.10375	4	0.35	0.74
	positive	57	66	7	10.36	0.0041	1.88	0.31	6.0548815	7	0.39	0.84

two half middle strip	negative	1	66	7	0.12	0.0000	1.01	0.31	3.2574194	4	0.23	0.48
	positive	39	66	7	7.16	0.0028	1.28	0.31	4.1357975	5	0.28	0.60

Appendix -C

Table C.1 Database used for training of ANN ($fr = 0.62\sqrt{f'c}$)

Varying parameters		Input parameters							stress N/mm ²	Output results						
		Span		column size						Deflection						
		x direction (mm)	y direction (mm)	x direction (mm)	y direction (mm)	Total load KN/m ²	Slab thickness (mm)	Concrete strength N/mm ²		elastic	craked (fr = 0.62sqrt(f'c))	Corner (mm)	Edge (mm)	center (mm)	Corner (mm)	Edge (mm)
Increase load	8400	8400	600	600	11.49	265	20.69	12.107	stress N/mm ²	11.710	10.166	8.340	18.992	15.695	12.292	
	8400	8400	600	600	12.45	265	20.69	13.119		12.689	11.015	9.037	21.963	17.784	13.481	
	8400	8400	600	600	13.41	265	20.69	14.130		13.667	11.865	9.734	25.151	19.910	14.562	
	8400	8400	600	600	14.37	265	20.69	15.142		14.645	12.714	10.431	28.351	22.083	15.573	
Increase steel area	10%	8400	8400	600	600	12.45	265	20.69	stress N/mm ²	13.119	12.689	11.015	9.037	21.395	17.293	13.182
	20%	8400	8400	600	600	12.45	265	20.69		13.119	12.689	11.015	9.037	20.901	16.895	12.886
Change slab thickness	0.8t	8400	8400	600	600	11.49	215	20.69	19.715	20.605	18.102	15.296	42.961	34.061	25.401	
	1.1t	8400	8400	600	600	13.41	300	20.69	10.815	9.853	8.479	6.795	15.227	12.851	10.094	
	1.2t	8400	8400	600	600	14.12	325	20.69	10.155	8.431	7.209	5.677	12.125	10.658	8.678	
change concrete strength	8400	8400	600	600	12.45	265	17.24	13.119	13.900	12.067	9.900	25.559	20.389	14.859		
	8400	8400	600	600	12.45	265	24.14	13.119	11.747	10.198	8.367	19.195	15.797	12.313		
	8400	8400	600	600	12.45	265	27.69	13.119	10.968	9.522	7.812	17.099	14.512	11.563		
change in column size	8400	8400	500	500	12.45	265	20.69	14.723	13.946	11.728	8.952	26.259	20.607	14.217		
	8400	8400	400	400	12.45	265	20.69	18.091	15.777	12.646	8.469	28.772	21.189	12.195		
	8400	8400	300	300	12.45	265	20.69	22.093	18.713	13.924	7.316	35.191	24.128	9.492		
Increase load	8400	6900	600	600	11.49	265	20.69	10.121	8.273	7.726	6.088	12.521	12.075	8.951		
	8400	6900	600	600	12.45	265	20.69	10.966	8.964	8.372	6.597	14.448	13.926	9.838		
	8400	6900	600	600	13.41	265	20.69	11.812	9.655	9.018	7.105	16.622	15.950	10.748		
	8400	6900	600	600	14.37	265	20.69	12.658	10.346	9.663	7.614	18.840	17.901	11.793		

Varying parameters		Input parameters							Output results						
		Span		column size					stress N/mm ²	Deflection					
		x direction (mm)	y direction (mm)	x direction (mm)	y direction (mm)	Total load kN/m ²	Slab thickness (mm)	Concrete strength N/mm ²		elastic			craked (fr = 0.62sqrt(f'c))		
Increase steel area	10%	8400	6900	600	600	12.45	265	20.69	10.966	8.964	8.372	6.597	14.157	13.601	9.646
	20%	8400	6900	600	600	12.45	265	20.69	10.966	8.964	8.372	6.597	13.858	13.304	8.964
Change slab thickness	0.8t	8400	6900	600	600	11.49	215	20.69	16.471	14.504	13.608	11.118	29.450	27.743	19.860
	1.1t	8400	6900	600	600	13.41	300	20.69	8.910	6.979	6.497	4.967	9.928	9.623	7.242
	1.2t	8400	6900	600	600	14.12	325	20.69	8.058	5.983	5.559	4.167	8.029	7.755	6.127
change concrete strength		8400	6900	600	600	12.45	265	17.24	10.966	9.820	9.171	7.227	17.037	16.400	11.060
		8400	6900	600	600	12.45	265	24.14	10.966	8.299	7.751	6.107	12.606	12.144	8.986
		8400	6900	600	600	12.45	265	27.69	10.966	7.748	7.237	5.702	11.230	10.867	8.333
change in column size		8400	6900	500	500	12.45	265	20.69	12.141	9.903	9.100	6.576	16.515	15.852	9.934
		8400	6900	400	400	12.45	265	20.69	14.452	11.270	10.113	6.269	19.341	18.423	9.484
		8400	6900	300	300	12.45	265	20.69	17.839	13.473	11.663	5.473	23.937	22.353	8.053
Increase load		8400	5400	600	600	11.49	265	20.69	8.323	6.236	6.188	4.890	9.105	9.283	6.906
		8400	5400	600	600	12.45	265	20.69	9.018	6.757	6.705	5.299	10.802	11.063	7.784
		8400	5400	600	600	13.41	265	20.69	9.714	7.278	7.222	5.708	12.626	12.902	8.884
		8400	5400	600	600	14.37	265	20.69	10.409	7.799	7.739	6.116	14.528	14.847	10.357
Increase steel area	10%	8400	5400	600	600	12.45	265	20.69	9.018	6.757	6.705	5.299	10.643	10.891	7.678
	20%	8400	5400	600	600	12.45	265	20.69	9.018	6.757	6.705	5.299	10.472	10.712	7.540
Change slab thickness	0.8t	8400	5400	600	600	11.49	215	20.69	13.519	10.914	10.827	8.907	23.791	24.282	18.925
	1.1t	8400	5400	600	600	13.41	300	20.69	7.192	5.268	5.230	4.005	7.126	7.262	5.587
	1.2t	8400	5400	600	600	14.12	325	20.69	6.420	4.521	4.491	3.358	5.756	5.846	4.558
change concrete strength		8400	5400	600	600	12.45	265	17.24	9.018	7.402	7.346	5.805	13.025	13.323	9.225
		8400	5400	600	600	12.45	265	24.14	9.018	6.256	6.208	4.906	9.171	9.352	6.931

Varying parameters		Input parameters							Output results						
		Span		column size					stress N/mm ²	Deflection					
		x direction (mm)	y direction (mm)	x direction (mm)	y direction (mm)	Total load KN/m ²	Slab thickness (mm)	Concrete strength N/mm ²		elastic	craked (fr = 0.62sqrt(f'c))	Corner (mm)	Edge (mm)	center (mm)	Corner (mm)
change concrete str.		8400	5400	600	600	12.45	265	27.69	9.018	5.841	5.796	4.580	8.000	8.128	6.349
change in column size		8400	5400	500	500	12.45	265	20.69	9.849	7.488	7.390	5.315	12.588	12.941	8.058
		8400	5400	400	400	12.45	265	20.69	11.388	8.571	8.392	5.111	15.164	15.630	7.886
		8400	5400	300	300	12.45	265	20.69	14.186	10.375	10.018	4.494	19.545	20.160	6.993
Increase load		8400	4200	600	600	11.49	265	20.69	7.547	5.967	6.049	5.002	9.132	9.373	7.276
		8400	4200	600	600	12.45	265	20.69	8.177	6.466	6.554	5.420	11.083	11.390	8.805
		8400	4200	600	600	13.41	265	20.69	8.808	6.964	7.059	5.838	13.043	13.381	10.572
		8400	4200	600	600	14.37	265	20.69	9.438	7.463	7.565	6.256	15.208	15.546	12.543
Increase steel area	10%	8400	4200	600	600	12.45	265	20.69	8.177	6.466	6.554	5.420	10.929	11.230	8.669
	20%	8400	4200	600	600	12.45	265	20.69	8.177	6.466	6.554	5.420	10.786	11.084	8.564
Change slab thickness	0.8t	8400	4200	600	600	11.49	215	20.69	11.270	9.915	9.304	7.986	20.830	21.297	18.434
	1.1t	8400	4200	600	600	13.41	300	20.69	6.027	4.432	4.500	3.599	5.658	5.763	4.657
	1.2t	8400	4200	600	600	14.12	325	20.69	5.329	3.803	3.865	3.019	4.624	4.709	3.660
change concrete strength		8400	4200	600	600	13.41	265	17.24	8.177	7.083	7.180	5.938	13.525	13.900	11.083
		8400	4200	600	600	13.41	265	24.14	8.177	5.986	6.067	5.018	9.231	9.477	7.310
		8400	4200	600	600	13.41	265	27.69	8.177	5.589	5.665	4.685	7.829	7.998	6.530
change in column size		8400	4200	500	500	13.41	265	20.69	8.257	6.297	6.376	4.799	10.504	10.801	7.368
		8400	4200	400	400	13.41	265	20.69	9.337	7.224	7.301	4.658	12.838	13.235	7.446
		8400	4200	300	300	13.41	265	20.69	11.497	8.846	8.885	4.120	17.218	17.754	6.595
Increase load		6900	6900	600	600	10.53	215	20.69	10.019	8.236	7.348	6.343	12.392	11.058	9.461
		6900	6900	600	600	11.49	215	20.69	10.932	8.987	8.017	6.922	14.367	12.462	10.507
		6900	6900	600	600	12.45	215	20.69	11.846	9.738	8.687	7.500	16.748	14.059	11.512

		Input parameters							Output results						
Varying parameters		Span		column size					stress N/mm ²	Deflection					
		x direction (mm)	y direction (mm)	x direction (mm)	y direction (mm)	Total load KN/m ²	Slab thickness (mm)	Concrete strength N/mm ²		elastic			craked (fr = 0.62sqrt(f'c))		
Increase load		6900	6900	600	600	13.40	215	20.69	12.750	10.481	9.350	8.072	19.123	15.640	12.330
Increase steel area	10%	6900	6900	600	600	11.49	215	20.69	10.932	8.987	8.017	6.922	14.046	12.212	10.298
	20%	6900	6900	600	600	11.49	215	20.69	10.932	8.987	8.017	6.922	13.787	11.979	10.088
Change slab thickness	0.8t	6900	6900	600	600	10.53	175	20.69	15.914	14.438	12.990	11.426	29.447	23.991	18.878
	1.1t	6900	6900	600	600	11.97	240	20.69	8.844	6.976	6.188	5.272	10.123	9.072	7.836
	1.2t	6900	6900	600	600	12.45	260	20.69	7.758	5.875	5.187	4.369	8.067	7.322	6.490
change concrete strength		6900	6900	600	600	11.49	215	17.24	10.932	9.846	8.783	7.583	16.330	13.647	10.949
		6900	6900	600	600	11.49	215	24.14	10.932	8.320	7.422	6.408	12.315	10.809	9.190
		6900	6900	600	600	11.49	215	27.69	10.932	7.769	6.930	5.983	11.139	9.940	8.552
change in column size		6900	6900	500	500	11.49	215	20.69	12.309	9.915	8.611	7.054	16.487	13.691	10.692
		6900	6900	400	400	11.49	215	20.69	14.313	11.195	9.331	6.936	19.353	15.171	10.328
		6900	6900	300	300	11.49	215	20.69	18.023	13.282	10.336	6.288	23.799	17.288	9.196
Increase load		6900	5400	600	600	10.53	215	20.69	8.018	5.398	5.177	4.336	7.364	7.296	6.031
		6900	5400	600	600	11.49	215	20.69	8.749	5.890	5.649	4.732	8.516	8.461	6.715
		6900	5400	600	600	12.45	215	20.69	9.480	6.382	6.121	5.127	9.847	9.768	7.426
		6900	5400	600	600	13.40	215	20.69	10.204	6.869	6.589	5.518	11.420	11.311	8.239
Increase steel area	10%	6900	5400	600	600	11.49	215	20.69	8.749	5.890	5.649	4.732	8.409	8.348	6.583
	20%	6900	5400	600	600	11.49	215	20.69	8.749	5.890	5.649	4.732	8.289	8.237	6.500
Change slab thickness	0.8t	6900	5400	600	600	10.53	175	20.69	12.729	9.423	9.057	7.774	21.545	21.350	15.956
	1.1t	6900	5400	600	600	11.97	235	20.69	7.059	4.584	4.391	3.615	6.046	5.957	4.998
	1.2t	6900	5400	600	600	12.45	255	20.69	6.123	4.238	4.056	3.291	5.130	5.056	4.215
change conc. str.		6900	5400	600	600	11.49	215	17.24	8.749	6.452	6.189	5.184	9.784	9.661	7.268

Varying parameters		Input parameters							Output results						
		Span		column size					stress N/mm ²	Deflection					
		x direction (mm)	y direction (mm)	x direction (mm)	y direction (mm)	Total load KN/m ²	Slab thickness (mm)	Concrete strength N/mm ²		elastic	cracked (fr = 0.62sqrt(f'c))	Corner (mm)	Edge (mm)	center (mm)	Corner (mm)
change concrete strength	6900	5400	600	600	11.49	215	24.14	8.749	5.453	5.230	4.381	7.403	7.302	5.961	
	6900	5400	600	600	11.49	215	27.69	8.749	5.091	4.883	4.090	6.671	6.549	5.497	
change in column size	6900	5400	500	500	11.49	215	20.69	9.843	6.542	6.205	4.863	9.965	9.861	7.179	
	6900	5400	400	400	11.49	215	20.69	11.271	7.444	6.940	4.829	11.809	11.735	7.411	
	6900	5400	300	300	11.49	215	20.69	13.749	8.921	8.092	4.435	14.922	14.741	6.952	
Increase load	6900	4200	600	600	10.53	215	20.69	6.584	4.153	4.168	3.559	5.192	5.286	4.476	
	6900	4200	600	600	11.49	215	20.69	7.184	4.532	4.548	3.883	6.082	6.235	5.096	
	6900	4200	600	600	12.45	215	20.69	7.784	4.911	4.928	4.207	7.268	7.505	5.835	
	6900	4200	600	600	13.40	215	20.69	8.378	5.285	5.304	4.528	8.648	8.910	6.954	
Increase steel area	10%	6900	4200	600	600	11.49	215	20.69	7.184	4.532	4.548	3.883	5.053	6.171	6.014
	20%	6900	4200	600	600	11.49	215	20.69	7.184	4.532	4.548	3.883	5.967	6.122	5.017
Change slab thickness	0.8t	6900	4200	600	600	10.53	175	20.69	10.436	7.243	7.262	6.367	13.879	14.203	12.057
	1.1t	6900	4200	600	600	11.97	240	20.69	5.803	3.529	3.545	2.970	4.291	4.348	3.541
	1.2t	6900	4200	600	600	12.45	260	20.69	5.515	3.451	3.480	2.870	4.157	4.220	3.359
change concrete strength	6900	4200	600	600	11.49	215	17.24	7.184	4.965	4.982	4.254	7.413	7.638	5.956	
	6900	4200	600	600	11.49	215	24.14	7.184	4.196	4.210	3.595	5.299	5.392	4.545	
	6900	4200	600	600	11.49	215	27.69	7.184	3.917	3.931	3.356	4.827	4.892	4.056	
change in column size	6900	4200	500	500	11.49	215	20.69	8.094	5.041	5.042	4.011	7.331	7.547	5.671	
	6900	4200	400	400	11.49	215	20.69	9.068	5.754	5.726	4.015	9.050	9.373	6.070	
	6900	4200	300	300	11.49	215	20.69	10.875	6.958	6.863	3.729	11.894	12.326	5.916	
Increase load	5400	5400	600	600	9.09	165	20.69	7.367	5.071	4.653	4.205	6.656	6.197	5.657	
	5400	5400	600	600	10.05	165	20.69	8.145	5.607	5.144	4.649	7.714	7.159	6.391	

Varying parameters		Input parameters							Output results						
		Span		column size					stress N/mm ²	Deflection					
		x direction (mm)	y direction (mm)	x direction (mm)	y direction (mm)	Total load KN/m ²	Slab thickness (mm)	Concrete strength N/mm ²		Corner (mm)	Edge (mm)	center (mm)	Corner (mm)	Edge (mm)	center (mm)
Increase load	5400	5400	600	600	11.01	165	20.69	8.923	6.143	5.636	5.093	8.934	8.189	7.378	
	5400	5400	600	600	11.97	165	20.69	9.701	6.678	6.127	5.537	10.421	9.422	8.270	
Increase steel area	10%	5400	5400	600	600	10.05	165	20.69	8.145	5.607	5.144	4.649	7.606	7.094	6.315
	20%	5400	5400	600	600	10.05	165	20.69	8.145	5.607	5.144	4.649	7.503	6.981	6.240
Change slab thickness	0.8t	5400	5400	600	600	9.58	135	20.69	11.973	9.262	8.544	7.803	17.200	15.069	12.752
	1.1t	5400	5400	600	600	10.77	190	20.69	6.371	4.109	3.752	3.357	5.322	4.964	4.518
	1.2t	5400	5400	600	600	11.01	200	20.69	5.811	3.665	3.339	2.976	4.631	4.318	3.909
change concrete strength	5400	5400	600	600	10.05	165	17.24	8.145	6.143	5.636	5.093	8.908	8.177	7.389	
	5400	5400	600	600	10.05	165	24.14	8.145	5.191	4.763	4.304	6.929	6.468	5.873	
	5400	5400	600	600	10.05	165	27.69	8.145	4.847	4.447	4.019	6.370	5.943	5.430	
change in column size	5400	5400	500	500	10.05	165	20.69	9.503	6.273	5.635	4.917	9.170	8.366	7.364	
	5400	5400	400	400	10.05	165	20.69	11.172	7.118	6.189	5.062	10.833	9.499	7.850	
	5400	5400	300	300	10.05	165	20.69	13.564	8.412	6.907	4.906	13.431	10.845	7.582	
Increase load	5400	4200	600	600	9.09	165	20.69	5.851	3.257	3.162	2.814	3.857	3.797	3.321	
	5400	4200	600	600	10.05	165	20.69	6.469	3.601	3.496	3.111	4.417	4.337	3.838	
	5400	4200	600	600	11.01	165	20.69	7.087	3.945	3.830	3.408	5.065	5.032	4.372	
	5400	4200	600	600	11.97	165	20.69	7.705	4.289	4.164	3.705	5.865	5.864	5.024	
Increase steel area	10%	5400	4200	600	600	10.05	165	20.69	6.469	3.601	3.496	3.111	4.383	4.306	3.812
	20%	5400	4200	600	600	10.05	165	20.69	6.469	3.601	3.496	3.111	4.354	4.277	3.788
Change slab thickness	0.8t	5400	4200	600	600	9.58	135	20.69	9.514	5.922	5.775	5.195	9.468	9.399	7.818
	1.1t	5400	4200	600	600	10.77	190	20.69	5.061	2.649	2.570	2.256	3.072	3.011	2.574
	1.2t	5400	4200	600	600	11.01	200	20.69	4.504	2.314	2.245	1.959	2.600	2.546	2.144

Varying parameters		Input parameters							Output results								
		Span		column size					stress N/mm ²	Deflection							
		x direction (mm)	y direction (mm)	x direction (mm)	y direction (mm)	Total load KN/m ²	Slab thickness (mm)	Concrete strength N/mm ²		elastic	craked (fr = 0.62sqrt(f'c))	Corner (mm)	Edge (mm)	center (mm)	Corner (mm)	Edge (mm)	center (mm)
change concrete strength	5400	4200	600	600	10.05	165	17.24	6.469	3.945	3.830	3.408	5.018	4.989	4.339			
	5400	4200	600	600	10.05	165	24.14	6.469	3.334	3.237	2.880	3.995	3.930	3.448			
	5400	4200	600	600	10.05	165	27.69	6.469	3.113	3.022	2.689	3.661	3.602	3.118			
change in column size	5400	4200	500	500	10.05	165	20.69	7.554	4.064	3.915	3.326	5.255	5.205	4.470			
	5400	4200	400	400	10.05	165	20.69	8.749	4.654	4.424	3.463	6.353	6.275	4.983			
	5400	4200	300	300	10.05	165	20.69	10.604	5.559	5.165	3.403	8.022	7.973	5.404			
Increase load	4200	4200	600	600	8.37	125	20.69	5.501	3.228	3.028	2.826	3.832	3.642	3.385			
	4200	4200	600	600	9.33	125	20.69	6.132	3.599	3.376	3.150	4.410	4.176	3.879			
	4200	4200	600	600	10.29	125	20.69	6.763	3.969	3.723	3.474	5.100	4.839	4.459			
	4200	4200	600	600	11.25	125	20.69	7.394	4.339	4.070	3.798	5.892	5.545	5.170			
Increase steel area	10%	4200	4200	600	600	9.33	125	20.69	6.132	3.599	3.376	3.150	4.375	4.141	3.849		
	20%	4200	4200	600	600	9.33	125	20.69	6.132	3.599	3.376	3.150	4.343	4.109	3.820		
Change slab thickness	1.1t	4200	4200	600	600	9.57	140	20.69	4.939	2.718	2.544	2.364	3.170	3.005	2.785		
	1.2t	4200	4200	600	600	10.29	150	20.69	4.571	2.430	2.271	2.104	2.788	2.626	2.431		
change concrete strength	4200	4200	600	600	9.33	125	17.24	6.132	3.942	3.698	3.451	5.001	4.748	4.381			
	4200	4200	600	600	9.33	125	24.14	6.132	3.332	3.125	2.916	4.017	3.807	3.539			
	4200	4200	600	600	9.33	125	27.69	6.132	3.111	2.918	2.723	3.694	3.510	3.260			
change in column size	4200	4200	500	500	9.33	125	20.69	7.482	4.146	3.828	3.490	5.392	5.050	4.588			
	4200	4200	400	400	9.33	125	20.69	9.115	4.795	4.319	3.775	6.648	6.131	5.421			
	4200	4200	300	300	9.33	125	20.69	11.405	5.688	4.899	3.907	8.334	7.312	6.004			

Appendix -D

Table D.1 Database used for training of ANN ($fr = 0.33\sqrt{f'c}$)

Varying parameters		Input parameters							stress N/mm ²	Output results						
		Span		column size						Deflection						
		x direction (mm)	y direction (mm)	x direction (mm)	y direction (mm)	Total load KN/m ²	Slab thickness (mm)	Concrete strength N/mm ²		Corner (mm)	Edge (mm)	center (mm)	Corner (mm)	Edge (mm)	center (mm)	
Increase load	8400	8400	600	600	11.49	265	20.69	12.107	11.710	10.166	8.340	31.279	25.673	18.822		
	8400	8400	600	600	12.45	265	20.69	13.119	12.689	11.015	9.037	34.262	28.226	21.000		
	8400	8400	600	600	13.41	265	20.69	14.130	13.667	11.865	9.734	37.246	30.643	22.855		
	8400	8400	600	600	14.37	265	20.69	15.142	14.645	12.714	10.431	40.428	32.935	24.471		
Increase steel area	10%	8400	8400	600	600	12.45	265	20.69	13.119	12.689	11.015	9.037	32.581	26.896	20.052	
	20%	8400	8400	600	600	12.45	265	20.69	13.119	12.689	11.015	9.037	31.142	25.777	19.332	
Change slab thickness	0.8t	8400	8400	600	600	11.49	215	20.69	19.715	20.605	18.102	15.296	54.959	47.437	39.845	
	1.1t	8400	8400	600	600	13.41	300	20.69	10.815	9.853	8.479	6.795	26.844	21.071	14.519	
	1.2t	8400	8400	600	600	14.12	325	20.69	10.155	8.431	7.209	5.677	22.265	17.203	11.256	
change concrete strength	8400	8400	600	600	12.45	265	17.24	13.119	13.900	12.067	9.900	36.798	30.861	23.572		
	8400	8400	600	600	12.45	265	24.14	13.119	11.747	10.198	8.367	32.307	26.051	18.700		
	8400	8400	600	600	12.45	265	27.69	13.119	10.968	9.522	7.812	30.076	23.979	16.950		
change in column size	8400	8400	500	500	12.45	265	20.69	14.723	13.946	11.728	8.952	41.510	33.335	22.756		
	8400	8400	400	400	12.45	265	20.69	18.091	15.777	12.646	8.469	40.902	31.242	19.107		
	8400	8400	300	300	12.45	265	20.69	22.093	18.713	13.924	7.316	47.229	33.464	14.413		
Increase load	8400	6900	600	600	11.49	265	20.69	10.121	8.273	7.726	6.088	22.512	20.787	15.327		
	8400	6900	600	600	12.45	265	20.69	10.966	8.964	8.372	6.597	25.302	22.973	17.126		
	8400	6900	600	600	13.41	265	20.69	11.812	9.655	9.018	7.105	27.964	24.923	18.775		
	8400	6900	600	600	14.37	265	20.69	12.658	10.346	9.663	7.614	30.309	26.848	20.342		

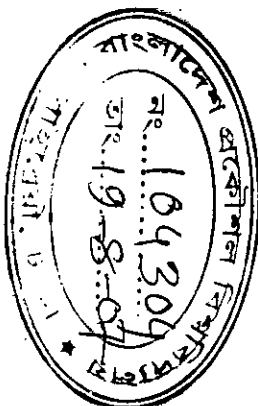
Varying parameters		Input parameters							Output results						
		Span		x direction (mm)		y direction (mm)		Total load KN/m ²	Slab thickness (mm)	Concrete strength N/mm ²	stress N/mm ²	Deflection			
				x direction (mm)	y direction (mm)	x direction (mm)	y direction (mm)					elastic	crazed(fr = 0.33sqrt(f'c))	Corner (mm)	Edge (mm)
Increase steel area	10%	8400	6900	600	600	12.45	265	20.69	10.966	8.964	8.372	6.597	24.191	21.969	16.431
	20%	8400	6900	600	600	12.45	265	20.69	10.966	8.964	8.372	6.597	23.209	21.047	15.803
Change slab thickness	0.8t	8400	6900	600	600	11.49	215	20.69	16.471	14.504	13.608	11.118	42.490	37.918	31.457
	1.1t	8400	6900	600	600	13.41	300	20.69	8.910	6.979	6.497	4.967	18.440	17.179	11.543
	1.2t	8400	6900	600	600	14.12	325	20.69	8.058	5.983	5.559	4.167	14.904	14.219	8.866
change concrete strength		8400	6900	600	600	12.45	265	17.24	10.966	9.820	9.171	7.227	27.917	25.077	19.298
		8400	6900	600	600	12.45	265	24.14	10.966	8.299	7.751	6.107	23.046	21.191	15.392
		8400	6900	600	600	12.45	265	27.69	10.966	7.748	7.237	5.702	20.921	19.506	13.833
change in column size		8400	6900	500	500	12.45	265	20.69	12.141	9.903	9.100	6.576	27.642	24.598	16.776
		8400	6900	400	400	12.45	265	20.69	14.452	11.270	10.113	6.269	30.748	26.877	15.809
		8400	6900	300	300	12.45	265	20.69	17.839	13.473	11.663	5.473	36.101	30.551	12.650
Increase load		8400	5400	600	600	11.49	265	20.69	8.323	6.236	6.188	4.890	18.148	18.712	14.795
		8400	5400	600	600	12.45	265	20.69	9.018	6.757	6.705	5.299	20.496	21.012	17.066
		8400	5400	600	600	13.41	265	20.69	9.714	7.278	7.222	5.708	22.635	23.034	18.948
		8400	5400	600	600	14.37	265	20.69	10.409	7.799	7.739	6.116	24.764	25.114	20.505
Increase steel area	10%	8400	5400	600	600	12.45	265	20.69	9.018	6.757	6.705	5.299	19.628	20.113	16.347
	20%	8400	5400	600	600	12.45	265	20.69	9.018	6.757	6.705	5.299	18.877	19.334	15.697
Change slab thickness	0.8t	8400	5400	600	600	11.49	215	20.69	13.519	10.914	10.827	8.907	35.392	35.742	32.011
	1.1t	8400	5400	600	600	13.41	300	20.69	7.192	5.268	5.230	4.005	14.660	15.087	11.072
	1.2t	8400	5400	600	600	14.12	325	20.69	6.420	4.521	4.491	3.358	11.526	11.992	8.220
change concrete strength		8400	5400	600	600	12.45	265	17.24	9.018	7.402	7.346	5.805	22.643	23.092	19.091
		8400	5400	600	600	12.45	265	24.14	9.018	6.256	6.208	4.906	18.597	19.157	15.060
		8400	5400	600	600	12.45	265	27.69	9.018	5.841	5.796	4.580	16.731	17.275	13.265

Varying parameters		Input parameters						Output results								
		Span		column size				stress N/mm ²	Deflection				elastic		craked($fr = 0.33\sqrt{f'c}$)	
		x direction (mm)	y direction (mm)	x direction (mm)	y direction (mm)	Total load KN/m ²	Slab thickness (mm)		Concrete strength N/mm ²	Corner (mm)	Edge (mm)	center (mm)	Corner (mm)	Edge (mm)	center (mm)	
change in column size	8400	5400	500	500	12.45	265	20.69	9.849	7.488	7.390	5.315	22.520	23.146	16.961		
	8400	5400	400	400	12.45	265	20.69	11.388	8.571	8.392	5.111	25.395	25.922	16.326		
	8400	5400	300	300	12.45	265	20.69	14.186	10.375	10.018	4.494	30.211	30.607	14.121		
Increase load	8400	4200	600	600	11.49	265	20.69	7.547	5.967	6.049	5.002	19.258	19.865	17.935		
	8400	4200	600	600	12.45	265	20.69	8.177	6.466	6.554	5.420	21.874	22.632	20.551		
	8400	4200	600	600	13.41	265	20.69	8.808	6.964	7.059	5.838	24.075	24.867	22.549		
	8400	4200	600	600	14.37	265	20.69	9.438	7.463	7.565	6.256	26.706	27.541	25.079		
Increase steel area	10%	8400	4200	600	600	12.45	265	20.69	8.177	6.466	6.554	5.420	20.968	21.699	19.564	
	20%	8400	4200	600	600	12.45	265	20.69	8.177	6.466	6.554	5.420	20.148	20.865	18.728	
Change slab thickness	0.8t	8400	4200	600	600	11.49	215	20.69	11.270	9.915	9.304	7.986	33.941	34.951	33.325	
	1.1t	8400	4200	600	600	13.41	300	20.69	6.027	4.432	4.500	3.599	12.846	13.183	10.900	
	1.2t	8400	4200	600	600	14.12	325	20.69	5.329	3.803	3.865	3.019	9.783	10.101	7.921	
change concrete strength	8400	4200	600	600	13.41	265	17.24	8.177	7.083	7.180	5.938	24.304	25.197	22.844		
	8400	4200	600	600	13.41	265	24.14	8.177	5.986	6.067	5.018	19.746	20.402	18.324		
	8400	4200	600	600	13.41	265	27.69	8.177	5.589	5.665	4.685	17.796	18.375	16.276		
change in column size	8400	4200	500	500	13.41	265	20.69	8.257	6.297	6.376	4.799	20.427	21.069	17.108		
	8400	4200	400	400	13.41	265	20.69	9.337	7.224	7.301	4.658	23.149	23.852	16.713		
	8400	4200	300	300	13.41	265	20.69	11.497	8.846	8.885	4.120	28.366	29.170	14.861		
Increase load	6900	6900	600	600	10.53	215	20.69	10.019	8.236	7.348	6.343	22.422	18.891	14.652		
	6900	6900	600	600	11.49	215	20.69	10.932	8.987	8.017	6.922	25.250	21.293	16.800		
	6900	6900	600	600	12.45	215	20.69	11.846	9.738	8.687	7.500	27.847	23.367	18.361		
	6900	6900	600	600	13.40	215	20.69	12.750	10.481	9.350	8.072	30.069	25.188	19.660		

Varying parameters		Input parameters							Output results						
		Span		column size					stress N/mm ²	Deflection					
		x direction (mm)	y direction (mm)	x direction (mm)	y direction (mm)	Total load KN/m ²	Slab thickness (mm)	Concrete strength N/mm ²		elastic	craked(fr = 0.33sqrt(f'c))	Corner (mm)	Edge (mm)	center (mm)	Corner (mm)
Increase steel area	10%	6900	6900	600	600	11.49	215	20.69	10.932	8.987	8.017	6.922	24.137	20.390	16.178
	20%	6900	6900	600	600	11.49	215	20.69	10.932	8.987	8.017	6.922	23.150	19.587	15.600
Change slab thickness	0.8t	6900	6900	600	600	10.53	175	20.69	15.914	14.438	12.990	11.426	41.608	36.498	30.550
	1.1t	6900	6900	600	600	11.97	240	20.69	8.844	6.976	6.188	5.272	19.080	15.608	11.526
	1.2t	6900	6900	600	600	12.45	260	20.69	7.758	5.875	5.187	4.369	15.070	12.121	8.736
change concrete strength		6900	6900	600	600	11.49	215	17.24	10.932	9.846	8.783	7.583	25.883	21.652	16.706
		6900	6900	600	600	11.49	215	24.14	10.932	8.320	7.422	6.408	22.294	18.149	13.730
		6900	6900	600	600	11.49	215	27.69	10.932	7.769	6.930	5.983	20.463	16.641	12.631
change in column size		6900	6900	500	500	11.49	215	20.69	12.309	9.915	8.611	7.054	27.456	22.572	16.540
		6900	6900	400	400	11.49	215	20.69	14.313	11.195	9.331	6.936	30.564	24.037	15.779
		6900	6900	300	300	11.49	215	20.69	18.023	13.282	10.336	6.288	34.879	25.642	13.431
Increase load		6900	5400	600	600	10.53	215	20.69	8.018	5.398	5.177	4.336	13.862	13.762	10.863
		6900	5400	600	600	11.49	215	20.69	8.749	5.890	5.649	4.732	16.157	15.940	12.724
		6900	5400	600	600	12.45	215	20.69	9.480	6.382	6.121	5.127	18.248	17.626	14.454
		6900	5400	600	600	13.40	215	20.69	10.204	6.869	6.589	5.518	20.501	16.809	15.828
Increase steel area	10%	6900	5400	600	600	11.49	215	20.69	8.749	5.890	5.649	4.732	15.539	15.315	12.230
	20%	6900	5400	600	600	11.49	215	20.69	8.749	5.890	5.649	4.732	14.985	14.770	11.825
Change slab thickness	0.8t	6900	5400	600	600	10.53	175	20.69	12.729	9.423	9.057	7.774	29.091	27.446	24.012
	1.1t	6900	5400	600	600	11.97	235	20.69	7.059	4.584	4.391	3.615	11.546	11.423	8.450
	1.2t	6900	5400	600	600	12.45	255	20.69	6.123	4.238	4.056	3.291	8.807	6.340	8.825
change concrete strength		6900	5400	600	600	11.49	215	17.24	8.749	6.452	6.189	5.184	17.469	16.750	13.514
		6900	5400	600	600	11.49	215	24.14	8.749	5.453	5.230	4.381	13.955	13.682	10.553
		6900	5400	600	600	11.49	215	27.69	8.749	5.091	4.883	4.090	12.498	12.326	9.226

Input parameters									Output results						
Varying parameters		Span		column size					stress N/mm ²	Deflection					
		x direction (mm)	y direction (mm)	x direction (mm)	y direction (mm)	Total load KN/m ²	Slab thickness (mm)	Concrete strength N/mm ²		elastic			craked(fr = 0.33sqrt(f'c))		
change in column size	6900	5400	500	500	11.49	215	20.69	9.843	6.542	6.205	4.863	18.331	17.629	13.204	
	6900	5400	400	400	11.49	215	20.69	11.271	7.444	6.940	4.829	20.686	19.649	12.795	
	6900	5400	300	300	11.49	215	20.69	13.749	8.921	8.092	4.435	24.671	22.610	11.250	
Increase load	6900	4200	600	600	10.53	215	20.69	6.584	4.153	4.168	3.559	10.996	11.420	10.019	
	6900	4200	600	600	11.49	215	20.69	7.184	4.532	4.548	3.883	12.989	13.473	11.976	
	6900	4200	600	600	12.45	215	20.69	7.784	4.911	4.928	4.207	14.816	15.381	13.695	
	6900	4200	600	600	13.40	215	20.69	8.378	5.285	5.304	4.528	16.731	15.331	15.500	
Increase steel area	10%	6900	4200	600	600	11.49	215	20.69	7.184	4.532	4.548	3.883	12.502	12.960	11.497
	20%	6900	4200	600	600	11.49	215	20.69	7.184	4.532	4.548	3.883	12.087	12.532	11.097
Change slab thickness	0.8t	6900	4200	600	600	10.53	175	20.69	10.436	7.243	7.262	6.367	23.352	24.039	22.828
	1.1t	6900	4200	600	600	11.97	240	20.69	5.803	3.529	3.545	2.970	8.895	9.239	7.682
	1.2t	6900	4200	600	600	12.45	260	20.69	5.515	3.451	3.480	2.870	8.517	8.825	7.208
change concrete strength	6900	4200	600	600	11.49	215	17.24	7.184	4.965	4.982	4.254	14.702	15.235	13.803	
	6900	4200	600	600	11.49	215	24.14	7.184	4.196	4.210	3.595	11.464	11.882	10.397	
	6900	4200	600	600	11.49	215	27.69	7.184	3.917	3.931	3.356	10.135	10.493	9.003	
change in column size	6900	4200	500	500	11.49	215	20.69	8.094	5.041	5.042	4.011	6.693	6.866	5.453	
	6900	4200	400	400	11.49	215	20.69	9.068	5.754	5.726	4.015	16.998	17.630	12.569	
	6900	4200	300	300	11.49	215	20.69	10.875	6.958	6.863	3.729	20.431	21.107	11.803	
Increase load	5400	5400	600	600	9.09	165	20.69	7.367	5.071	4.653	4.205	11.966	10.463	8.743	
	5400	5400	600	600	10.05	165	20.69	8.145	5.607	5.144	4.649	14.391	12.568	10.733	
	5400	5400	600	600	11.01	165	20.69	8.923	6.143	5.636	5.093	16.428	14.392	12.113	
	5400	5400	600	600	11.97	165	20.69	9.701	6.678	6.127	5.537	18.662	16.315	13.643	

Varying parameters		Input parameters							Output results						
		Span		column size					stress N/mm ²	Deflection					
		x direction (mm)	y direction (mm)	x direction (mm)	y direction (mm)	Total load KN/m ²	Slab thickness (mm)	Concrete strength N/mm ²		elastic	corner (mm)	edge (mm)	center (mm)	corner (mm)	edge (mm)
Increase steel area	10%	5400	5400	600	600	10.05	165	20.69	8.145	5.607	5.144	4.649	13.891	12.267	10.416
	20%	5400	5400	600	600	10.05	165	20.69	8.145	5.607	5.144	4.649	13.405	11.869	10.120
Change slab thickness	0.8t	5400	5400	600	600	9.58	135	20.69	11.973	9.262	8.544	7.803	27.321	24.522	21.073
	1.1t	5400	5400	600	600	10.77	190	20.69	6.371	4.109	3.752	3.357	9.358	8.048	6.558
	1.2t	5400	5400	600	600	11.01	200	20.69	5.811	3.665	3.339	2.976	7.806	6.725	5.446
change concrete strength		5400	5400	600	600	10.05	165	17.24	8.145	6.143	5.636	5.093	16.108	14.244	11.999
		5400	5400	600	600	10.05	165	24.14	8.145	5.191	4.763	4.304	12.827	11.215	9.336
		5400	5400	600	600	10.05	165	27.69	8.145	4.847	4.447	4.019	11.472	9.998	8.288
change in column size		5400	5400	500	500	10.05	165	20.69	9.503	6.273	5.635	4.917	16.621	14.194	11.455
		5400	5400	400	400	10.05	165	20.69	11.172	7.118	6.189	5.062	19.115	15.694	11.384
		5400	5400	300	300	10.05	165	20.69	13.564	8.412	6.907	4.906	22.584	17.355	10.340
Increase load		5400	4200	600	600	9.09	165	20.69	5.851	3.257	3.162	2.814	6.408	6.455	5.367
		5400	4200	600	600	10.05	165	20.69	6.469	3.601	3.496	3.111	7.806	7.840	6.653
		5400	4200	600	600	11.01	165	20.69	7.087	3.945	3.830	3.408	9.304	9.306	8.054
		5400	4200	600	600	11.97	165	20.69	7.705	4.289	4.164	3.705	10.865	10.815	9.606
Increase steel area	10%	5400	4200	600	600	10.05	165	20.69	6.469	3.601	3.496	3.111	7.579	7.608	6.471
	20%	5400	4200	600	600	10.05	165	20.69	6.469	3.601	3.496	3.111	7.361	7.392	6.307
Change slab thickness	0.8t	5400	4200	600	600	9.58	135	20.69	9.514	5.922	5.775	5.195	16.540	15.960	14.726
	1.1t	5400	4200	600	600	10.77	190	20.69	5.061	2.649	2.570	2.256	4.955	4.985	3.980
	1.2t	5400	4200	600	600	11.01	200	20.69	4.504	2.314	2.245	1.959	3.926	3.995	3.157
change concrete strength		5400	4200	600	600	10.05	165	17.24	6.469	3.945	3.830	3.408	9.002	8.997	7.797
		5400	4200	600	600	10.05	165	24.14	6.469	3.334	3.237	2.880	6.863	6.901	5.736
		5400	4200	600	600	10.05	165	27.69	6.469	3.113	3.022	2.689	6.056	6.104	4.999



Input parameters									Output results						
Varying parameters	Span		column size		Total load KN/m ²	Slab thickness (mm)	Concrete strength N/mm ²	stress N/mm ²	Deflection			craked($f_r = 0.33\sqrt{f'_c}$)			
	x direction (mm)	y direction (mm)	x direction (mm)	y direction (mm)					Corner (mm)	Edge (mm)	center (mm)	Corner (mm)	Edge (mm)	center (mm)	
change in column size	5400	4200	500	500	10.05	165	20.69	7.554	4.064	3.915	3.326	9.506	9.497	7.721	
	5400	4200	400	400	10.05	165	20.69	8.749	4.654	4.424	3.463	11.485	11.347	8.390	
	5400	4200	300	300	10.05	165	20.69	10.604	5.559	5.165	3.403	14.258	13.779	8.226	
Increase load	4200	4200	600	600	8.37	125	20.69	5.501	3.228	3.028	2.826	6.017	5.500	4.890	
	4200	4200	600	600	9.33	125	20.69	6.132	3.599	3.376	3.150	7.486	6.802	6.080	
	4200	4200	600	600	10.29	125	20.69	6.763	3.969	3.723	3.474	8.916	8.122	7.309	
	4200	4200	600	600	11.25	125	20.69	7.394	4.339	4.070	3.798	10.333	9.450	8.529	
Increase steel area	10%	4200	4200	600	600	9.33	125	20.69	6.132	3.599	3.376	3.150	7.264	6.609	5.920
Change slab thickness	20%	4200	4200	600	600	9.33	125	20.69	6.132	3.599	3.376	3.150	7.069	6.432	5.783
Change slab thickness	1.1t	4200	4200	600	600	9.57	140	20.69	4.939	2.718	2.544	2.364	4.865	4.331	3.812
change concrete strength	4200	4200	600	600	10.29	150	20.69	4.571	2.430	2.271	2.104	4.075	3.645	3.239	
	4200	4200	600	600	9.33	125	17.24	6.132	3.942	3.698	3.451	8.532	7.791	7.013	
	4200	4200	600	600	9.33	125	24.14	6.132	3.332	3.125	2.916	6.604	5.970	5.326	
change in column size	4200	4200	600	600	9.33	125	27.69	6.132	3.111	2.918	2.723	5.799	5.250	4.670	
	4200	4200	500	500	9.33	125	20.69	7.482	4.146	3.828	3.490	9.325	8.308	7.156	
	4200	4200	400	400	9.33	125	20.69	9.115	4.795	4.319	3.775	11.501	9.975	8.165	
	4200	4200	300	300	9.33	125	20.69	11.405	5.688	4.899	3.907	14.210	11.651	8.379	